

AD-A081 893

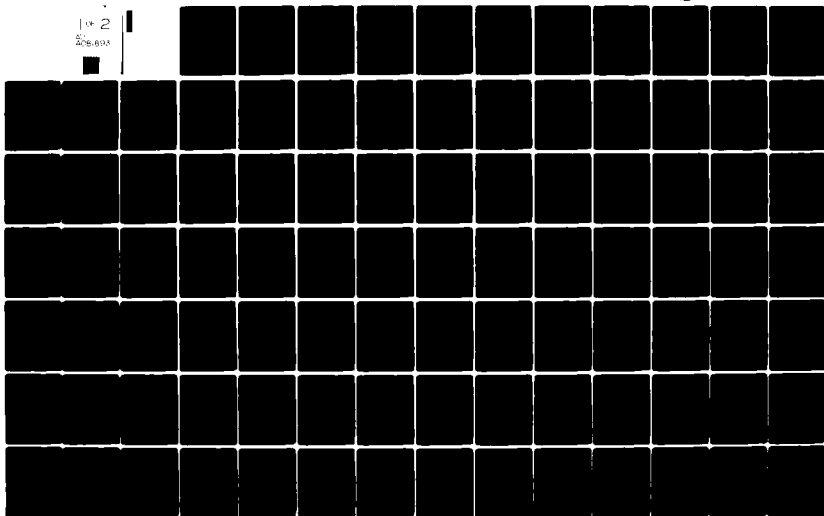
AIR FORCE INST OF TECH WRIGHT-PATTERSON AFB OH SCH00--ETC F/6 19/6
ANALYSIS OF A CONTROLLER FOR THE M61 MOVABLE GUN.(U)
DEC 78 D E JONES
AFIT/6A/AA/78D-5

UNCLASSIFIED

NL

1 of 2

206,808



AFIT/GA/AA/78D-5

1

ANALYSIS OF A CONTROLLER FOR THE
M61 MOVABLE GUN

THESIS

AFIT/GA/AA/78D-5✓

DONALD E. JONES
LIEUTENANT USAF

Approved for public release; distribution unlimited

14
AFIT/GA/AA/78D-5

6
ANALYSIS OF A CONTROLLER FOR THE
M61 MOVABLE GUN .

THESIS *D. Mat. is th*

Presented to the Faculty of the School of Engineering
of the Air Force Institute of Technology
Air University
in Partial Fulfillment of the
Requirements for the Degree of
Master of Science

Approved For	
1.1.1.1	<input checked="" type="checkbox"/>
1.1.1.2	<input type="checkbox"/>
1.1.1.3	<input type="checkbox"/>
1.1.1.4	<input type="checkbox"/>
1.1.1.5	<input type="checkbox"/>
1.1.1.6	<input type="checkbox"/>
1.1.1.7	<input type="checkbox"/>
1.1.1.8	<input type="checkbox"/>
1.1.1.9	<input type="checkbox"/>
1.1.1.10	<input type="checkbox"/>

12 123
by

(10)
Donald E. Jones
Lieutenant USAF

11 December 1978

A

Approved for public release; distribution unlimited

01-20-78 *13*

Preface

This analysis of the M61 movable gun is intended to be an overall evaluation of the control system. Originally, the concept of the thesis was to design a digital controller for the system. But the gun servo subsystem dynamics are good enough and the sampling rate so low that a conventional digital controller is neither required nor feasible. Thus the motivation became one of answering questions which were raised in the review of readily available literature.

The gun system analysis is based on locally available Delco Corporation and McDonnell Aircraft Company reports. No attempt was made to contact either contractor regarding specific questions, so portions of the given information may not be in agreement with current data or design.

I extend my appreciation to my thesis advisor, Capt James Silverthorne, and Professor C. H. Houppis for their assistance throughout this study and to Professors D. W. Breuer and Robert Calico for their interest in reviewing my thesis. I am also indebted to Lt Col Anthony Leatham who sponsored this thesis and to Joe Rogers and Major K. E. Hudson who provided additional background material.

Finally, and most dearly, I would like to thank my wife, Pat, for the time she spent with and without me over the course of my studies. Her encouragement and understanding were invaluable.

Donald E. Jones

Contents

	Page
Preface	ii
List of Figures	v
List of Tables	vii
Symbols	viii
Abstract	x
I Introduction	1
Historical Background	1
System Definition	2
Purpose	2
Assumptions	4
Performance Criteria	5
Approach	7
II Technical Description of the Gun System	8
Gun Servo Subsystem	10
Digital Controller	16
Coordinate Transformation	17
III Analysis of the Gun Servo Subsystem	21
Differential Pressure Compensator	21
Feedforward Compensator	30
Effect of Rate Commands and Rate Feedforward	34
IV Analysis of Digital Portion of Gun System	36
System Gain	36
Digital Rate Feedforward	42
Sensor Filters	42
Computation Time	46
Word Length Considerations	51
V Analysis of Muzzle Response	52
Effect of Structural Modes on Muzzle Response	52
Controller for Structural Modes	56
VI Conclusion	66
Summary	66
Recommendations	67

	Page
Bibliography	68
Appendix A: Derivation of Gun Dynamics Model	70
Appendix B: Determination of Gun Output Coefficients	73
Appendix C: Gun Servo Subsystem State Variable Representation . .	81
Appendix D: M61 Simulation Program	88
Appendix E: Z and S Plane Relationships	108
VITA	109

List of Figures

<u>Figure</u>		<u>Page</u>
1	M61 Movable Gun Servo Subsystem	3
2	Basic Gun System Model	8
3	Gun System Model	9
4	Gun Servo Subsystem Model	10
5	Sensor Frequency Response	12
6	Gun Geometry	15
7	Gun System Interface	16
8	Continuous Complementary Filter	18
9	Baseline Gun System Response	22
10	Differential Pressure Compensation Loop	23
11	Differential Pressure Compensator Root Locus	24
12	Differential Pressure Loop Time Responses	26
13	Gun Servo Subsystem Reduction	31
14	Gun Servo Subsystem Root Locus	32
15	Gun Servo Subsystem Response Using Position Inputs	35
16	Discrete Gun System Model	36
17	Discrete Gun System Root Locus	40
18	Response of Gun System with No Digital Rate Feedforward	43
19	Effect of 10 Hz Sensor Filter on System Response	45
20	Gun System Model Including Computational Delay	47
21	Effect of Computation Time on System Response	50
22	Gun Structural Mode Slopes	53
23	Muzzle Frequency Response	54
24	Muzzle Time Response	55
25	Structural Mode Compensator	59

<u>Figure</u>	<u>Page</u>
26 Structural Mode Compensator Root Locus	60
27 Structural Mode Compensator Discrete Root Locus	61
28 Structural Mode Compensator Time Response	62
29 Modeled Muzzle Frequency Response	74
30 Modeled Sensor Frequency Response	79
31 State Variable Block Diagram	81
32 Z Domain Unit Circle	108

List of Tables

<u>Table</u>		<u>Page</u>
I	Gun Servo Subsystem Specifications	5
II	Differential Pressure Compensator Gun Response	25
III	Differential Pressure Compensator System Response	25
IV	Gun Servo Subsystem Ramp Errors	33
V	Effect of K_{OL} on Gun System Performance	33
VI	Effect of Rate Feedforward on Gun Response	34
VII	Comparison of Analytical and Simulation Response	41
VIII	Poles of Closed Loop Gun System as a Function of Gain	41
IX	Effect of Sensor Filter on System Response	44
X	Effect of Digital Filter Gain on System Response	46
XI	Comparison of Simulation and Analytical Computation Time Effects	49
XII	System Response for Different Computation Times	51
XIII	Structural Mode Compensator Response	64

Symbols

A_i	Gun dynamics output coefficient for i th mode
C	Computation time delay (T_C)
F	Actuator piston force
f_s	Sampling frequency (Hertz)
G_1	Feedforward compensation
G_2	Servo valve dynamics
G_3	Gun dynamics
G_{3D}	2 mode gun dynamics model
G_{3C}	4 mode gun dynamics model
G_{3M}	Muzzle dynamics model
G_4	Differential pressure compensator
G_f	Sensor filter (analog)
G_g	Gun system transfer function
G_{gss}	Gun servo subsystem transfer function
G'_{gss}	s G_{gss}
G_p	Gun dynamics with differential pressure compensator
G_{ZOH}	Zero order hold dynamics
H_p	Differential pressure compensator
H_s	Feedback structural compensator
k	Sample period
K_1	System gain
K_3	Digital sensor filter gain
K_{OL}	Gun servo subsystem gain
L_x	X actuator length
L_y	Y actuator length

L_{xo}	Centered x actuator length		
L_{yo}	Centered y actuator length		
M_p	Peak overshoot		
mrad	Milliradians		
MSE	Mean Squared Error		
R_p	Input to compensated servovalve-actuator-gun subsystem		
s	Laplace domain variable		
T	Sample time		
T_c	Computation time		
T_p	Peak overshoot time		
T_r	Rise time		
T_s	Settling time		
x	State variable; X actuator position		
\hat{x}	Estimated position; Estimated state		
x_s	Sensor output (X channel)		
x_M	Muzzle output (X channel)		
\dot{x}_c	GSS rate command		
\dot{x}_{cd}	Digital rate command		
y_s	Sensor output (Y channel)		
y_M	Muzzle output (Y channel)		
z	Discrete domain variable		
Z	Z transform operator		
θ	Elevation		
θ_c	Elevation command		
ω	Natural frequency		
ψ	Azimuth	ζ	Damping ratio
ψ_c	Azimuth command	Δ	$1 - C/T$

Abstract

The effects of changing control parameters of the movable M61 gun system proposed for the F-15 aircraft are examined using time response and root locus methods. In the course of the analysis, a Fortran IV simulation program, state space model, and gun servo subsystem Z transform are developed.

The gun servo subsystem design has little effect on system response. The system settled in under 0.2 sec and had less than 10% overshoot for any open loop gain from 0 to 200 sec^{-1} and with or without differential pressure compensation. *7/80*

The overall system is stable for a system gain of 0 to 39 and exhibits nearly deadbeat responses for a gain of 20. Digital rate feed-forward is required to keep ramp following error below 1 mrad for a $5^\circ/\text{sec}$ ramp. Digital filtering improves response and analog low-pass sensor filters with a cutoff of 30 Hz eliminate aliasing while moderately reducing system performance. Computation delays of less than 0.005 sec were found to have negligible effect on the system response.

The muzzle response is examined and a compensator, which neglects barrel cluster rotation, is designed to reduce the 50% overshoot and over 2 sec settling time for a step input. This, however, degraded tracking of more realistic (lower frequency content) inputs indicating that a better compensator should be designed or that muzzle response at target acquisition should be allowed to settle before firing.

Overall, the movable M61 was found to be an extremely fast gun system, insensitive to most control parameters. *✓*

ANALYSIS OF A CONTROLLER FOR THE M61 MOVABLE GUN

I Introduction

Historical Background

Since World War I, fighter aircraft have been armed with rapid firing guns to perform the close in air superiority role. Although it has been suggested that air superiority aircraft can function without a gun, experience has shown that the gun has a place on the highest technology aircraft (Ref 2:1). Gunsights have been improved dramatically since the use of cross hairs and the gun itself has been improved over the years. However, the same method of aiming the gun is still being used, i.e., point the aircraft.

Although this has proven effective in the past, increasing speed and maneuverability have put an extremely heavy burden on the pilot to track the target with his aircraft. If a means were available to relieve the pilot of a portion of this task and avoid the dynamic constraints of the aircraft, aircraft gunnery could be much more effective.

The movable gun concept was investigated by the RAND Corporation in 1968 (Ref 16). This study indicated that the movable gun greatly improved firing opportunities. In addition, the greatest performance increase occurred within the first few degrees of movement.

The movable gun concept was further explored in the EXPO series of air to air fire control studies performed by the McDonnell Aircraft Company (MCAIR). EXPO V not only confirmed the RAND findings, but

generated a preliminary hardware design for a movable M61 cannon for the F-15 aircraft.

System Definition

The movable M61 was designed by Delco Electronics Division to MCAIR specifications. The Gun-Servo Subsystem (GSS), consisting of the gun, hydraulic actuators and associated hardware and electronics, is shown in Figure 1. The gun servo subsystem includes a failure monitor which centers the gun if an error is detected in its response. This portion of the gun servo subsystem will not be included in any of the analysis.

The gun system is composed of the gun servo subsystem, portions of the F-15 mission computer (MC) and the connecting data bus.

Purpose

The purpose of this study is to examine the effects of varying control parameters of the gun servo subsystem as designed by Delco, examine digital components of the system, and examine time response of the muzzle. Delco dealt primarily with frequency domain responses in their reports; this study will focus on time domain effects.

At this time there have been no final descriptions of a digital controller algorithm appearing in Delco or MCAIR literature. This study will examine some of the aspects of the digital controller including open loop gain, digital rate feedforward and digital filtering of sensor outputs.

Finally, the effects of the gun structural modes on the muzzle response will be examined. The muzzle frequency response is given by

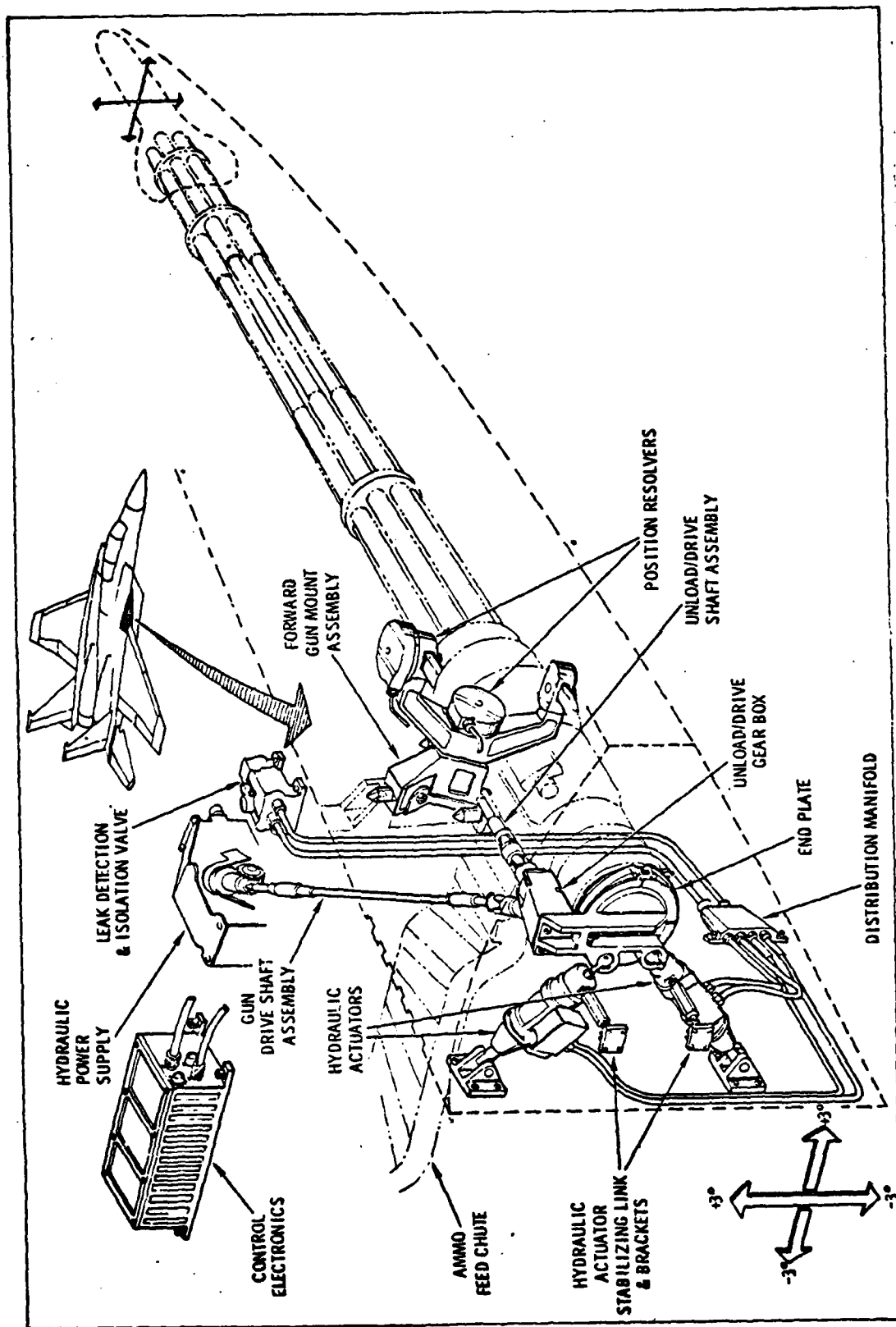


Fig. 1. M61 Movable Gun Servo Subsystem (Ref 4)

Delco reports but its time domain consequences are not discussed. A preliminary design for a compensator to reduce structural resonance will be discussed.

Assumptions

This thesis will make several simplifying assumptions regarding the gun dynamics and command inputs. These assumptions and their implications follow.

Gun Dynamics. The gun will be treated as a single body, neglecting barrel cluster rotation and projectile motion. The six barrel gun has a firing rate of 6000 rounds per minute, so gun firing occurs at 100 Hz and the barrels rotate at 16.7 revolutions per second. Gun firing will be an impulsive input along the gun axis, and therefore should have a negligible effect on the system response.

Since the barrel cluster rotation is a relatively low frequency effect (the first structural mode is at 11.6 Hz), it may cause some coupling of the gun dynamics in the azimuth and elevation axes. This effect will have its greatest impact on the structural mode analysis.

By neglecting nonlinear friction and treating structural damping in the gun as viscous damping, the system can be examined using linear models. The use of linear models greatly simplifies the analysis.

Command Inputs. It is assumed that rate and position commands for the gun azimuth and elevation are available within the mission computer. It is not the intent of this study to become involved with processes of target and projectile prediction or aircraft dynamics.

Performance Criteria

The Delco reports placed emphasis on frequency domain criteria for the gun servo subsystem. This thesis will deal almost exclusively with time domain analysis. Most of the specifications supplied by MCAIR are related to gun servo subsystem performance rather than to the gun system which contains the digital control loop. Time domain specifications must then be developed for the entire gun system based on the gun servo subsystem requirements and some engineering judgment.

The available performance specifications are listed in Table I. When a specification appears in more than one reference, the primary source is cited. When in disagreement, the most recent source is used.

Table I
Gun Servo Subsystem Specifications

Specification		Reference
Steady State Oscillation	$\leq 0.1\%$	14
GSS Overshoot	$< 20\%$	3
Bandwidth of GSS	100 Hz	5
Static Accuracy	.5 mrad	14
Rate Following Error (GSS)	≤ 1 mrad for $5^\circ/\text{sec}$	3
Angular Excursion	$\pm 3^\circ$	14
Angular Velocity	$\geq 45^\circ/\text{sec}$	14
Angular Acceleration	≥ 200 Rad/sec ²	5
80% of 100 Round burst in 8 mrad Dia Circle		15

The steady state oscillation and static accuracy are primarily related to hardware tolerance and sensor errors, so will not be used except in a short discussion of digital word length.

The GSS bandwidth, overshoot, and rate following error specifications will be addressed when discussing the Gun Servo Subsystem. The bandwidth of 100 Hz cannot be applied to the discrete system since the sampling rate is 20 Hz.

The GSS overshoot criterion seems to be high for the system overshoot based on the dispersion specification, so will not be used in system analysis. The rate following specification will be used, however.

The angular excursion, velocity, acceleration are functions of the hydraulics and actuators so are not used as control criteria, but as limits in the gun simulation.

From the dispersion specification, the maximum error which will place the target in the area of a probable hit is 4 mrad. Based on this, it would be desirable to keep the overshoot less than 4 mrad to maximize probability of a hit. For the maximum excursion of 52 mrad this is about 10%. Since the gun has a dispersion of 4 mrad, a 5% settling criterion (2.5 mrad at maximum excursion) is used rather than 2%. It would be desirable to have the gun settle as fast as possible but 0.2 seconds (20 rounds) seems reasonable.

The design criteria to be used for the system are then:

T_s (5%)	0.2 sec
M_p	$\leq 10\%$
Rate following error	$\leq 1.5\%$

Approach

The GSS and gun system will be analyzed using both analytical methods and a computer simulation. For the analytical portion of the analysis, the interactive computer aided design program TOTAL (Ref 10) was used. The simulation program (described in Appendix D) is a FORTRAN IV program executed on the CDC 6600/CYBER digital computer. The computer simulation includes some of the nonlinearities of the system and uses more complete gun dynamics.

II Technical Description of the Gun System

The basic gun system can be modeled as shown in Figure 2. This non-linear servo system is driven by azimuth and elevation commands internal to the F-15 mission computer. These commands are generated using outputs of the lead computation routines within the mission computer along with target tracking information from the APG-63 Radar. As a result of the limited data rates of these inputs and the computational burden of the mission computer, position commands are available at a 20 Hz rate.

A more detailed gun system model is shown in Figure 3. In the following sections, this model will be broken down and each of its components described.

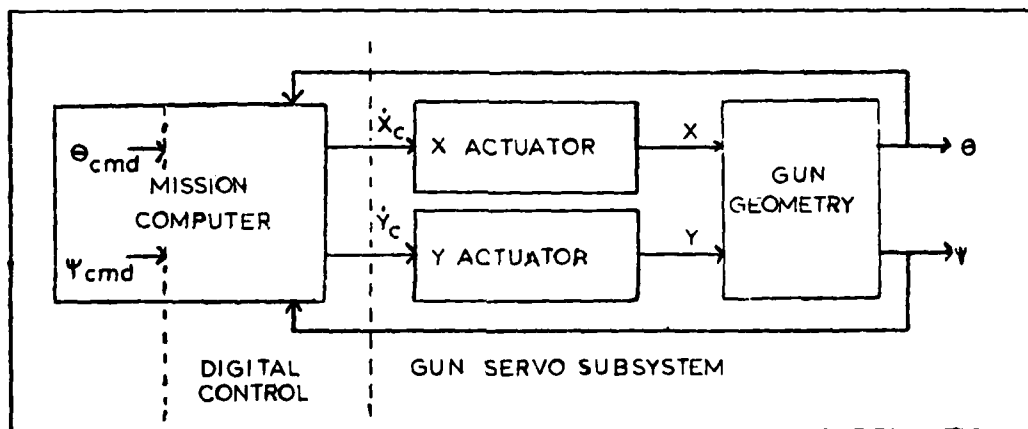


Figure 2. Basic Gun System Model.

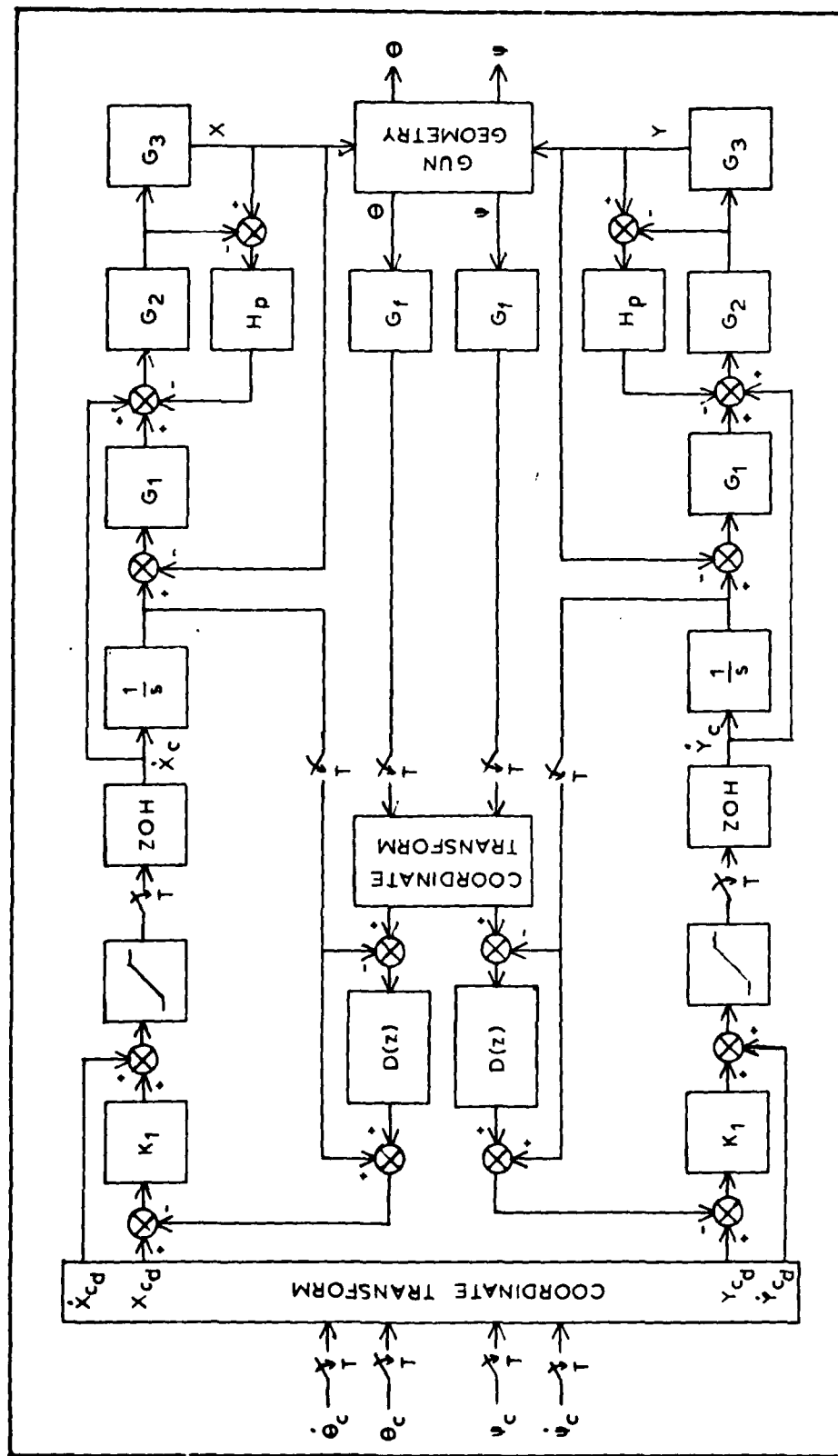


Figure 3. Gun System Model.

Gun Servo Subsystem

The gun servo subsystem contains two nearly orthogonal actuator channels. Each channel consists of the actuator, servovalve, sensors and the associated compensation networks. A model for each of the identical channels, including gun dynamics, is shown in Figure 4 (Ref 3).

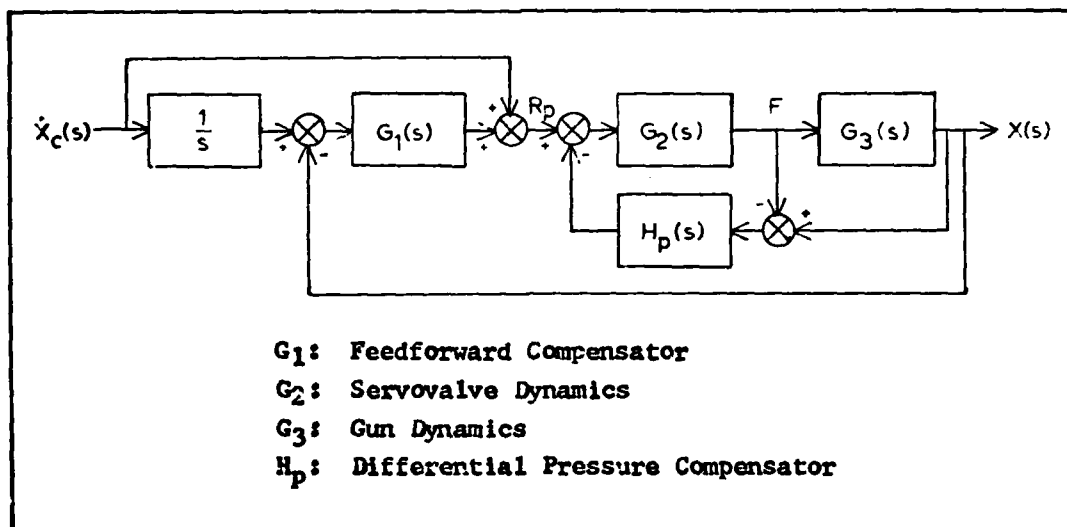


Figure 4. Gun Servo Subsystem Model.

Feedforward Compensation. The feedforward compensation, $G_1(s)$, is simply a gain in the current design.

$$G_1(s) = K_{OL} = 100 \text{ sec}^{-1} \quad (1)$$

Other compensators and gains will be discussed in chapter III.

Servovalve Dynamics. The servovalve dynamics relate electrical inputs to a force exerted on the actuator piston. A model of these dynamics is given by the manufacturer as

$$G_2(s) = \frac{A_v \omega_v^2}{s(s^2 + 2\zeta_v \omega_v s + \omega_v^2)} \quad (2)$$

where

$$A_v = 1$$

$$\zeta_v = .70$$

$$\omega_v = 200 \text{ Hz} = 1256 \text{ rad/sec}$$

Gun Dynamics. The gun dynamics represent the relationship between the actuator forces and the gun displacement. Because the gun is not a rigid body, a finite element analysis was performed by Delco to obtain the structural response of the gun and actuator body. The finite element program provided the parameters for use in an elaborate gun model described in Ref 13. The program also produced the frequency response of the gun sensor to an actuator input shown in Figure 5. This frequency response is used to generate a model for the gun dynamics.

Two sensors are being considered for the gun system. The first is a linear variable differential transformer (LVDT) which senses actuator length. The second is an angular resolver which measures gun angle at the pivot position. The gun has nearly identical frequency response at both of these sensor locations so the LVDT response can be used for both sensors.

Two sets of gun dynamics based on this frequency response were used in this gun system analysis. The first is a model used by Delco in their gun servo subsystem design and is used in the analytical analysis. The second is a more detailed model, using the first four structural modes, and is used in the computer simulation.

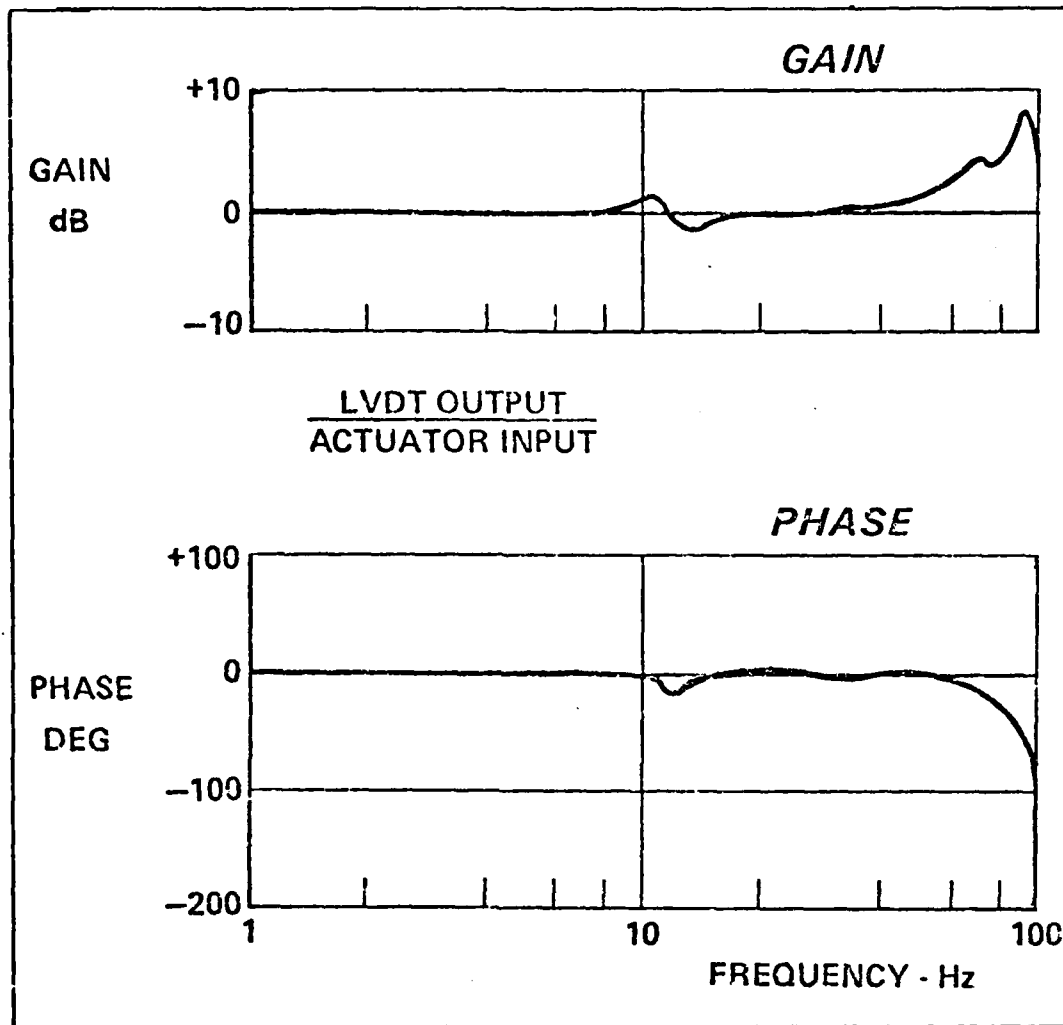


Figure 5. Sensor Frequency Response (Ref 5).

The gun dynamics used by Delco were obtained by fitting a fourth order transfer function to the response of Figure 4. This transfer function is

$$G_{3D}(s) = \frac{\omega_1^2 \omega_2^2}{\omega_z^2} \frac{(s^2 + 2\zeta \omega_z s + \omega_z^2)}{(s^2 + 2\zeta \omega_1 s + \omega_1^2)(s^2 + 2\zeta \omega_2 s + \omega_2^2)} \quad (3)$$

where

$$\omega_1 = 11.5 \text{ Hz} = 72.26 \text{ rad/sec}$$

$$\omega_2 = 95 \text{ Hz} = 596.9 \text{ rad/sec}$$

$$\omega_z = 12 \text{ Hz} = 75.4 \text{ rad/sec}$$

$$\zeta = .15$$

A more detailed gun model is obtained by treating the gun as a structurally damped beam. There are many ways of modeling structural damping. While viscous damping is one of the least accurate for a steel structure, it does allow the use of a linear model.

Equation (4) (derived in Appendix A) models the gun dynamics as a sum of "n" second order modes.

$$G_{3C}(s) = \frac{X(s)}{F(s)} = \sum_{i=1}^n \frac{A_i}{s^2 + 2\zeta\omega_i s + \omega_i^2} \quad (4)$$

where ω_i is the frequency of the i th mode, A_i is the output coefficient of the i th mode and ζ the gun damping ratio.

The first four natural modes ($n=4$) of the gun were used in the computer model. The frequencies of these modes are given as (Ref 5):

$$\omega_1 = 11.6 \text{ Hz} = 72.88 \text{ rad/sec}$$

$$\omega_2 = 34.9 \text{ Hz} = 219.7 \text{ rad/sec}$$

$$\omega_3 = 68.7 \text{ Hz} = 431.6 \text{ rad/sec}$$

$$\omega_4 = 83.5 \text{ Hz} = 524.6 \text{ rad/sec}$$

The output coefficients ($A_1 - A_4$) and damping ratio (ζ) are found in Appendix B using the gun frequency response. These coefficients

are:

$$\begin{aligned}A_1 &= 356.2 \\A_2 &= 0 \\A_3 &= 48170 \\A_4 &= 185600 \\f &= 0.05\end{aligned}$$

Differential Pressure Compensator. The differential pressure compensator was developed by Delco to provide damping of the 68 and 83 hertz gun structural modes. This compensator uses as its input the pressure differential across the actuator piston. This compensator is given by

$$H_p(s) = \frac{K_{hyd}}{A} G_4(s) \quad (5)$$

where K_{hyd} is the hydraulic spring constant and A is the piston area.

$$\begin{aligned}K_{hyd} &= 100,000 \text{ lb/in} \\A &= .9 \text{ in}^2\end{aligned}$$

$$G_4(s) = \frac{K_{\Delta p} (\tau_1)}{(\tau_1 s + 1)(\tau_2 s + 1)} \quad (6)$$

where

$$\begin{aligned}K_{\Delta p} &= 3.15 \times 10^{-3} \text{ in/sec/psi} \\1/\tau_1 &= 500 \\1/\tau_2 &= 2500\end{aligned}$$

Gun Geometry. The actuators are mounted on the rear of the M61 gun as shown in Figure 6. The transformation from actuator lengths to gun angles is given by (Ref 5)

$$\sin \theta = - \frac{L_x^2 - L_y^2}{4bd} \quad (7)$$

$$\sin \psi = \frac{1}{2b} [2L_x^2 L_y^2 + 2(2b)^2 L_y^2 + 2(2b)^2 L_x^2 - L_x^4 - L_y^4 - (2b)^4]^{\frac{1}{2}} - \frac{a}{d}$$

where θ is the elevation angle, ψ the azimuth angle, L_x and L_y the x and y actuator lengths, respectively, and

$$a = b = 10.25 \text{ in}$$

$$d = 24.1 \text{ in}$$

While these transformations are not exact, they have a maximum error of 0.002 mrad over the 3° excursion.

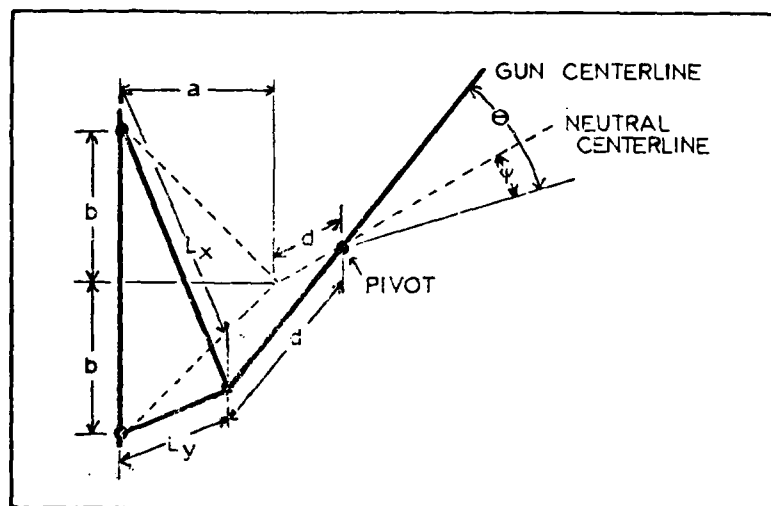


Figure 6. Gun Geometry

Interfaces to Mission Control Computer. The gun servo subsystem also includes interface elements to the mission computer. Those of interest in the control analysis are shown in Figure 7. The interface contains 10 bit analog to digital and digital to analog converters, a

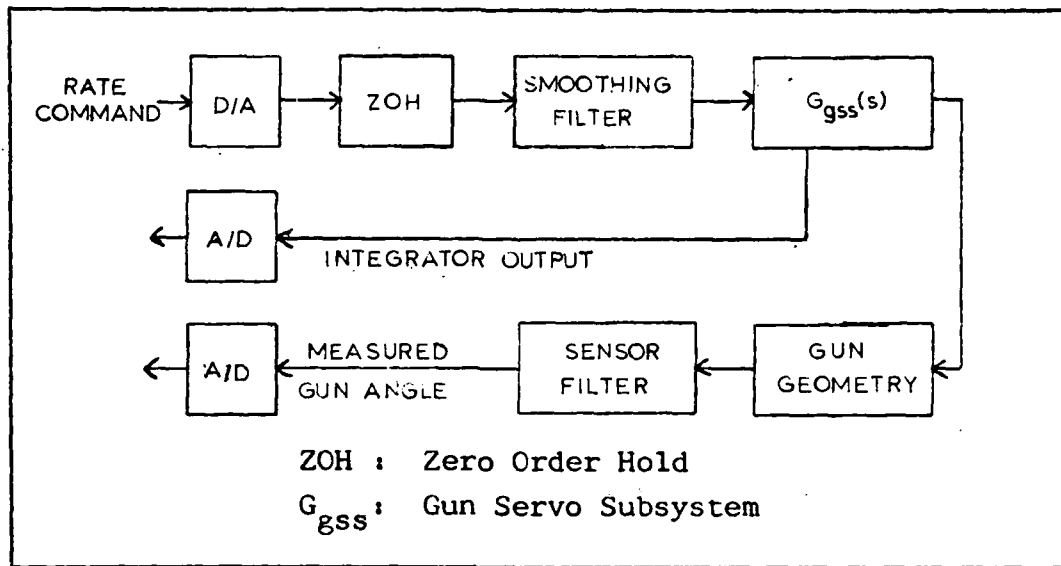


Figure 7. Gun System Interface.

zero order hold, and two low pass filters. One of these filters is used to smooth zero order hold output and the other is a filter for the sensor. The smoothing filter was not included in the simulation due to an oversight. However, some of the filter effect can be determined based on analysis of the sensor filter since the two are essentially in series. The integrator output is fed back to the mission computer for a digital filtering algorithm.

Digital Controller

The digital portion of the gun system was not well defined. Figure 3 contains a composite of the controllers described in References 5, 12, and 13. The location of the coordinate transformations is arbitrary; however, the specific transform used is dependent upon their location.

The system gain is given by K_1 . The digital rate feedforward is included in the system per Reference 12. This rate information could be generated inside the controller by differentiating the position input signal, but should be available from the tracker/predictor algorithm. The actuator commands are limited to ± 18 inches/sec corresponding to a $45^\circ/\text{sec}$ angular rate.

Coordinate Transformation

There are essentially two coordinate transformations employed in this version of the digital controller. The first is for the position commands and measurements. The actuator positions are given by

$$\begin{aligned} X &= L_x - L_{x0} \\ Y &= L_y - L_{y0} \end{aligned} \tag{8}$$

where L_{x0} and L_{y0} are the neutral position actuator lengths and L_x and L_y are the current lengths.

$$L_{x0} = L_{y0} = \sqrt{a^2 + b^2} \tag{9}$$

The actuator lengths are given by (Ref 5)

$$\begin{aligned} L_x &= [(\psi d + a)^2 + (\theta d - b)^2]^{\frac{1}{2}} \\ L_y &= [(\psi d + a)^2 + (\theta d + b)^2]^{\frac{1}{2}} \end{aligned} \tag{10}$$

where a , b , and d are as defined above. Note that this transformation uses the small angle approximations for the sine so is less accurate than the gun geometry transformation of Eq (7).

The second transformation is for the rate command. It is found by differentiating Eq (8). The result is

$$\begin{aligned}\dot{\hat{X}} &= \frac{d}{dx} [(d\psi + a)\dot{\psi} + (d\theta - b)\dot{\theta}] \\ \dot{\hat{Y}} &= \frac{d}{dy} [(d\psi + a)\dot{\psi} + (d\theta + b)\dot{\theta}]\end{aligned}\quad (11)$$

Digital Filter. The digital complementary filter containing $D(z)$ shown in Figure 3 is used for iterative correction of coordinate transformation errors (Ref 5). The continuous form of this complementary filter is shown in Figure 8.

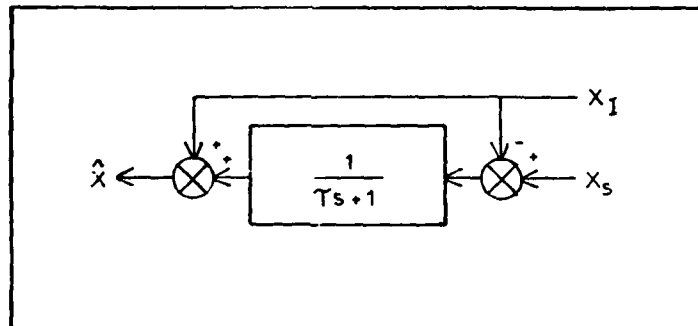


Figure 8. Continuous Complementary Filter

From the figure,

$$\hat{X}(s) = D(s) [X_S(s) - X_I(s)] + X_I(s) \quad (12)$$

where

$$D(s) = \frac{1}{Ts + 1}$$

which can be written as

$$\hat{X}(s) = \frac{1}{\tau s + 1} X_S(s) + \frac{\tau s}{\tau s + 1} X_I(s)$$

From this, it can be seen that the filter generates an estimate of the gun position by summing the low frequency components of the sensor measurements and the high frequency components of the integrator output. A discrete version of Eq (12) must be developed for implementation in the digital computer.

Since the inputs to the digital filter are discrete impulses, a zero order hold must be placed on the input to $D(s)$. Then

$$D'(s) = G_{ZOH}(s) D(s)$$

and

$$\hat{X}^*(s) = [D'(s)X_S^*(s) - D'(s)X_I^*(s)] + X_I(s) \quad (13)$$

where the star indicates a sampled input. Since the samplers lie between the continuous inputs and $D'(s)$, the inputs can be separated from $D'(s)$. The Z transform of Eq (13) is given by Eq (14).

$$\hat{X}(z) = Z[D'(s)] [X_S(z) - X_I(z)] + X_I(z) \quad (14)$$

Let

$$\begin{aligned} D'(z) &= Z[D'(s)] \\ &= Z\left[\frac{1-e^{-sT}}{s(\tau s + 1)}\right] \\ &= (1-z^{-1}) \frac{(1-e^{-T/\tau}) z^{-1}}{(1-z^{-1})(1-e^{-T/\tau} z^{-1})} \end{aligned}$$

Since z^{-1} is a delay operator, use of $D'(z)$ in the complementary filter will cause the current estimate of the actuator position to be

based on its past position. This delay is a result of including the zero order hold in $D'(s)$ to provide continuous inputs to $D(s)$. The filter will be implemented in the digital computer so it is possible to eliminate this delay by multiplying by z .

$$D(z) = z D'(z)$$

or

$$D(z) = \frac{1 - e^{-T/\tau}}{1 - e^{-T/\tau} z^{-1}} \quad (15)$$

$D(z)$ is not the Z transform of $D(s)$ but is its functional equivalent for use in the digital computer.

Letting $K_3 = 1 - e^{-T/\tau}$, the filter output is given by

$$\hat{X}(z) = \frac{K_3}{1 - (K_3 - 1) z^{-1}} [X_S(z) - X_I(z)] + X_I(z)$$

The difference equation for the filter is then

$$\hat{X}(k) = K_3 [X_S(k) - X_I(k)] + (1 - K_3) [\hat{X}(k-1) - X_I(k-1)] + X_I(k) \quad (16)$$

It is interesting to note that Eq(16) can be shown to be a constant gain optimal observer for the gun servo subsystem.

III Analysis of the Gun Servo Subsystem

The gun servo subsystem frequencies are all above half the sampling frequency. Due to Shannon's sampling theorem (Ref 8) these frequencies are misrepresented in the Z domain; the effect of these frequencies will appear to be at frequencies between 0 and 10 hertz for the 20 hertz sample rate. As a result, the gun servo subsystem analysis must be performed in the continuous time domain.

In analysis of the gun servo subsystem, the Delco design will be taken as a baseline and changes to this baseline will be examined. The baseline response of Figure 9 uses the given GSS with a K_{OL} of 100 and including the differential pressure compensation. The digital gain is 20 and the digital rate feedforward is included. No sensor filters are included in the baseline. Notice that the system azimuth and elevation commands are indicated by an asterisk.

In the following sections the effects of the differential pressure compensator, feedforward compensator, and rate feedforward will be examined. The analyses are based on S plane root locus methods and simulation results.

Differential Pressure Compensator

The differential pressure (ΔP) loop is intended to provide damping of the high frequency structural modes. This is important, for as Figure 5 shows, the 83 hertz structural mode is dominant at the sensor location.

The ΔP compensator is evaluated using the section of the gun servo subsystem shown by Figure 10. Using block diagram reduction, it can

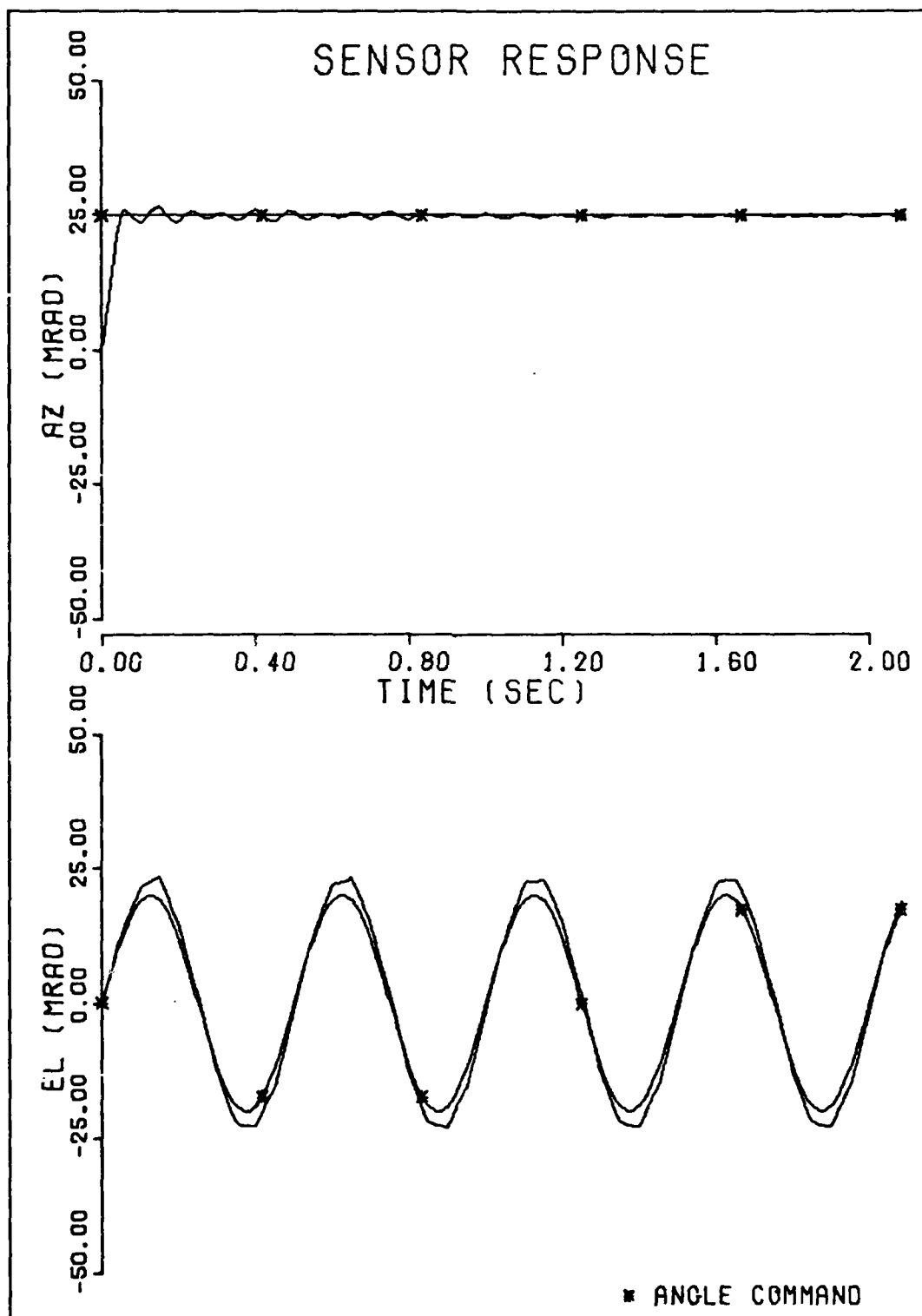


Figure 9. Baseline Gun System Response.

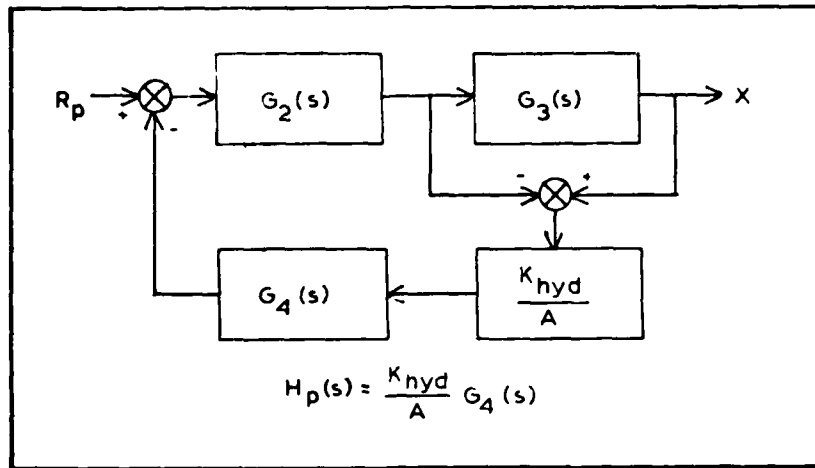


Figure 10. Differential Pressure Compensation Loop.

be shown

$$G_p(s) = \frac{X(s)}{R_p(s)} = \frac{G_2 G_3}{1 + (1-G_3) G_2 H_p} \quad (17)$$

Figure 11 shows the root locus of $(1-G_3) G_2 H_p = -1$. The primary effect of the compensator is to pull the high frequency structural poles to the left, increasing their damping. Also, the frequency of the servo-valve poles is reduced as they are moved to the right.

The $G_p(s)$ for a gain $(K_{\Delta P})$ of 3.15×10^{-3} is given below.

$$G_p(s) = \frac{5.17 \times 10^{11} (s^2 + 22.6s + 5690)(s + 500)(s + 2500)}{s(s^2 + 22.3s + 4940)(s^2 + 667s + 296000)(s^2 + 568s + 765000)(s + 1500)(s + 2210)} \quad (18)$$

The ΔP compensator has increased damping of the high frequency mode and slightly reduced the first mode frequency.

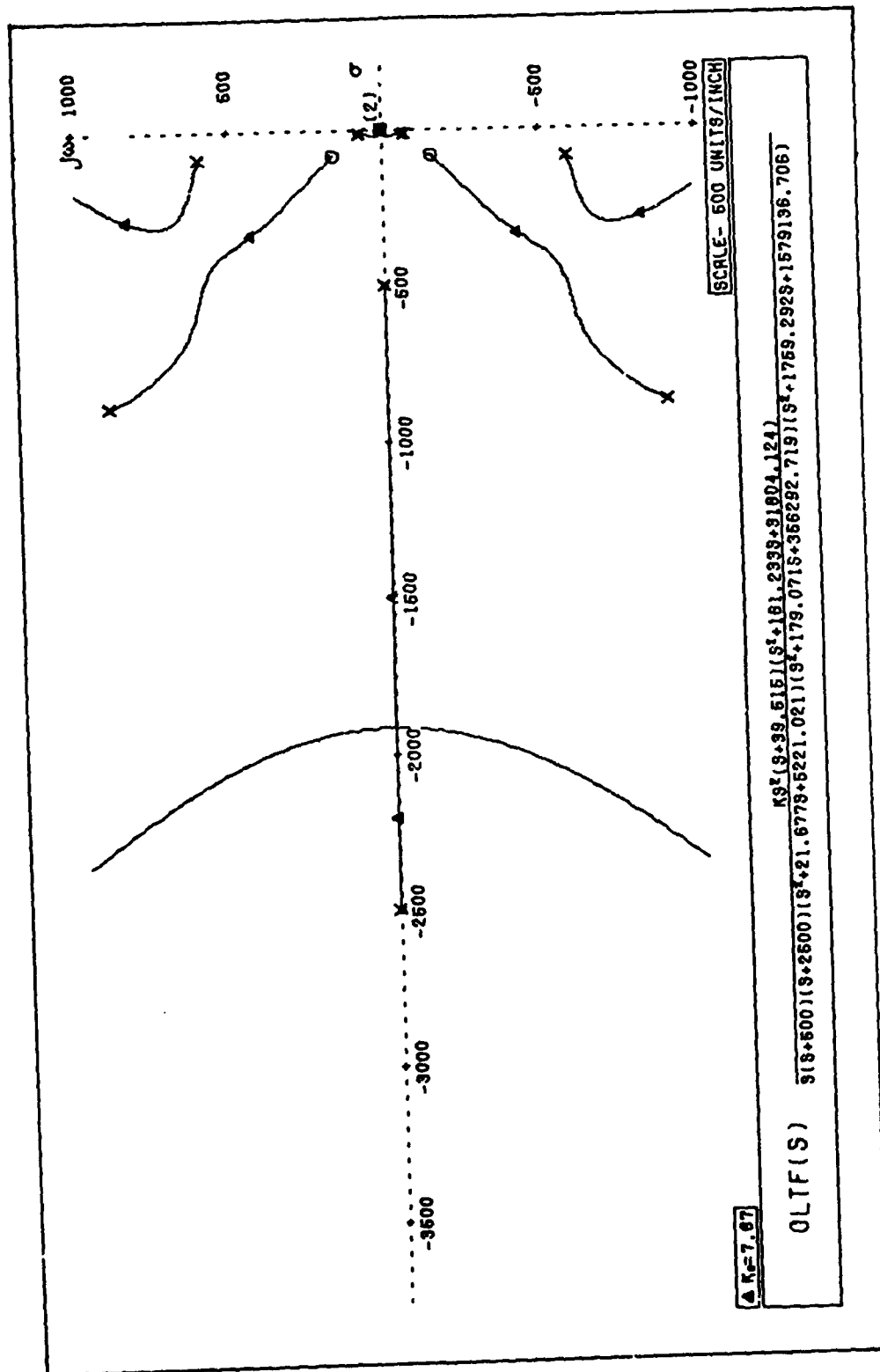


Figure 11. Differential Pressure Compensator Root Locus.

Figures 12a and b compare the time response of the gun and actuator with and without the compensator. Figures 12c and d make the same comparison for the system response. Table II gives rise time (T_r), settling time (T_s), peak time (T_p) and peak overshoot (M_p) for an impulse to $G_p(s)$ for both the two mode and four mode dynamics. Table III contains the same information for a step input command to the gun simulation.

Table II
Differential Pressure Compensator Gun Response*

Model	T_r	T_p	T_s	M_p
Without ΔP				
2 Mode	0.00206	0.00533	0.131	1.50
4 Mode	0.00223	0.00628	0.308	1.71
With ΔP				
2 Mode	0.00246	0.00617	0.149	1.23
4 Mode	0.00260	0.00720	0.405	1.38

*unit step input

Table III
Differential Pressure Compensator System Response*

	T_r	T_p	T_s	M_p
With ΔP	0.05	0.054	0.158	26.99
Without ΔP	0.05	0.054	0.108	26.73

*25 mrad step input

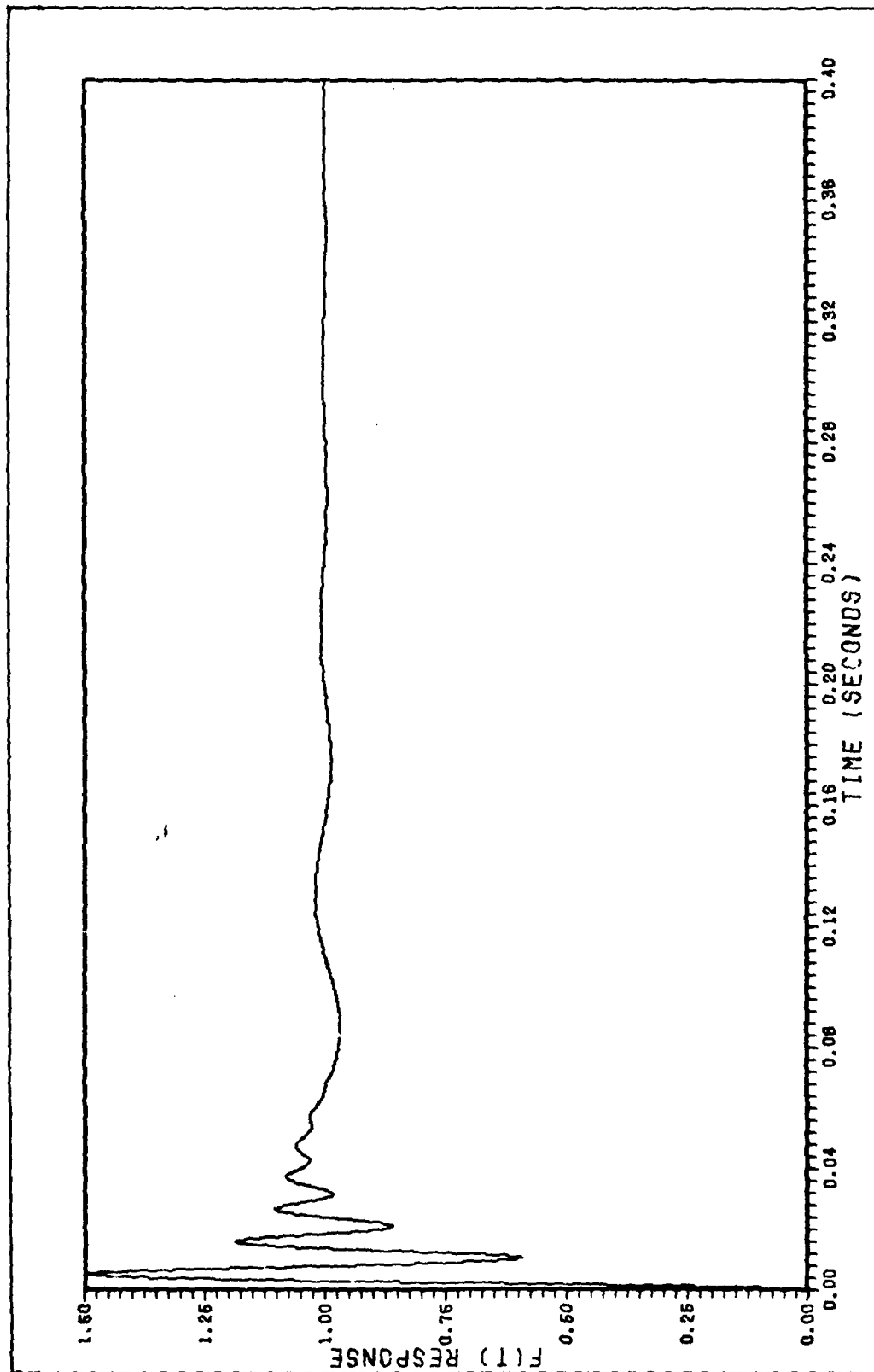
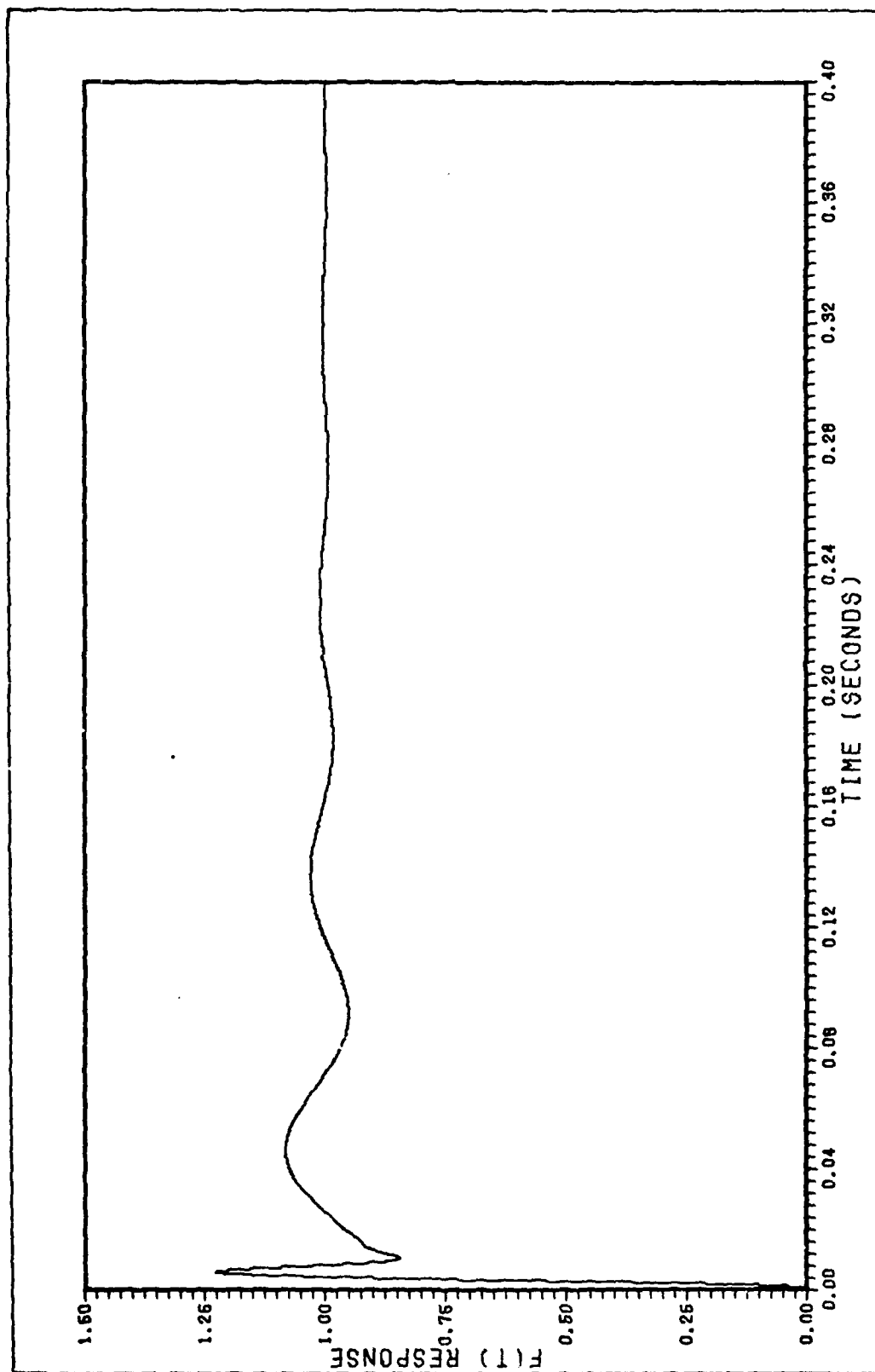
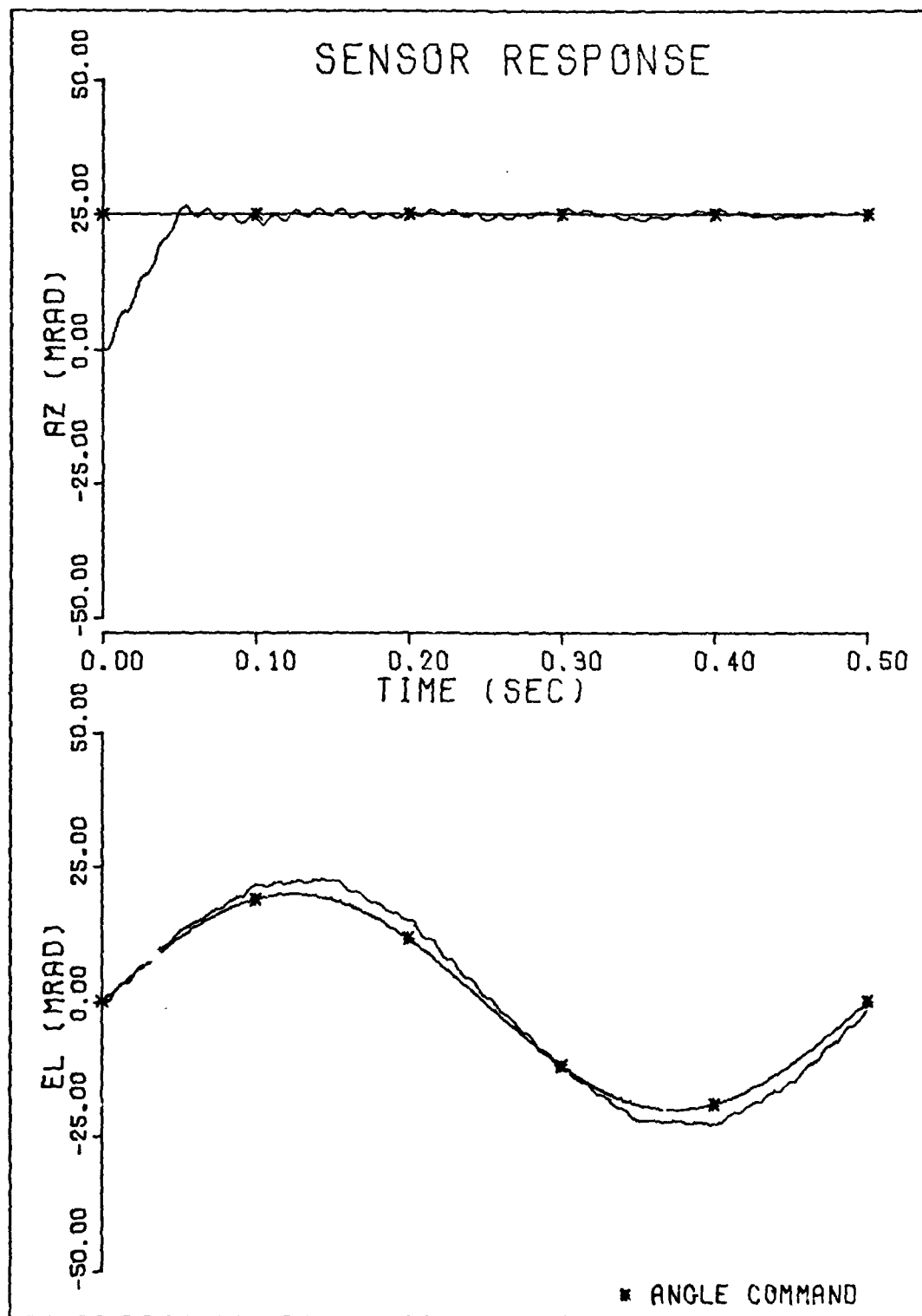


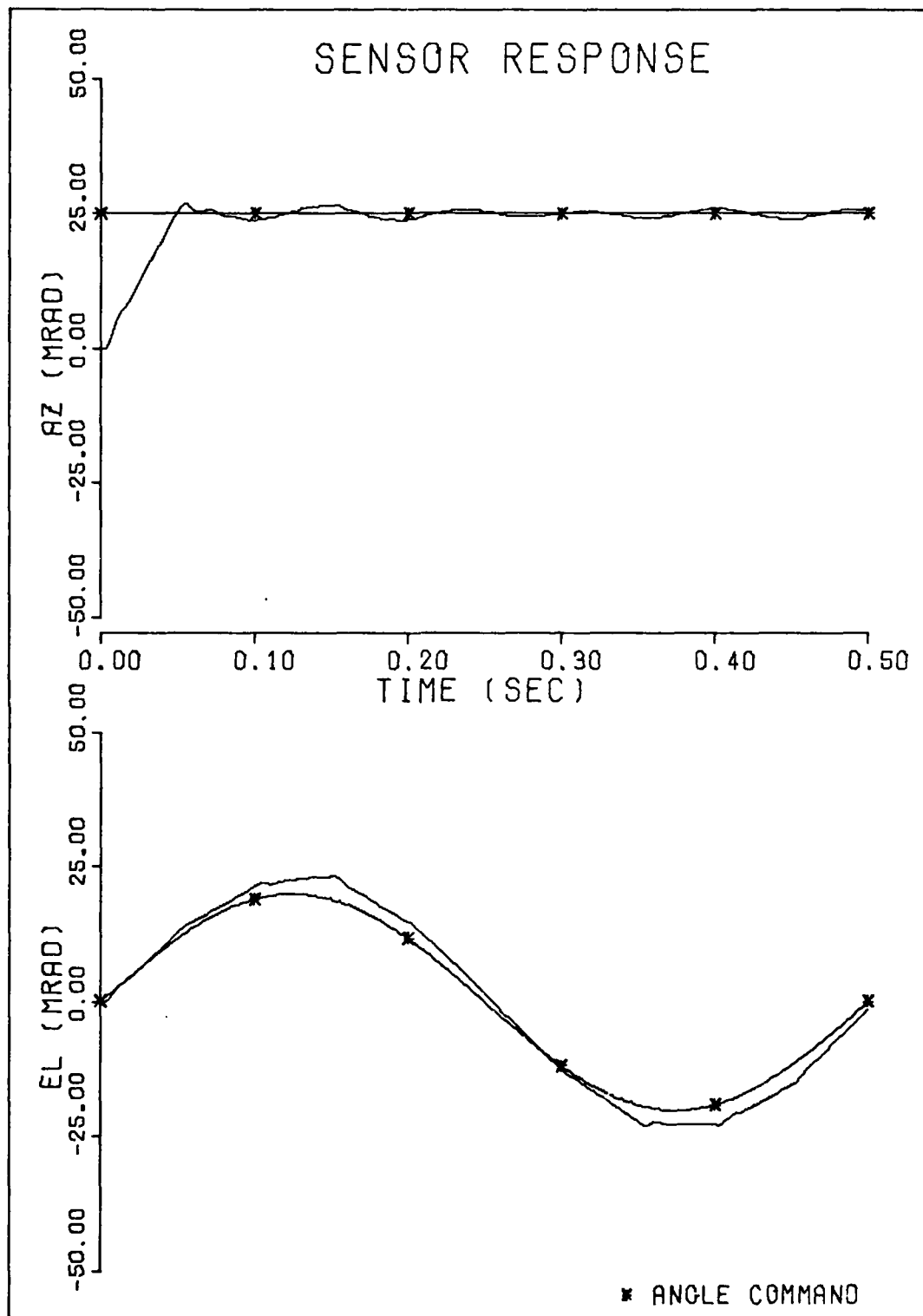
Figure 12. Differential Pressure Loop Time Responses.
a. Sensor Response with no Compensator.



b. Sensor Response with Compensator.



c. System Response with no Compensator.



d. System Response with Compensator.

Although it appears from Table III that response has been degraded with the compensator, this is due to the simulation using no sensor filters for this portion of testing. Figures 12a, b, c and d demonstrate that the high frequency oscillations are effectively damped.

Feedforward Compensator

The feedforward compensator is an optional compensator to provide additional low frequency gain and structural damping if ground firing tests indicate they are necessary (Ref 3). In the present design, however, $G_1(s)$ is simply a gain, K_{OL} .

Using the $G_p(s)$ obtained in the previous section, one gun servo subsystem channel can be represented by Figure 13(a). Figure 13(b) shows the system after block diagram manipulation. The closed loop transfer function is therefore given by

$$G_{gss}(s) = \frac{X(s)}{\hat{X}_c(s)} = \frac{(s + G_1)G_p}{s(1 + G_1G_p)} \quad (19)$$

It is interesting to note that if $G_p(s)$ is taken to be $\frac{1}{s}$ (i.e., neglect structural and valve dynamics), then $G_{gss}(s)$ is given by

$$\frac{1}{s} \left(\frac{s + G_1}{s + G_1} \right)$$

so $G_1(s)$ has no effect on the rigid body dynamics.

Returning to the true $G_p(s)$ and letting $G_1(s) = K_{OL}$, then

$$G_{gss}(s) = \frac{(s + K_{OL}) G_p}{s(1 + K_{OL} G_p)} \quad (20)$$

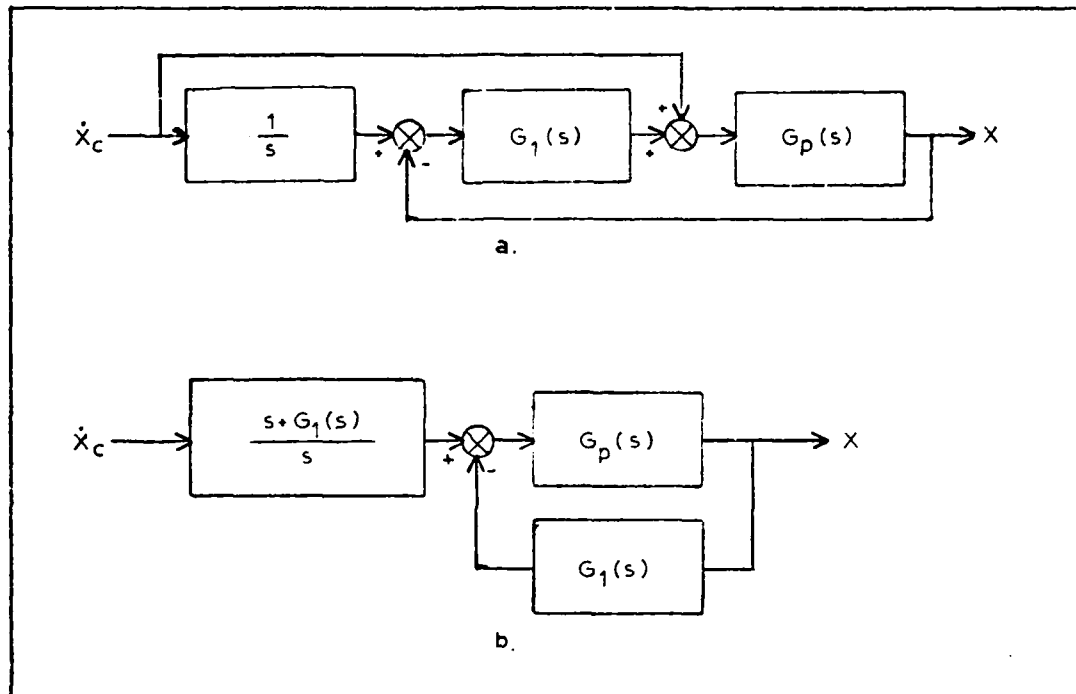


Figure 13. Gun Servo Subsystem Reduction.

The root locus of $K_{OL} G_p = -1$ is given by Figure 14. As the gain is increased, the dominant poles are no longer associated with the high frequency structural mode but become associated with the servovalve. The limit on gain for stability is $K_{OL} = 390$. Table IV gives the steady state tracking error of the system for a ramp input. Different values of open loop gain and rate feed forward (RFF) are presented. Table V gives the simulation time response figures of merit for various open loop gains.

The settling time is very sensitive to small changes in the high frequency components of the gun response since no sensor filters are employed. Realizing this, Tables IV and V indicate that the open loop gain, K_{OL} , has very little effect on the system response.

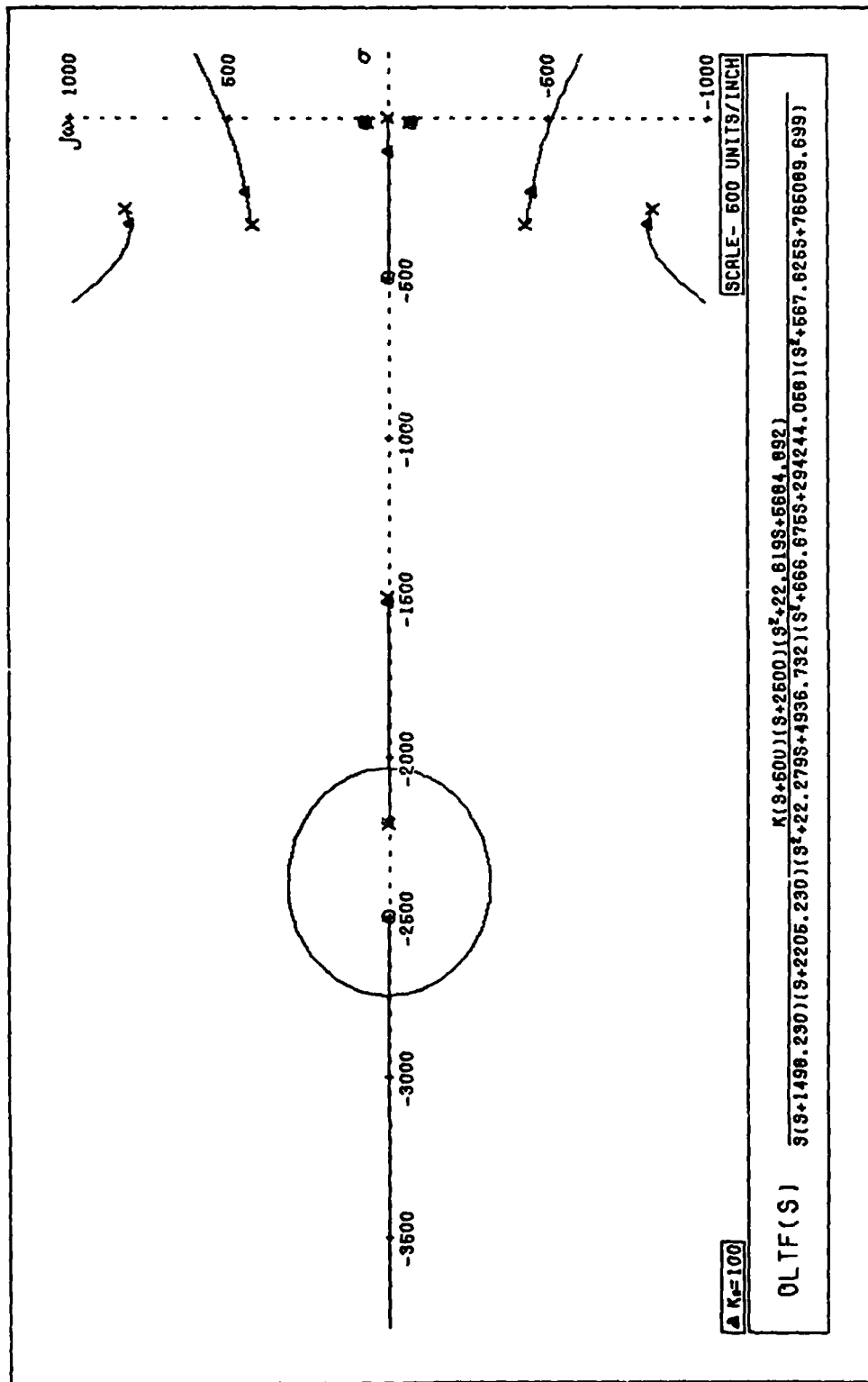


Figure 14. Gun Servo Subsystem Root Locus.

Table IV
Gun Servo Subsystem Ramp Errors

K_{OL}	With RFF	% Error	No RFF
0	0.23		∞
10	0		10
100	0		1
200	0		0.05

Table V
Effect of K_{OL} on Gun System Performance*

K_{OL}	T_r	T_p	T_s	M_p
0	0.052	0.074	0.208	26.77
10	0.052	0.072	0.306	26.84
100	0.050	0.054	0.158	26.99
200	0.052	0.056	0.058	26.56

*25 mrad step input

The closed loop transfer function for the gun servo subsystem with $K_{OL} = 100$ is

$$\frac{5.17 \times 10^{11}(s^2+22.6s + 5690)(s+500)(s+2500)(s+100)}{(s^2+17.78s+5390)(s^2+460s+255,000)(s^2+166s+1,320,000)(s+104)(s+1513)(s+2200)}$$

(21)

Effect of Rate Commands and Rate Feedforward

The reason for rate command inputs to the gun servo subsystem is shown by Figure 15. This figure shows the response of the gun servo subsystem without the integrator ($G'_{gss}(s) = s G_{gss}(s)$) to a step input. Although the overshoot would not be quite so high in the actual system due to rate and acceleration limits, it is still an undesirable feature. The large overshoot of the gun servo subsystem is reduced by giving ramp position commands consisting of integrated step rate commands from the digital computer.

The effect of feeding this rate command into the actuator input is demonstrated by Tables IV and VI. Table IV shows that the steady state ramp following error of the gun servo subsystem is zero when rate feedforward is used. Table VI indicates that the rate feedforward improves the gun transient response.

Table VI
Effect of Rate Feedforward on Gun Response*

	T_r	T_p	T_s	M_p
Without RFF	0.066	0.108	0.168	28.6
With RFF	0.05	0.148	0.158	26.7

*25 mrad step input

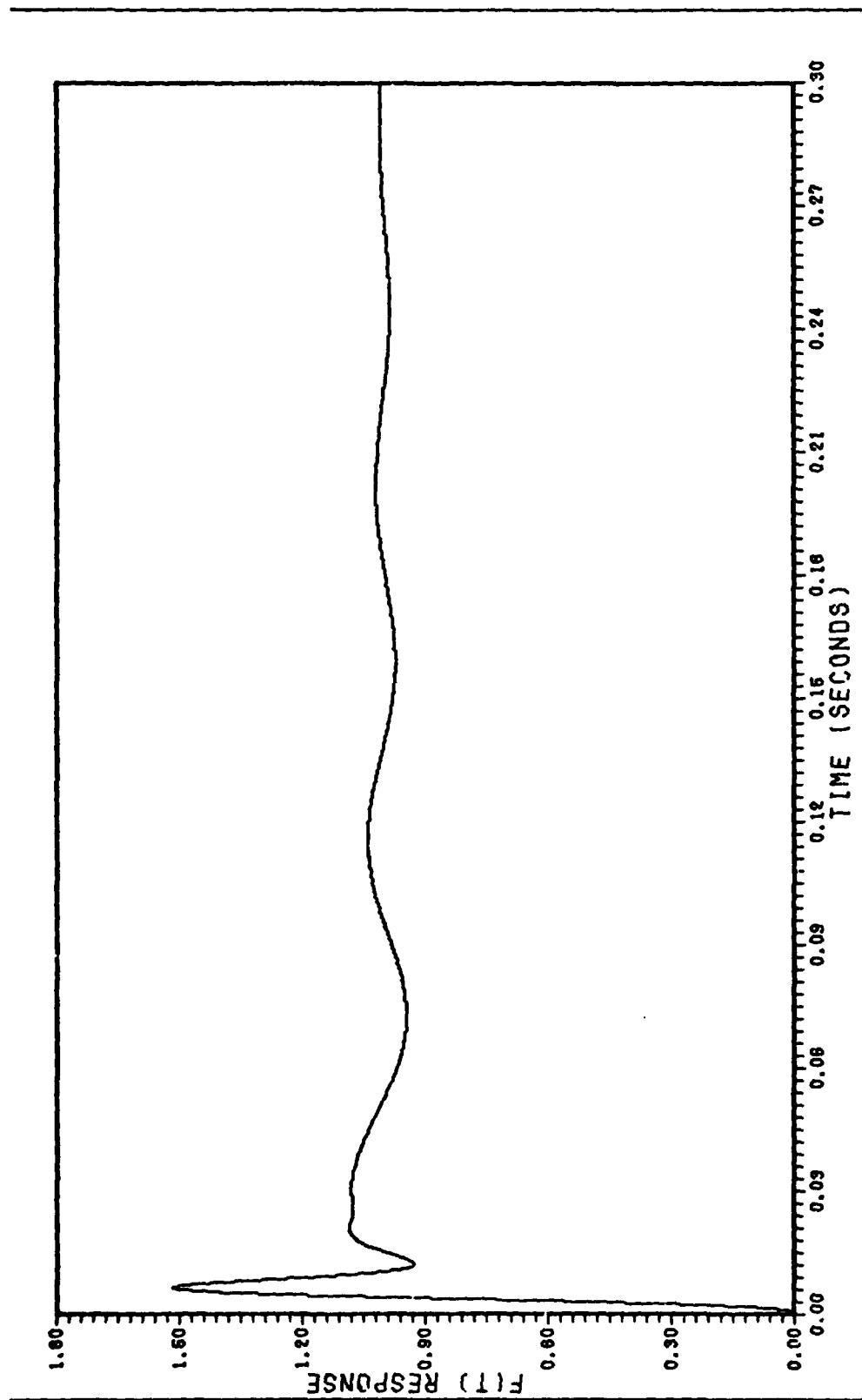


Figure 15. Gun Servo Subsystem Response Using Position Inputs.

IV Analysis of Digital Portion of Gun System

The gun servo subsystem discussed in the last section receives rate commands from the mission computer. This section will discuss the means of generating these commands. The effects of various elements of the digital portion of the gun system and interface elements will be evaluated using Z domain root locus methods and the digital simulation. For the analytical portion of the analysis, one channel of the gun system is modeled as shown in Figure 16a.

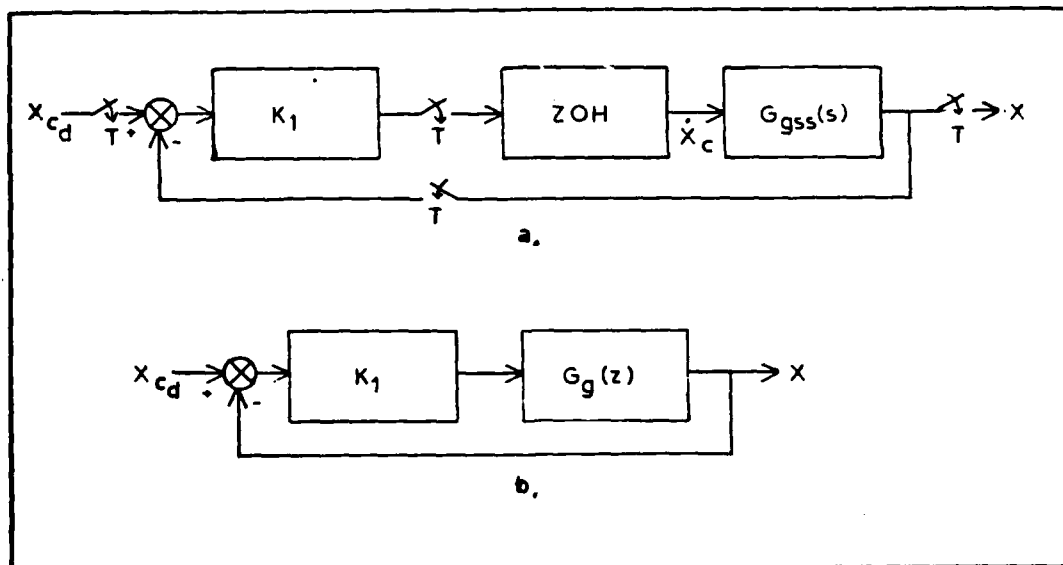


Figure 16. Discrete Gun System Model.

System Gain

The effect of the system gain K_1 on system response was examined using a discrete root locus. The Z transforms were found using the impulse invariance transformation function of the design program TOTAL.

The program uses an algorithm which first obtains the partial fraction expansion of $F(s)$, then finds

$$F(z) = \sum_{k=1}^n \frac{A_k z}{z - e^{-s_k T}} \quad (22)$$

where s_k is the s domain pole and A_k is its associated partial fraction coefficient.

Z Transform of Gun Servo Subsystem. The gun servo subsystem including the zero order hold is given by

$$G_g(s) = G_{ZOH}(s) G_{gss}(s)$$

where

$$G_{ZOH}(s) = \frac{1 - e^{-sT}}{s} \quad (23)$$

and T is the sample time of 0.05 seconds.

The discrete system can then be modeled by Figure 16b where

$$\begin{aligned} G_g(z) &= Z [G_{ZOH}(s) G_{gss}(s)] \\ &= Z \left[\frac{1 - e^{-sT}}{s} G_{gss}(s) \right] \end{aligned}$$

but since $z = e^{sT}$

$$G_g(z) = (1 - z^{-1}) Z \left[\frac{1}{s} G_{gss}(s) \right] \quad (24)$$

The s transform of $\frac{1}{s} G_{gss}(s)$ cannot be found directly using TOTAL since the algorithm of Eq (22) cannot handle repeated poles. The $\frac{1}{s^2}$

term which is formed by the zero order hold and integrator poles is expanded out as shown below.

$$\begin{aligned} \frac{1}{s} G_{gss}(s) &= \frac{1}{s^2} \frac{(s + K_{OL}) G_p(s)}{(1 + G_p(s) K_{OL})} \\ &= \frac{A}{s^2} + \frac{N(s)}{s(1 + G_p(s) K_{OL})} \end{aligned} \quad (24)$$

where

$$A = \frac{(s + K_{OL}) G_p(s)}{1 + G_p(s) K_{OL}} \bigg|_{s=0} \approx 1$$

Substituting $A = 1$ in Eq (24) and solving for $N(s)$,

$$N(s) = (s G_p(s) - 1)/s$$

Thus

$$\begin{aligned} G_g(z) &= \frac{z-1}{z} Z \left[\frac{1}{s^2} + \frac{s G_p(s) - 1}{s^2 (1 + G_p(s) K_{OL})} \right] \\ &= \frac{z-1}{z} \left[\frac{Tz}{(z-1)^2} + Z \left(\frac{s G_p(s) - 1}{s^2 (1 + G_p(s) K_{OL})} \right) \right] \end{aligned} \quad (25)$$

The Z transform of $[s G_p(s) - 1] / (1 + G_p(s) K_{OL})$ was found using TOTAL. However, numerical problems were encountered due to the extremely small poles of $G_g(z)$. This problem was overcome by a short program using the DMSL subroutine ZPOLR (Ref 9) to find the roots of the complete system. The discrete gun servo subsystem is given by Eq (26).

$$G_g(z) = \frac{0.0509 (z^2 + 1.11z + 0.416)(z^2 - 1.53 \times 10^{-8} z + 7.65 \times 10^{-16})}{(z + 0.0217)(z - 0.00713)(z + 1.92 \times 10^{-8})} \cdot \frac{(z - 1.43 \times 10^{-33})(z - 1.37 \times 10^{-48})}{(z^2 + 1.17z + .445)(z^2 + 1.77 \times 10^{-5}z + 1.01 \times 10^{-10})} \quad (26)$$

$$(z^2 + 1.25 \times 10^{-7} z + 4.09 \times 10^{-15}) (z - .00544)$$

$$(z - 1.43 \times 10^{-33})(z - 1.37 \times 10^{-48})(z - 1)$$

Since $z = 0$ corresponds to $s = -\infty$, most of the terms in Eq (26) are negligible so

$$G(z) \approx \frac{.05(z^2 + 1.11z + 0.416)(z + 0.0217)(z - 0.00713)(z + 1.92 \times 10^{-8})}{(z-1)(z^2 + 1.17z + 0.445)(z^2 + 1.77 \times 10^{-5} + 1.01 \times 10^{-10})(z-0.00544)} \quad (27)$$

The discrete root locus for the gun servo subsystem is shown in Figure 17. The maximum gain for stability ($\|z\| < 1$) is 36. For a gain of 20, the closed loop transfer function is given by

$$\frac{X(z)}{X_c(z)} = \frac{(z-0.00713)(z+0.0217)(z^2 + 1.11z + 0.416)(z + 1.92 \times 10^{-8})}{(z^2 + 0.0458z + 0.0183)(z^2 + 1.24z + 0.460)(z + 1.54 \times 10^{-8})(z-0.00777)} \quad (28)$$

The response of this model is compared against the results of the simulation in Table VII.

Table VIII gives the dominant pole locations for several values of gain. Notice that the first mode poles are still essentially cancelled by the zeros at $-0.55 \pm j 0.33$ so have little effect. The time response corresponding to these system poles can be determined by referring to Appendix E.

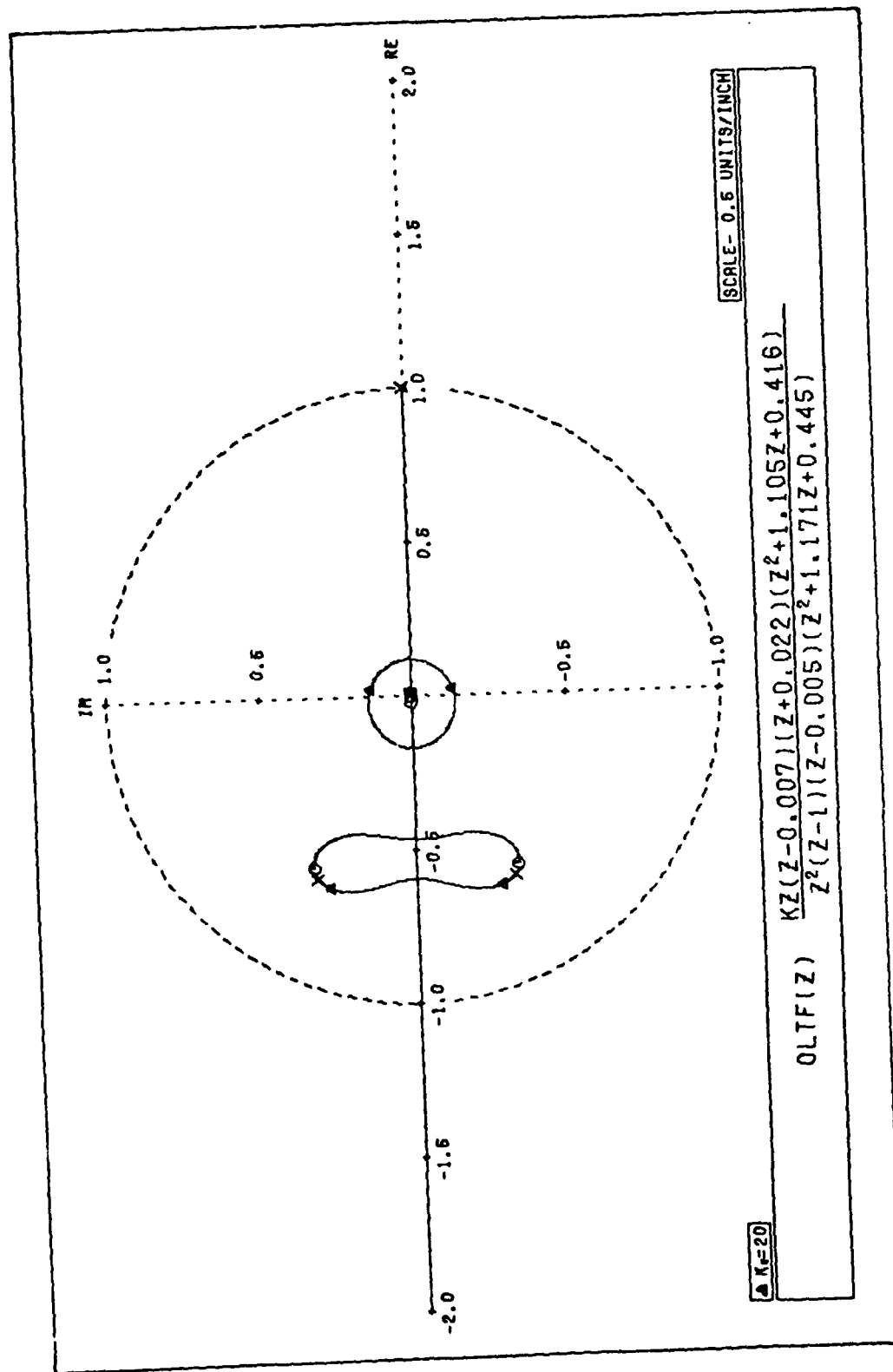


Figure 17. Discrete Gun System Root Locus

Table VII
Comparison of Analytical and Simulation Response*
($K_1 = 20$)

k	$\theta(k)$ (mrad)	
	Simulation	Analytical
0	0	0
1	25.4	25.4
2	23.8	23.8
3	26.5	26.2
4	23.9	24.2
5	25.4	25.4

*25 mrad step input

Table VIII
Poles of Closed Loop Gun System as a Function of Gain

K_1	Dominant Poles	
10	0.49	$-0.60 \pm j 0.31$
12.5	0.36	$-0.60 \pm j 0.31$
15	0.21	$-0.61 \pm j 0.30$
17.5	$0.080 \pm j 0.096$	$-0.61 \pm j 0.29$
20	$0.022 \pm j 0.13$	$-0.62 \pm j 0.28$
22.5	$-0.036 \pm j 0.14$	$-0.62 \pm j 0.26$

Additional insight into the effect of K_1 is obtained by completely neglecting the gun servo subsystem dynamics. The Z transform of the gun servo subsystem is then simply $\frac{0.05}{z-1}$. The root locus is then a line to the left from $z = 1$ crossing $z = 0$ at $K_1 = 20$ and $z = -1$ at $K_1 = 40$. This would indicate instability at a gain of 40 and a deadbeat response for a gain of 20. The simulation indicates instability at a gain of 39, so in this respect the simple model is better than the more complex model of Eq (27). This is probably due to numerical errors in finding $G_g(z)$ and deletion of the small roots.

Digital Rate Feedforward

This section will discuss the need for digital rate feedforward in the mission computer. Figure 18 shows the response of the system with a gain of 20 to a ramp input without rate feedforward. The gun output lags the command input by the sample time (0.05 seconds).

There are two methods of dealing with this problem. The first is to give the gun position commands which are one sample period in advance; however, this places an additional burden on the target prediction algorithms. The other alternative is to use the digital rate feedforward as discussed in section II.

Use of the rate feedforward reduces ramp following errors from 5% to zero.

Sensor Filters

Up to this point, none of the simulations have used a filter on the sensor. Although the system works well without a filter, the system performance can be improved through their use.

Analog Sensor Filter. As a result of Shannon's sampling theorem (Ref 8), any sampled input having a frequency greater than one half the sampling frequency (f_s) will appear to have a different frequency. In fact, it will have a frequency between 0 and $f_s/2$. This effect is called aliasing and in the case of the gun system, increases the settling time by causing low frequency ($< f_s/2$) oscillations.

To prevent this, a low pass filter can be placed on the input to the mission computer. Reference 3 suggests a first order lag filter with a 10 Hz cutoff. When such a filter is used, the system overshoot

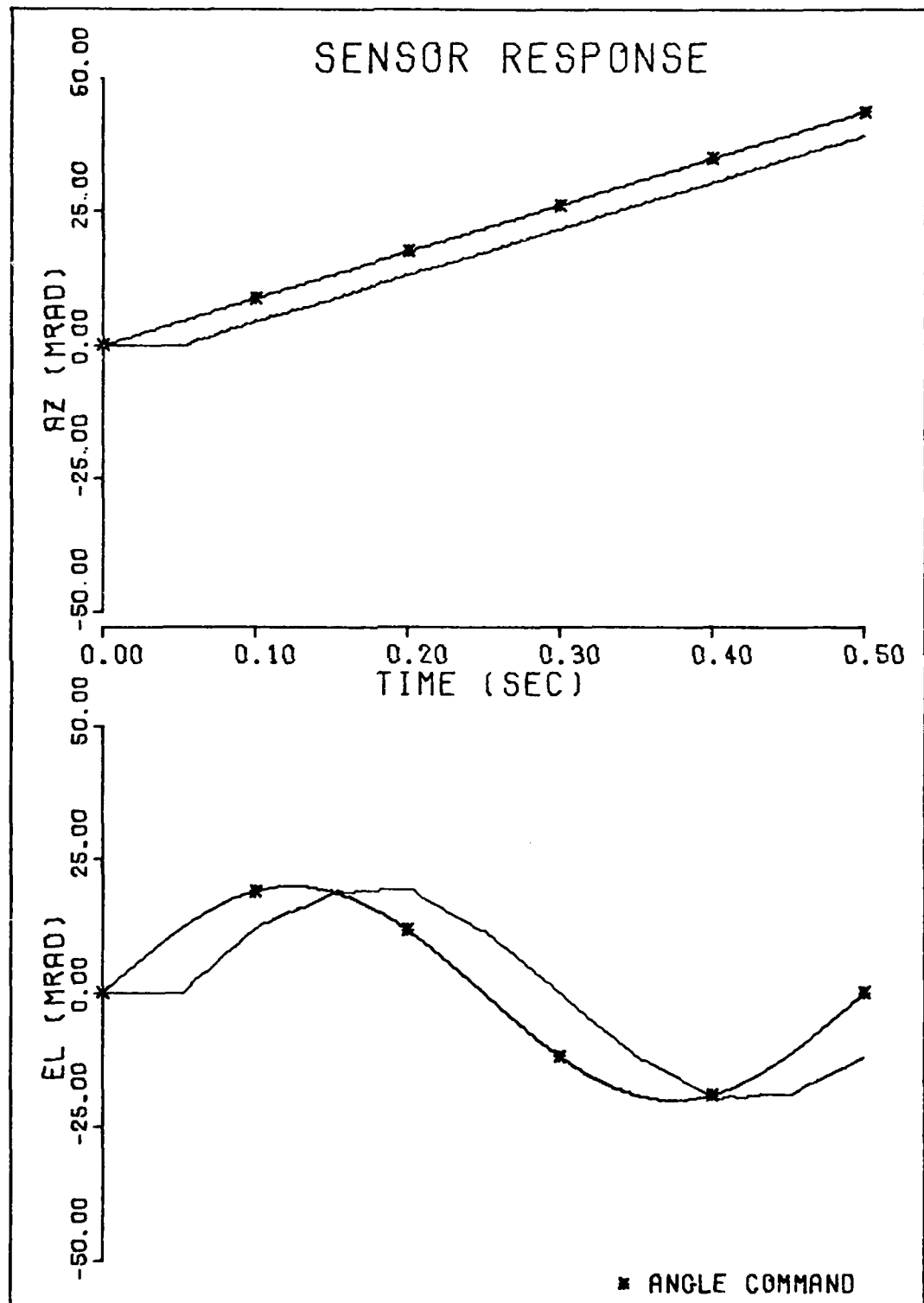


Figure 18. Response of Gun System with No Digital Rate Feedforward.

and settling time is increased as shown in Figure 19. This degradation of performance is due to decreasing the bandwidth of the system.

The output of the sensor filter with a cutoff of 10 Hz is down 3.7 dB at 11.6 Hz, thus the first mode is not attenuated much more than the desired 10 Hz signal which is down 3 dB. Fortunately, the sensor does not sense much of the first or second modes so the sensor filter cutoff frequency can be increased. As shown in Table IX, a sensor filter of 30 Hz provides better performance than the 10 Hz filter.

Table IX
Effect of Sensor Filters on System Response*

Cutoff Frequency	T_r	T_p	T_s	M_p
None	0.05	0.054	0.158	26.49
10 Hz	0.05	0.104	0.268	32.32
30 Hz	0.05	0.136	0.156	27.06

*25 mrad step input

The information in Table IX indicates that either sensor filter cutoff frequency increases the peak overshoot. This is because the servo bandwidth is reduced from 100 Hz to the sensor cutoff frequency. A smoothing filter on the output of the zero order hold will have the same effect, thus its cutoff frequency should also be somewhat greater than the 10 Hz suggested by Reference 3.

Digital Sensor Filter. The outputs of the analog sensor filter are inputs to the digital filtering algorithm. This algorithm estimates the position of the gun based on the measurement and the integrator output which provides rigid body response.

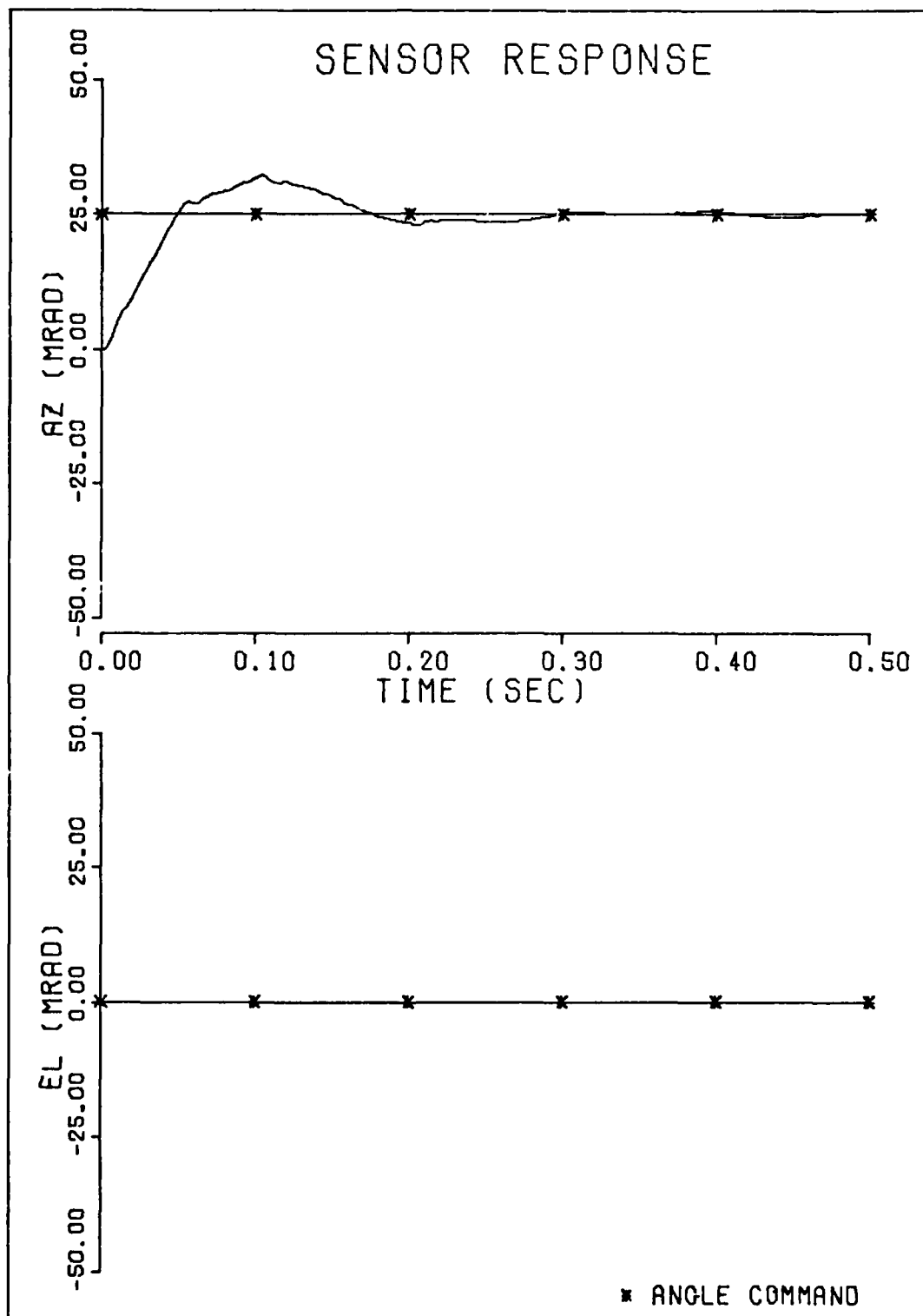


Figure 19. Effect of 10 Hz Sensor Filter on System Response.

The difference equation for the digital filter (Eq (16)) was employed in the simulation program. Table X compares the system performance for different filter gains. For a gain (K_3) of 0 the filter completely ignores measured outputs. With a gain of 1, the measured outputs are used directly.

Table X
Effect of Digital Filter Gains on System Response*
(4% settling criteria)

K_3	T_r	T_p	T_s	M_p
0	0.05	0.054	0.058	26.99
0.5	0.05	0.054	0.100	26.99
1	0.05	0.054	0.454	26.99

*25 mrad step input

A 4% settling criterion was used since a 5% criterion indicated no difference in the system performance for different gains. This would indicate that the errors caused by aliasing are less than 5%. Although the best response is obtained for $K_3 = 0$, this gain could not be used in the actual system since the system would be running open loop. The best gain for use in the system must be selected based on noise, and system error considerations.

Computation Time

When implemented on the mission computer, output measurements and control inputs corresponding to a given sample period are separated by some finite time delay. This computation time (T_c) is used for analog to digital and digital to analog conversions as well as time to perform digital computations.

When this time delay is included in the system, the single channel model is given by Figure 20a, where C is the computation time. A delay in the computer output is the same as a delay in the system output so the system can also be given by Figure 20b.

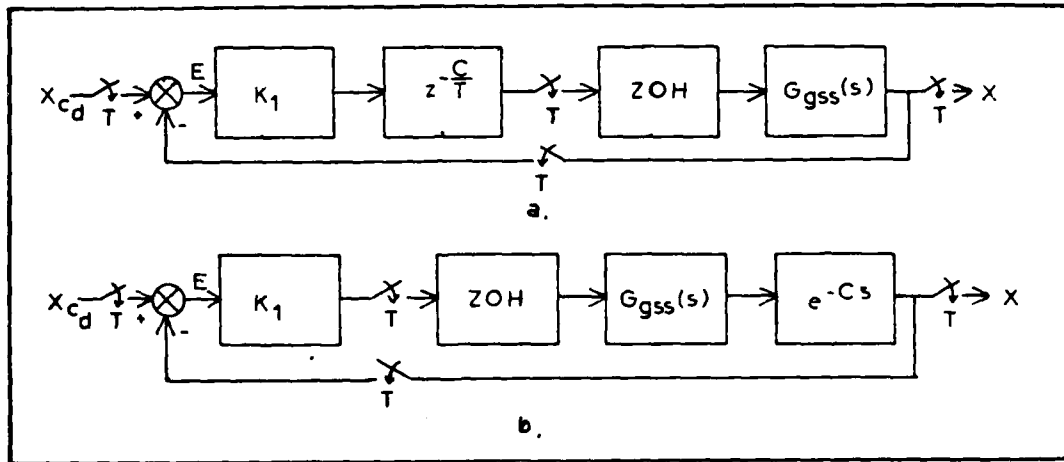


Figure 20. Gun System Model Including Computational Delay.

If $G_{gss}(s)$ is allowed to be $1/s$ (ignoring complex dynamics), then

$$\begin{aligned}
 G_g(s) &= G_{ZOH} \left(\frac{1}{s} \right) e^{-Cs} \\
 &= \left(\frac{1-e^{-sT}}{s} \right) \left(\frac{1}{s} \right) (e^{-Cs}) \\
 &= \frac{1-e^{-sT}}{s^2} e^{-Cs}
 \end{aligned} \tag{29}$$

Using the modified Z transform (Ref 1:234) the delay can be treated by letting

$$Z [X(t-C)] = z^{-m} Z [X(s) e^{\Delta Ts}] \quad (30)$$

$$= z^{-m} X(z, m)$$

where m is one plus the integer number of sampling periods delayed and Δ is a number between 0 and 1 such that

$$C = (m - \Delta) T$$

For our case it is reasonable to consider computation delays no greater than one time period so $m = 1$ and

$$\Delta = 1 - \frac{C}{T} \quad (31)$$

Now,

$$\begin{aligned} Z[X(t-C)] &= z^{-1} Z \left[\frac{1-e^{-sT}}{s^2} e^{\Delta Ts} \right] X_{cd}(z) \\ &= z^{-1} (1-z^{-1}) Z \left[\frac{1}{s^2} e^{\Delta Ts} \right] X_{cd}(z) \\ &= z^{-1} (1-z^{-1}) \frac{\Delta T + T(1-\Delta) z^{-1}}{(1-z^{-1})^2} X_{cd}(z) \\ &= \frac{\Delta T [z + (1/\Delta - 1)]}{z(z-1)} X_{cd}(z) \end{aligned} \quad (32)$$

The complete forward transfer function is then given by

$$\frac{X(z)}{E(z)} = \frac{K_1 T \Delta [z + (1/\Delta - 1)]}{z(z-1)} \quad (33)$$

where Δ is given by Eq (31).

For $K_1 = 20$ and $T = 0.05$, the closed loop response is given by

$$\frac{X(z)}{X_{cd}(z)} = \frac{\Delta z + (1 - \Delta)}{z^2 - (1 - \Delta)z + (1 - \Delta)} \quad (34)$$

Table XI compares the output of the simulation with the prediction of Eq (34). The theoretical results match the simulation results except for the transients caused by neglected dynamics.

Figure 20 shows the gun response for a computation time of 0.024 seconds. Table XII gives the figures of merit for the simulation with different computation times. Both show that computation time produces increased overshoot and settling time. Results indicate that the system gain must be reduced to compensate for computation times in excess of 0.005 seconds (10% of the sampling time).

Table XI
Comparison of Simulation and Analytical Computation Time Effects*

k	$\theta(k)$			
	$T_c = .01$		$T_c = .024$	
	Analytical	Simulation	Analytical	Simulation
0	0	0	0	0
1	20.0	18.1	13.0	9.4
2	29.0	28.2	31.2	30.2
3	26.8	28.0	33.8	35.0
4	29.6	23.9	26.2	26.7
5	24.6	25.0	21.4	21.5

*25 mrad step input

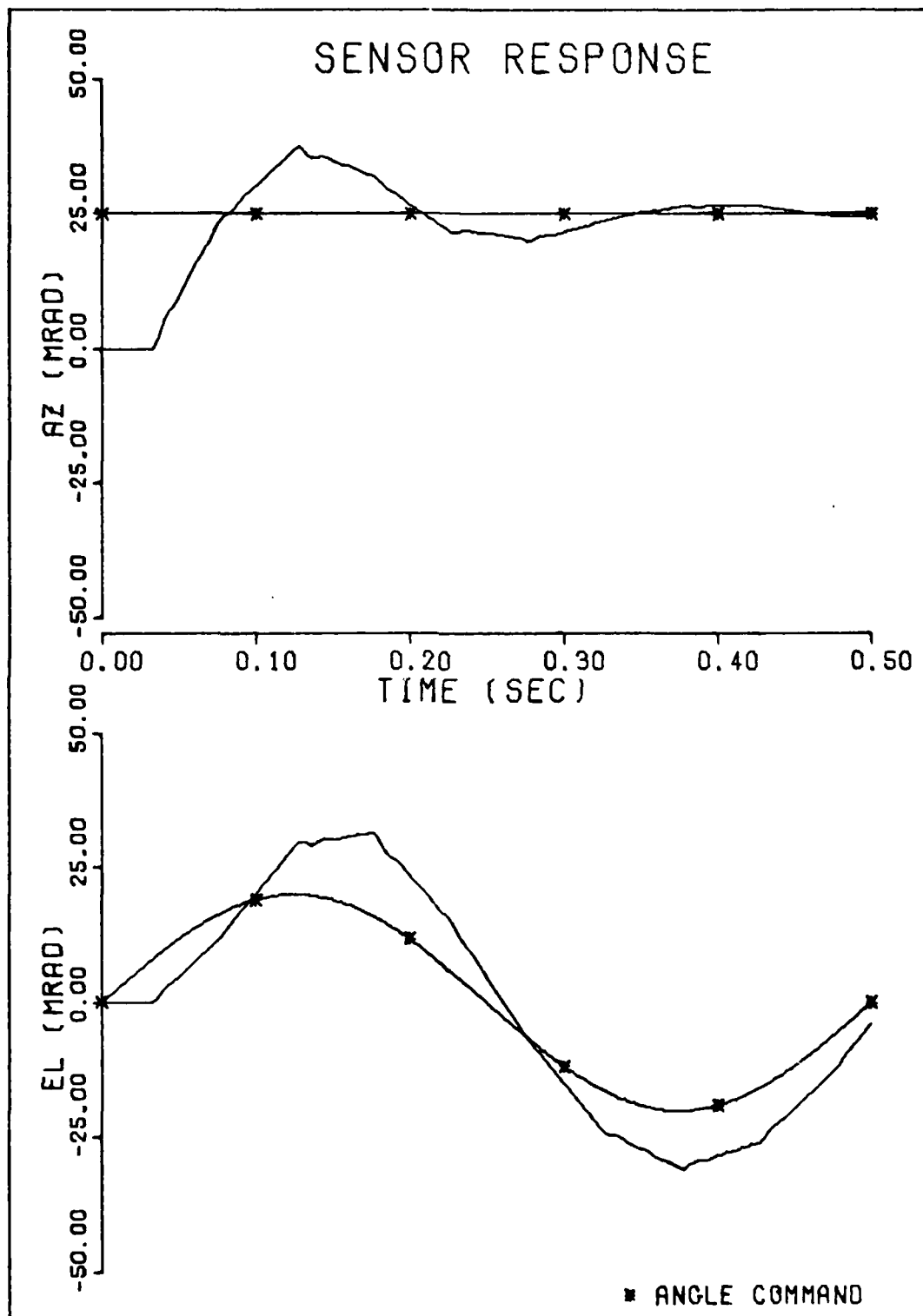


Figure 21. Effect of Computation Time on System Response ($T_c = .024$ sec).

Table XII
System Response for Different Computation Times*
(K₁ = 20)

C	T _r	T _p	T _s	M _p
0	0.05	0.054	0.158	26.99
0.004	0.056	0.144	0.162	26.91
0.01	0.064	0.114	0.218	29.67
0.024	0.082	0.128	0.432	37.75

*25 mrad step input

Word Length Considerations

Due to a finite word length, a digital control system must represent its data in quantitized units. The effects of wordlength in the computer are highly dependent on the specific algorithms used, so will not be discussed further. However, the word length of the data interface can be checked to determine its accuracy.

Although the data busses can carry 16 bits of information per channel, the A/D and D/A converters have a 10 bit word length (Ref 3). The ratio of the largest number to the smallest which can be represented by the word is given by

$$\frac{V_{\max}}{V_{\min}} = 2^n$$

where n is the number of magnitude bits. Subtracting one sign bit from the 10 bit word, 9 bits are available for magnitude information.

$$\frac{V_{\max}}{V_{\min}} = 2^9 = 512$$

If the largest angle to be represented is 52 mrad, then the minimum resolution is 52/512 or .1 mrad. This is well within the requirement of the .5 mrad static accuracy specification.

V Analysis of Muzzle Response

Up to this point, the gun system response has been examined only at the sensor location. This section will deal with the response of the gun at the muzzle. The muzzle response will be examined and a controller designed to improve damping of the first structural mode.

Effect of Structural Modes on Muzzle Response

By examining Figure 22 which shows the gun's structural mode shapes, it can be seen that the first (11.6 Hz) mode has a very small displacement at the rear of the gun and a low slope at the pivot position. This indicates that neither the actuator position sensor nor the angle resolver at the pivot can sense the first mode response. This is fortunate as simulation results indicated unacceptable oscillations for larger first mode output.

The gun muzzle, however, lies at the point of maximum mode shape slope. It is the muzzle which determines the projectile direction so the first mode oscillation has a significant effect on gun performance. The muzzle frequency response of Figure 23 also shows the high gain of the first structural mode at the muzzle.

Figure 24 shows the gun muzzle time response which can be compared against the sensor response of Figure 9. Two results can be seen. For a step input the muzzle has large overshoot and long settling time; for a sinusoidal input the muzzle tracks the input quite well. This means that the first structural mode will cause significant oscillation in target acquisition but target tracking will not be seriously affected.

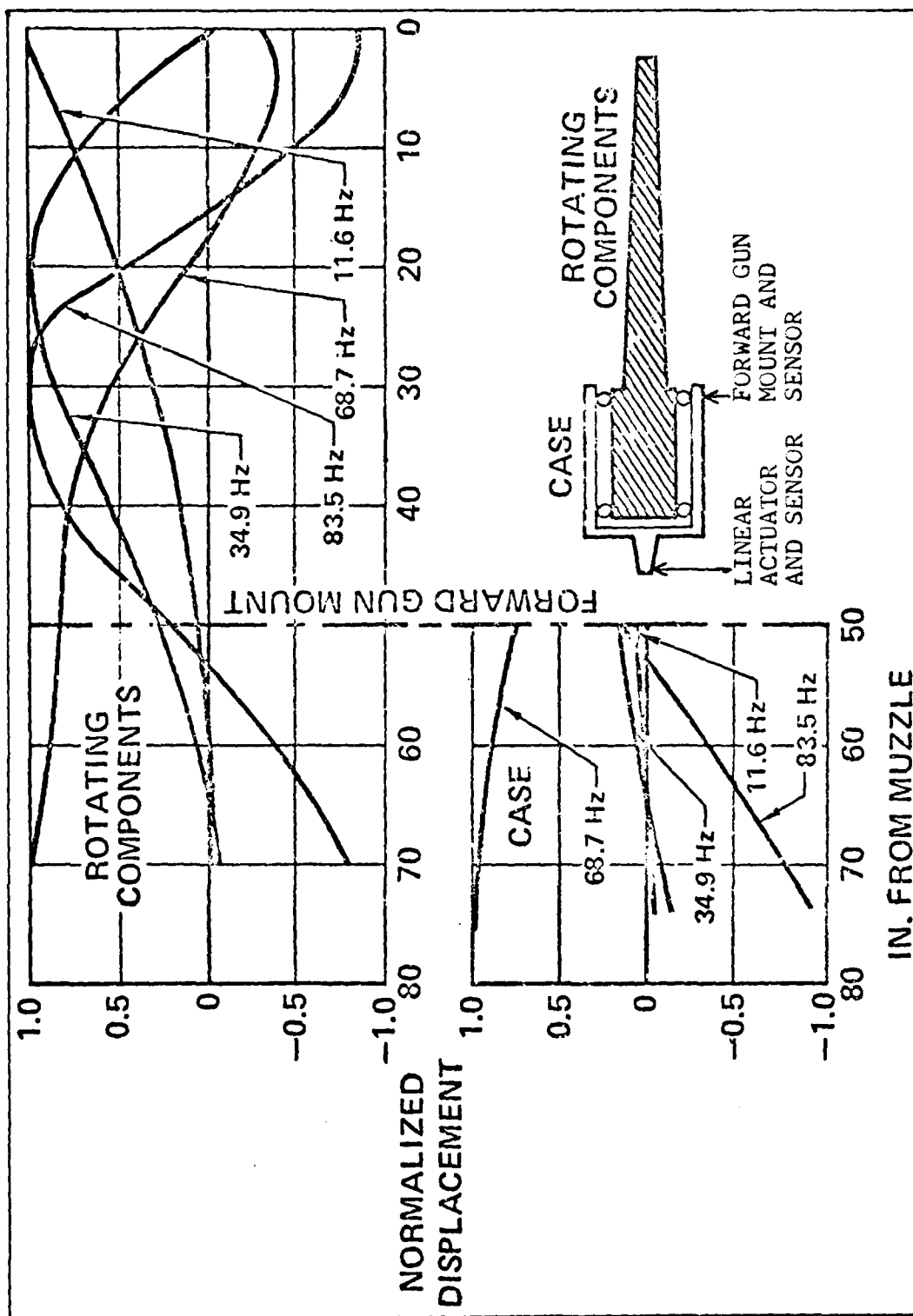


Figure 22. Gun Structural Mode Shapes (Ref 5).

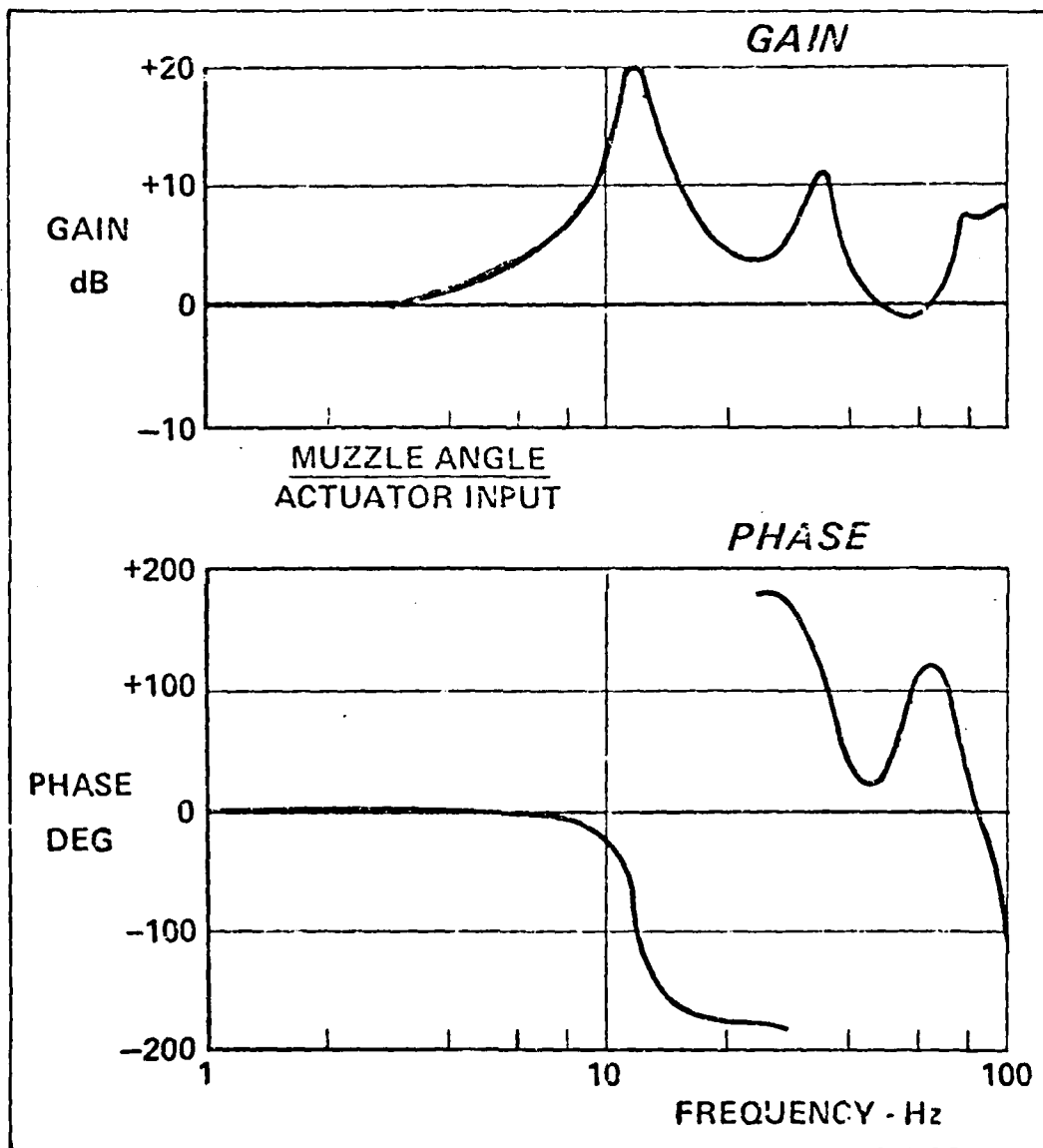


Figure 23. Muzzle Frequency Response (Ref 5)

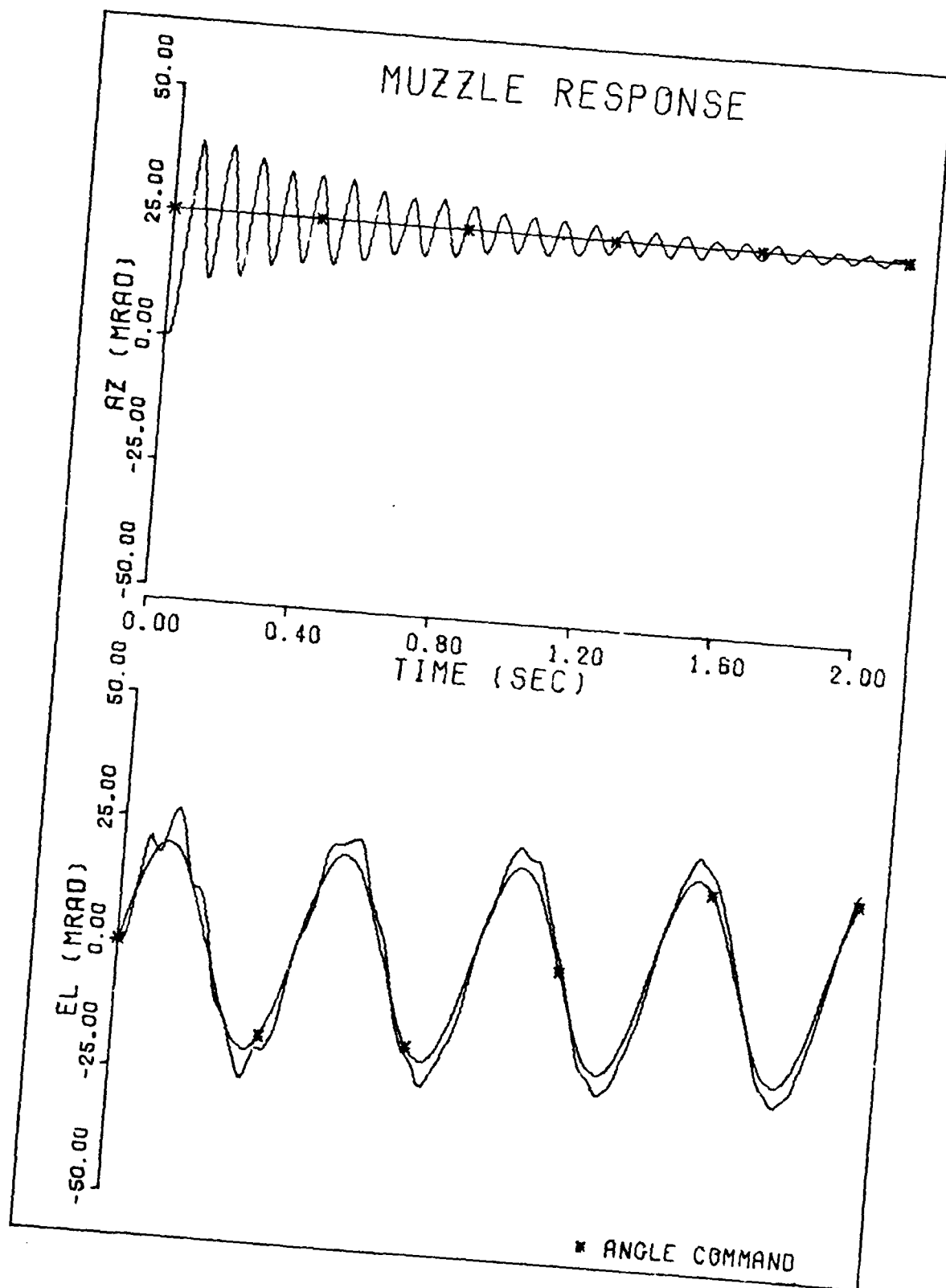


Figure 24. Muzzle Time Response.

It may be acceptable to have a two second settling period during target acquisition. If not, some form of compensation is required to increase the damping of the first mode. The next section will describe the preliminary design of such a compensator.

Controller for Structural Modes

This preliminary structural mode compensator design makes two important assumptions. First is that the controller is necessary and second is that the barrel cluster is non-rotating. The rotating barrel cluster will cause cross coupling between the axes due to gyroscopic precession. Although it is not known what the magnitude of this effect will be, it is suspected that it may be significant.

Three different controller configurations were considered, a digital controller, use of the existing feedforward compensation and a feedback compensator.

The structural modes cannot be controlled by the digital controller for, as mentioned earlier, the natural frequencies of the gun lie outside the controllable region of 10 Hz. An alternative approach would be to consider an intermediate digital processor which would operate at a higher frequency. A controller, having a sample rate of 100 Hz, was designed to control the first structural mode, but aliasing of the third and fourth modes caused unacceptable response.

As shown in Chapter III, the feedforward compensator, $G_1(s)$, has little effect on the low frequency response of the gun so this compensator will not be capable of controlling the first mode. Thus, feedback compensation becomes the only viable method of first mode control.

The sensors cannot directly measure the muzzle position since they have very low amplitude response to the first mode. It is conceivable that a high gain bandpass filter could pick out the first mode response from the sensor, but such an approach would require an extremely high order filter. Ideally, a sensor for first mode control should be located at the muzzle. The rotating barrels, however, make this a very complex hardware problem, not to mention the difficulties of working with a rotating coordinate frame. It is apparent then that some form of observer is required to find the barrel response based on sensor output.

A conventional observer for the Y channel of the gun servo subsystem has the form (Ref 6)

$$\begin{aligned}\dot{\hat{\mathbf{X}}} &= [\mathbf{A}] \hat{\mathbf{X}} + \mathbf{B} \dot{\mathbf{Y}}_c + \mathbf{L} [\mathbf{Y}_s - \mathbf{C}_s \hat{\mathbf{X}}] \\ \hat{\mathbf{Y}}_M &= \mathbf{C}_M \hat{\mathbf{X}}\end{aligned}\tag{35}$$

where \mathbf{A} is the system matrix, \mathbf{B} is the input matrix, \mathbf{L} is the observer gain matrix and \mathbf{C}_M and \mathbf{C}_s are the servo and muzzle output matrices. $\hat{\mathbf{X}}$ is the estimated state vector and \mathbf{Y}_s and $\hat{\mathbf{Y}}_M$ are the sensor output and estimated muzzle output, respectively. This was considered, but it appears that at least a five or possibly seven state system model would be required to include the integrator and gun structural modes.

The method chosen to determine muzzle response was to realize that

$$\frac{X_M(s)}{X_c(s)} \approx \frac{1}{s} \frac{\omega_1^2}{(s^2 + 2\zeta \omega_1 s + \omega_1^2)}\tag{36}$$

neglecting higher frequency dynamics, and that the sensor transfer function

$$\frac{X_s(s)}{\dot{X}_c(s)} \approx \frac{1}{s} \quad (37)$$

Eqs (36) and (37) yield

$$\frac{X_M(s)}{X_s(s)} \approx \frac{\omega_1^2}{s^2 + 2\zeta \omega_1 s + \omega_1^2} \quad (38)$$

Feedback of the estimated muzzle position causes the system roots to move toward the right half-plane as the gain is increased, so the rate-acceleration feedback of Eq (39) was employed.

$$H_s(s) = \frac{s(s + 10)}{s^2 + 2\zeta \omega_1 s + \omega_1^2} \quad (39)$$

It would be desirable to place this type of compensator in an inner feedback loop, perhaps the same as the ΔP compensator, leaving a unity feedback outer loop. However, for convenience, the compensator was placed in the outer loop as shown by Figure 25.

The root locus of Figure 26 shows that as open loop gain is increased, the dominant first mode poles move to the left. A K_{OL} of 0.003 gives a ζ of 0.17. Increasing the gain further increased the damping ratio, but overall system performance was degraded due to reducing the system bandwidth.

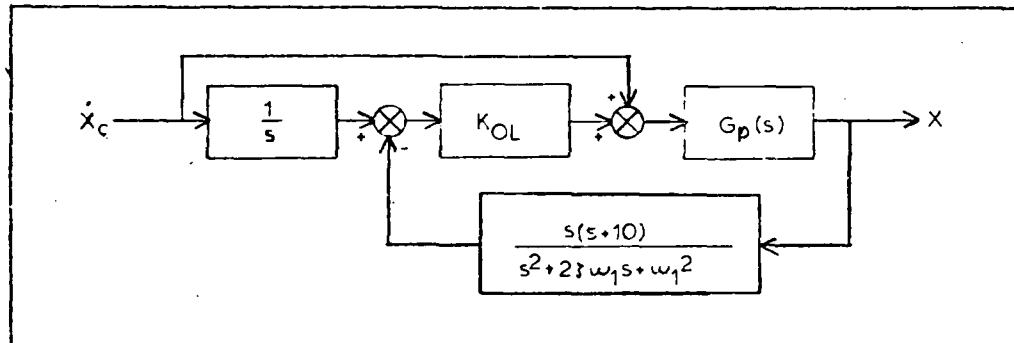


Figure 25. Structural Mode Compensator.

Using $K_{OL} = 0.003$, gun servo subsystem transfer function is

$$G_{gss}(s) \approx \frac{0.454 (s^2 + 7.29s + 5312)}{s(s^2 + 24.7s + 5066)} \quad (40)$$

after elimination of non-dominant poles and zeros.

Finding the Z transform of Eq (40) in series with a zero order hold, as was done in section IV,

$$G_g(z) = \frac{0.0428 (z + 1.25) + 0.426}{(z-1) (z^2 + 1z + 0.290)} \quad (41)$$

The root locus of Figure 27 indicates that the system damping ratio for a system gain of 20 is about 0.25 which is somewhat low. A gain of 15 produced the time response shown in Figure 28. This figure and Table XIII show that the compensator does help the step response of the muzzle by reducing settling time and peak overshoot. However, the square root of the mean square muzzle error (MSE) for a 2 Hz sine

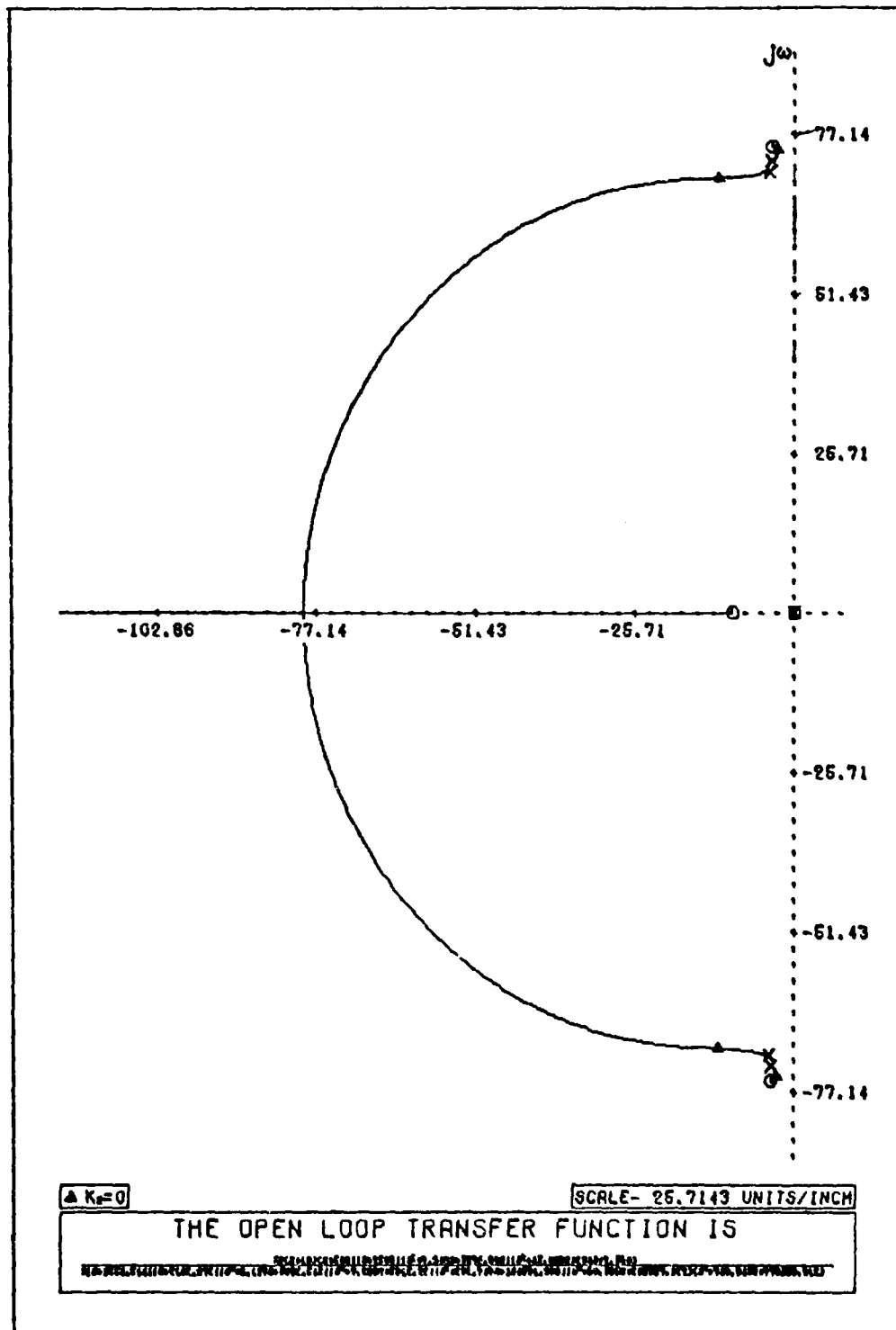


Figure 26. Structural Mode Compensator Root Locus

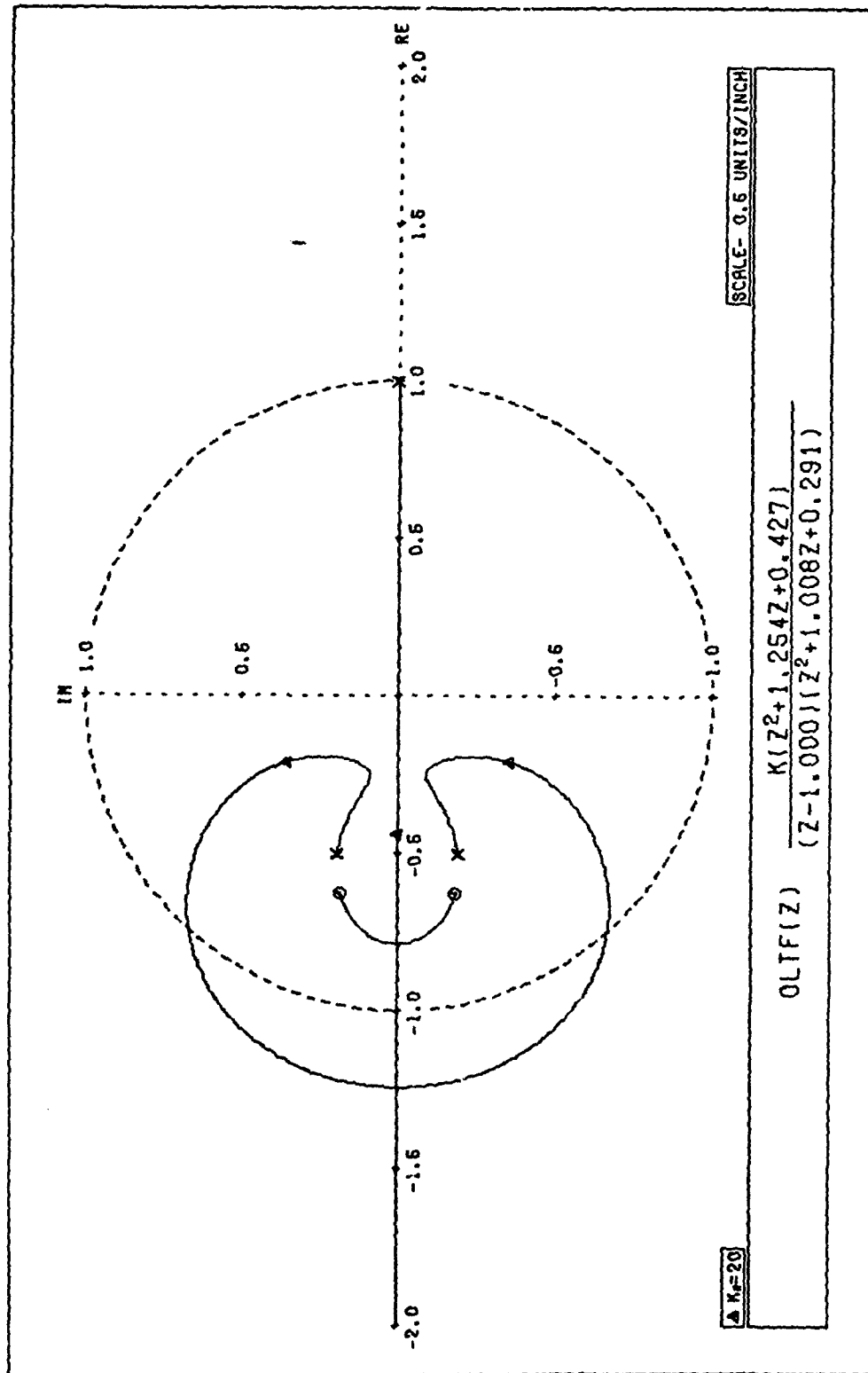


Figure 27. Structural Mode Compensator Discrete Root Locus

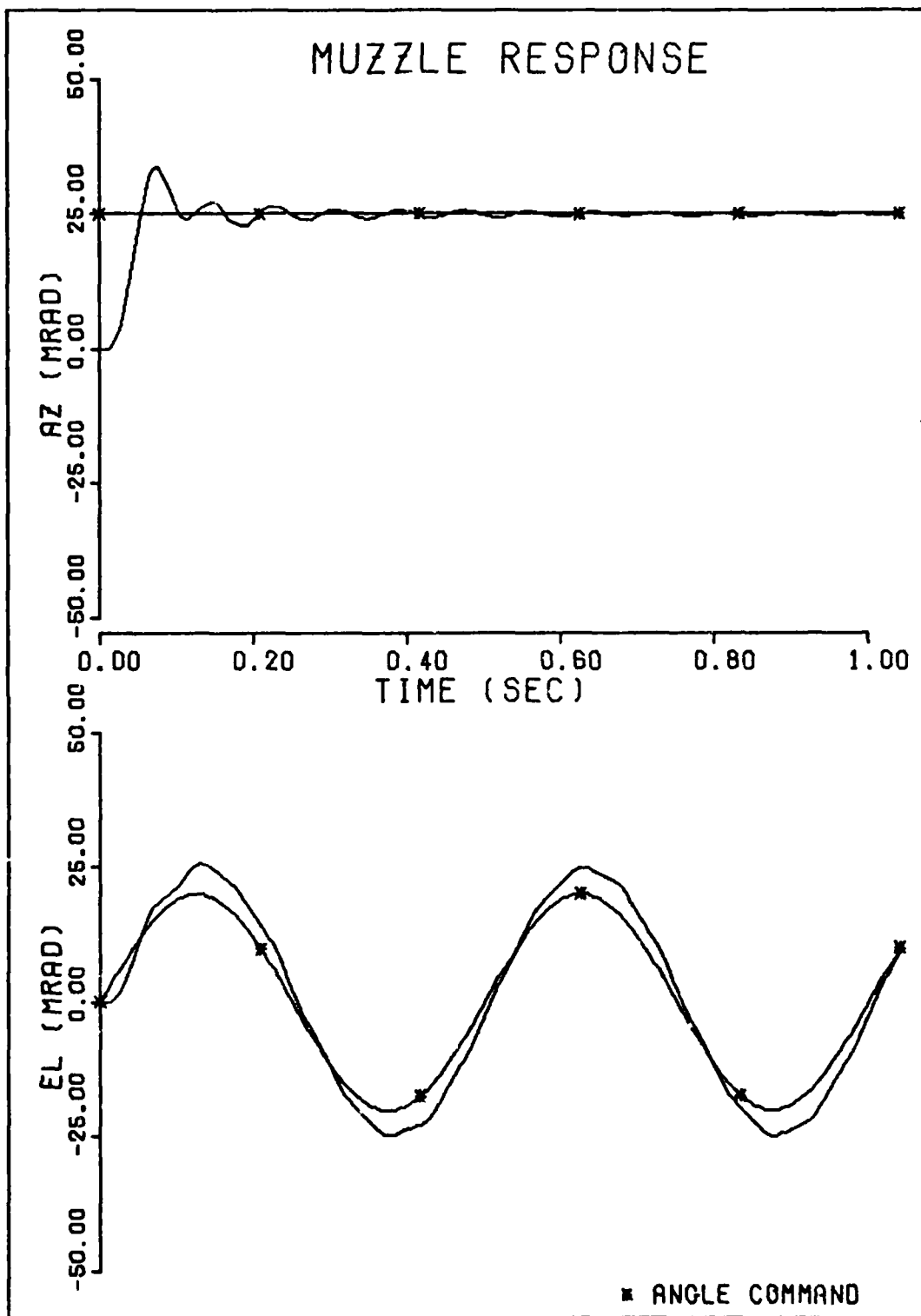


Figure 28a. Structural Mode Compensator Time Response.

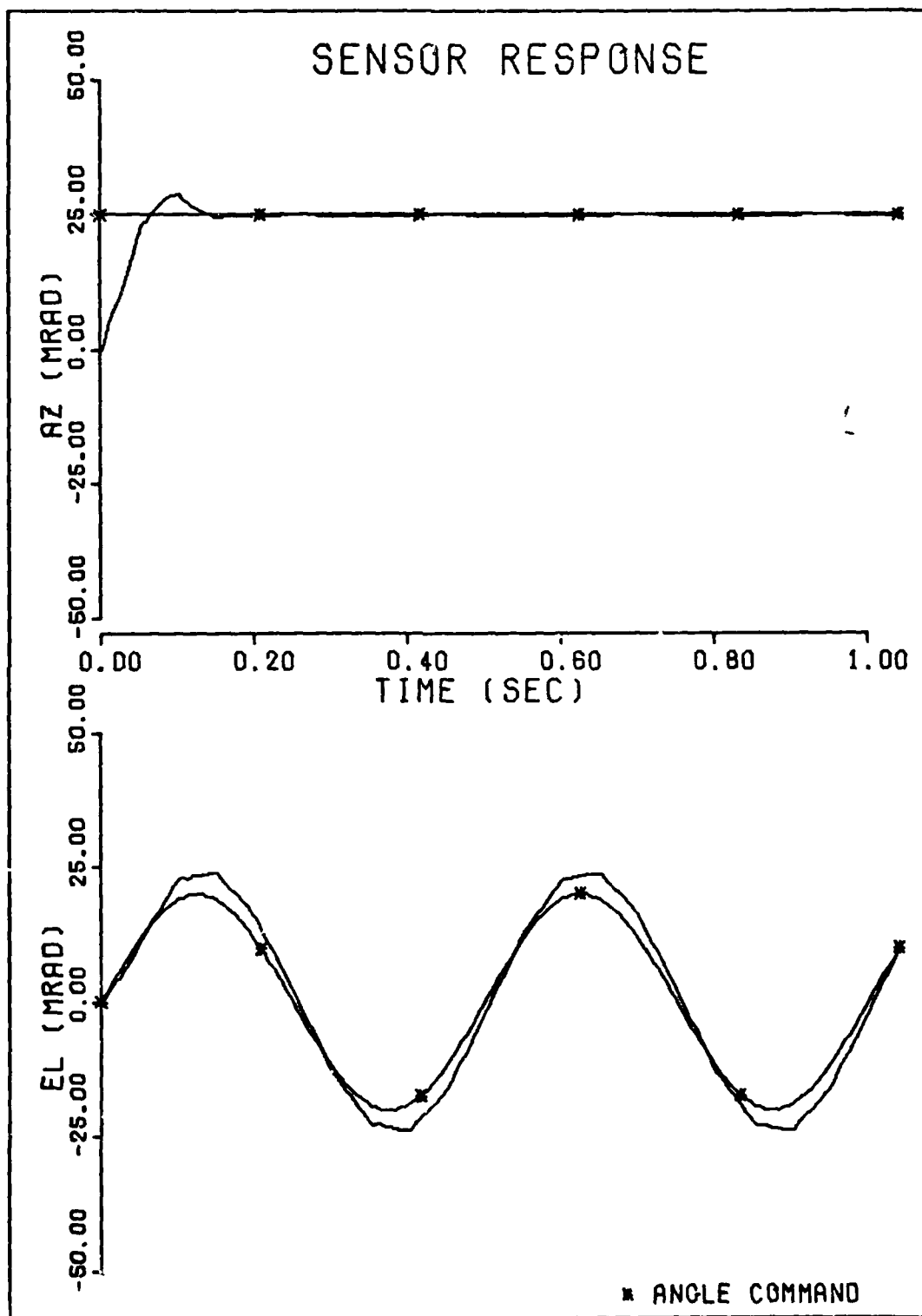


Figure 28b. Structural Mode Compensator Time Response.

input is increased by the compensator, indicating that the tracking ability of the gun has been reduced.

The structural modes of the gun can be controlled as demonstrated by this low level compensator design.

Table XIII
Structural Mode Compensator Response*

	T_s	T_r	T_p	M_p	\sqrt{MSE} **
Servo Responses					
Without Compensator	0.158	0.05	0.054	26.99	-
With Compensator	0.09	0.102	0.104	25.91	-
Muzzle Response					
Without Compensator	>2	0.048	0.07	39.28	3.62
With Compensator	0.156	0.070	0.150	26.45	4.49
*25 mrad step input			**20 mrad 2Hz sine input		

Additional simulations indicate that 10% errors in the estimation of first mode frequency and damping ratios have little effect on the controller's ability to damp step inputs. The primary drawbacks of this preliminary filter design are that low frequency tracking capabilities have been degraded and barrel cluster rotation has been ignored.

It is possible that a closed position loop could improve this response. In addition, a lag-lead compensator could be added at G_1 to allow a higher K_{OL} . Barrel rotation, however, would be a much more complex problem to deal with.

The difficulties associated with implementing a realistic compensator for the first structural mode appear to be more than the problem

warrants. Since the tracking response is acceptable with no compensation, it may be best to simply wait for the acquisition transients to die out before firing the gun.

VI Conclusion

The major results of this study will now be summarized and recommendations made based on these results.

Summary

The gun system easily meets all specifications developed in the Introduction. The gun system settles in under 0.2 seconds and has an overshoot of less than 10% for a system gain of 20, independent of K_{OL} and with or without a differential pressure compensator. Although the full dynamics of the gun servo subsystem are complex, it can be modeled as a pure integrator for discrete analysis. The slew rate and acceleration limits have little or no effect on the linear analysis at the gains used.

A system gain of 20 provides essentially a deadbeat response for the gun system. As computation time exceeds 10% of the sampling time it is necessary to reduce the system gain to stay within overshoot specifications. In order to meet ramp following specifications, a rate feedforward must be included in the mission computer.

The digital sensor filter has little effect on the gun response using the specifications in the Introduction; however, if response is examined at a closer level, the filter does reduce the system settling time. Use of a 10 Hz analog filter for the sensor output severely degrades performance; however, a 30 Hz filter eliminates high frequency inputs to the discrete controller while maintaining a reasonable time response.

The first gun structural mode causes overshoots of over 50% in the muzzle angle and settling times in excess of 2 seconds for a step input. The effect of the first mode is not as severe in tracking polynomial or sinusoidal inputs. If barrel cluster rotation is neglected, a compensator can be designed to control the acquisition (step input) oscillations. This controller degrades tracking of other inputs, however. The complexity of dealing with barrel cluster rotation and the uncompensated tracking response indicate that the acquisition problem is best handled by allowing the barrel vibrations to damp out before the gun is fired.

The M61 movable gun is an extremely fast system which does not require any compensation provided that commands to the gun servo subsystem are rate commands as in the current configuration. The addition of differential pressure compensation, sensor filters and selection of a good K_{OL} all improve the gun system response by small degrees, resulting in a highly effective gun pointing system.

Recommendations

This study has shown the M61 movable gun control system to be effective, neglecting barrel cluster rotation. It appears that additional investigation into the combined effects of first mode oscillation and barrel cluster rotation is required. Investigations in this area could also lead to a realistic method of reducing acquisition settling time.

Bibliography

1. Cadzow, J. R. and H. R. Martens. Discrete-Time and Computer Control Systems. Englewood Cliffs, N. J.: Prentice-Hall, Inc., 1970.
2. D'Azzo, J. J. and C. H. Houpis. Linear Control System Analysis and Design. New York: McGraw-Hill, 1975.
3. Delco Electronics Division. M61A1 Gun Servo Design, Phase II. AFATL-TR-77-15. Eglin AFB: Air Force Armament Laboratory, Feb 1977.
4. Delco Electronics Division. M61A1 Gun Servo Design, Phase III. AFATL-TR-77-120. Eglin AFB: Air Force Armament Laboratory.
5. Delco Electronics Division. Preliminary Design of a Movable Gun Subsystem for the F-15 Aircraft. R-75-94. Santa Barbara, CA, Oct 1975.
6. Gelb, Arthur, et al. Applied Optimal Estimation. Cambridge, Mass.: MIT Press, 1974.
7. Green, Jerrell E. A Guided Gun for Fighter Aircraft (U). Memorandum RM-5584-PR. Santa Monica, California: The Rand Corporation, Feb 1968.
8. Houpis, C. H. and G. B. Lamont. Digital Control Systems/Information Processing. Class Lecture Notes. School of Engineering, Air Force Institute of Technology, WPAFB, Ohio, December 1977.
9. MSL Library 3 Reference Manual. Houston, Texas: International Mathematical and Statistical Libraries, Inc., 1977.
10. Larimer, Stanley J. Users Manual for TOTAL. Wright-Patterson AFB, OH: Air Force Institute of Technology, January 1978.
11. Leatham, Anthony L. A New Approach to an Old Problem: Aircraft Gunnery. Conference Draft for Air University Airpower Symposium. Air War College, Maxwell AFB, Alabama, February 13, 1978.
12. McDonnell Aircraft Company. Air-to-Air Fire Control Exposition (EXPOV) Fourth Status Report. Attachment 3, "Central Interface with Gun Servo Subsystem." St. Louis, MO, September 1975.
13. McDonnell Aircraft Company. Air-to-Air Fire Control Exposition (EXPOV) Sixth Status Report. Attachment 3, "Technical Description Movable Gun Math Models." St. Louis, MO, November 1975.

14. McDonnell Aircraft Company. Installation Requirements - Movable Gun System for the F-15 Aircraft. MDC A3538. St. Louis, Mo., 19 June 1975.
15. McDonnell Aircraft Company. Procurement Specifications for the M61A1 20 mm Gun Accessory System. PS 68-730061. St. Louis, Mo., 30 November 1973.
16. Meirovitch, Leonard. Analytical Methods in Vibration. New York: The Macmillan Company, 1967.
17. Nikolai, Paul J. and Donald S. Clegg. Solution of Ordinary Differential Equations on the CDC/CYBER 74 Processors. AFFDL-TM-130-FBR. Air Force Flight Dynamics Laboratory, Wright-Patterson AFB, Ohio, January 1977.
18. Swisher, George M. Introduction to Linear Systems Analysis. Champaign, Illinois: Matrix Publishers Inc., 1976.

Appendix A

Derivation of Gun Dynamics Model

In the following discussion, the gun dynamics model will be derived based on a lumped parameter model which might be used in a finite element analysis.

The equation of motion for a lumped parameter model of a viscously damped structure is (Ref 16:390)

$$[M] \ddot{\underline{q}} + [C] \dot{\underline{q}} + [K] \underline{q} = \underline{Q} \quad (42)$$

where M , C , and K are the mass, damping and stiffness matrices, respectively, \underline{q} is the generalized coordinate vector and \underline{Q} the generalized force vector.

The mass matrix is symmetric and positive definite so it can be expressed

$$[M] = [M]^{1/2} [N]^{1/2}$$

Letting $\underline{q} = [M]^{-1/2} \underline{y}$,

$$\ddot{\underline{y}} + [A] \dot{\underline{y}} + [B] \underline{y} = [M]^{-1/2} \underline{Q} \quad (43)$$

where

$$[A] = [M]^{-1/2} [C] [M]^{-1/2}$$

$$[B] = [M]^{-1/2} [K] [M]^{-1/2}$$

It can be shown that if A can be expressed

$$[A] = \sum_{r=1}^{\infty} \sum_{p=0}^{n-1} \alpha_{rp} [B]^{p/r} \quad (44)$$

where α_{rp} is a different coefficient for each combination of r and p, then the system can be decoupled into its normal modes. The transformation to decouple the system is given by $\underline{u} = [\Phi] \underline{y}$ where Φ is the transformation matrix composed of the eigenvectors of the system and has the property $\Phi^{-1} = \Phi^T$.

Making the transformation, the system is given by

$$\ddot{\underline{u}} + [2\zeta \omega] \dot{\underline{u}} + [\omega^2] \underline{u} = [\Phi]^T [M]^{-1} \underline{Q} \quad (45)$$

where $[2\zeta \omega]$ and $[\omega^2]$ are both diagonal matrices if Eq (44) is satisfied.

One mode of Eq (45) is given by

$$\ddot{u}_i + 2\zeta_i \omega_i \dot{u}_i + \omega_i^2 u_i = \Phi_i^T [M]^{-1} \underline{Q} = \lambda_i(P_a) f \quad (46)$$

where Φ_i is the eigenvector associated with the ith mode and $\lambda_i(P_a)$ is defined as the mode shape at the actuator where the force f is applied. Equation (44) is satisfied if ζ_i is constant for $i = 1, n$.

The system output, y, can be given by

$$y(t) = \sum_{i=1}^n \lambda_i(P_s) u_i(t) \quad (47)$$

where $\lambda_i(P_s)$ is the mode shape evaluated at the output location. Taking the Laplace transform of Eq (46) and employing Eq (47),

$$\frac{Y(s)}{F(s)} = \sum_{i=1}^n \frac{A_i}{s^2 + 2\zeta \omega_i s + \omega_i^2} \quad (48)$$

where $A_i = \lambda_i(P_a) \lambda_i(P_s)$ and ζ is the constant damping ratio.

Appendix B

Determination of Gun Output Coefficients

The gun structural dynamics are based on the frequency response plots provided in Reference 5. Two sets of dynamics are derived; one is for the muzzle location, and the other for the sensor location.

Muzzle Dynamic Equation

From Appendix A, the gun muzzle output equation can be given by

$$G_{3_M}(s) = \frac{X_M(s)}{F(s)} = \sum_{i=1}^n \frac{A_{i_m}}{(s^2 + 2\zeta_i \omega_i s + \omega_i^2)} \quad (49)$$

where A_{i_m} are the muzzle output coefficients to be determined, ζ is the gun damping ratio to be determined and ω_i are the first four normal frequencies given by Reference 5 as

$$\omega_1 = 11.6 \text{ Hz} = 72.88 \text{ rad/sec}$$

$$\omega_2 = 74.9 \text{ Hz} = 219.2 \text{ rad/sec}$$

$$\omega_3 = 68.7 \text{ Hz} = 431.6 \text{ rad/sec}$$

$$\omega_4 = 83.5 \text{ Hz} = 524.6 \text{ rad/sec}$$

Figure 29 shows the frequency response for the gun muzzle. The dashed line indicates the response given in Reference 5 and the solid line the response of the model developed here. The figure indicates the maximum response is located near 11.6 Hz and has a value of 20 dB corresponding to a magnitude (M_m) of 10.

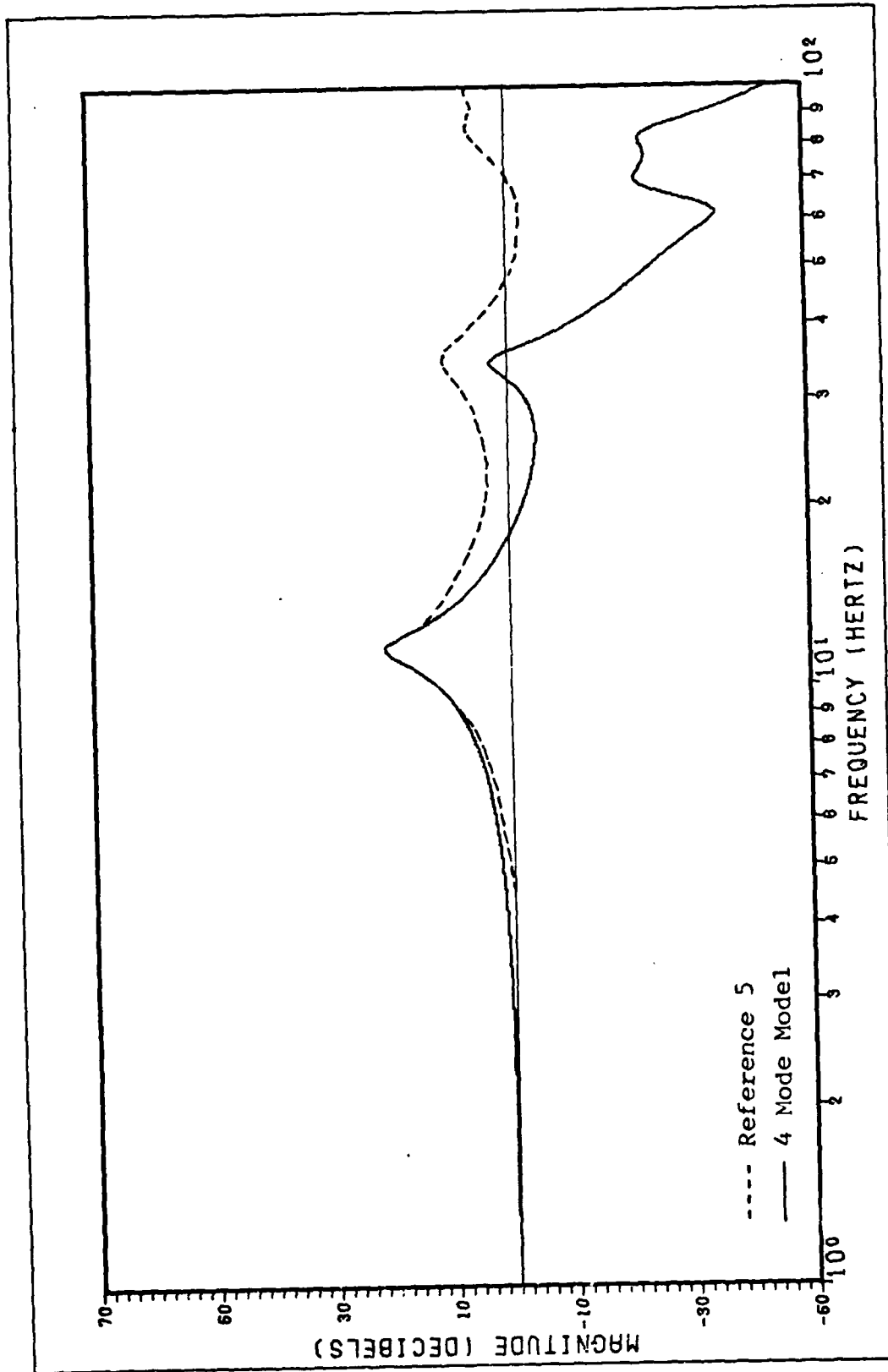


Figure 29a. Modeled Muzzle Frequency Response.

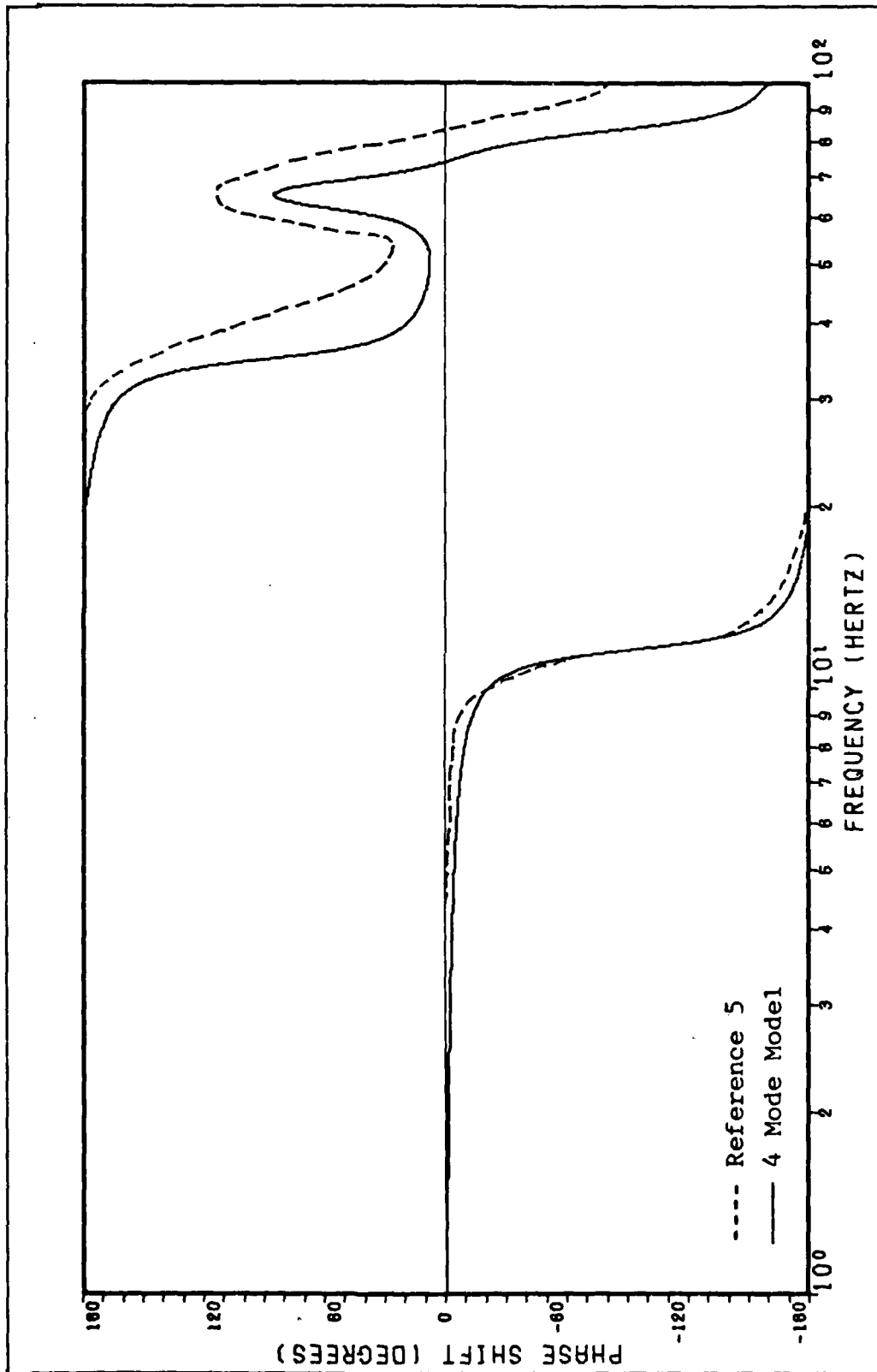


Figure 29b. Modeled Muzzle Frequency Response.

Using the relation (Ref 2:299)

$$M_m = \frac{1}{2\sqrt{1-\zeta^2}}$$

then

$$\zeta^2 = \frac{1 - \sqrt{1 - (1/M_m)^2}}{2} \quad (50)$$

so

$$\zeta = 0.05$$

We also know that

$$\lim_{s \rightarrow 0} G_{3M}(s) = \lim_{s \rightarrow 0} \sum_{i=1}^4 \frac{A_i}{s^2 + 2\zeta \omega_i s + \omega_i^2} = 1 \quad (51)$$

to satisfy the steady state (rigid body) requirements. Thus

$$\sum_{i=1}^4 \frac{A_i}{\omega_i^2} = 1 \quad (52)$$

If the expression for the magnitude of $G_{3M}(j\omega)$ were written as a function of ζ , ω_1 , ω , and A_1 , it would be possible to take three measurements of ω and M_m from the frequency response and form three equations in four unknowns ($A_i, i = 1, 4$). If Eq (52) were added, four equations in four unknowns could be solved for the A_i 's. This method was tried for finding A_i but the nonlinear algebraic equations became unwieldy, so a more conventional synthesis method was used.

The gun transfer function is given in its factored form as

$$G_{3M}(s) = K \frac{\prod_{j=1}^3 (s^2 + 2\zeta_j \omega_{nj} s + \omega_{nj}^2)}{\prod_{i=1}^4 (s^2 + 2\zeta \omega_i s + \omega_i^2)} \quad (53)$$

where

$$K = \frac{\prod_{i=1}^4 \omega_i^2}{3 \prod_{j=1}^3 \omega_{nj}^2}$$

to satisfy Eq (52).

The numerator damping ratios were arbitrarily chosen to be 0.05, the same as the gun damping ratios. ω_{n1} , ω_{n2} , and ω_{n3} were then chosen such that the frequency response of $G_m(s)$ was fit to the true gun response, as shown by the solid line of Figure 29. Note that the magnitude is not well matched at high frequencies. In order to match the magnitude response, zeros would be required near 20 and 45 Hz; however, the phase diagram does not show zeros at these locations.

The partial fraction expansion of Eq (53) was then found using the design program TOTAL. The form of this expansion is

$$\sum_{i=1}^4 \frac{A_i + B_i s}{s^2 + 2\zeta_i \omega_i s + \omega_i^2}$$

Since B does not affect the steady state response and was small compared to A, it was set to zero. A check of the frequency response indicated that no change from the factored form was detectable.

The muzzle output coefficients are then given by

$$\begin{aligned} A_1 &= 6041 \\ A_2 &= -6605 \\ A_3 &= -1319 \\ A_4 &= 1918 \end{aligned}$$

Sensor Dynamic Equations

Two different sensors were considered by Delco. The first, a linear sensor is mounted on the actuator. The second, an angle sensor, is located on the gun gimbals. The frequency response of the two sensors is nearly identical, so one transfer function is considered for both sensors.

The sensor output coefficients were determined using the same procedure as for the muzzle. Figure 30 shows the given and modeled frequency responses.

The sensor output coefficients are given by

$$A_1 = 356.2$$

$$A_2 = 0$$

$$A_3 = 48170$$

$$A_4 = 185624$$

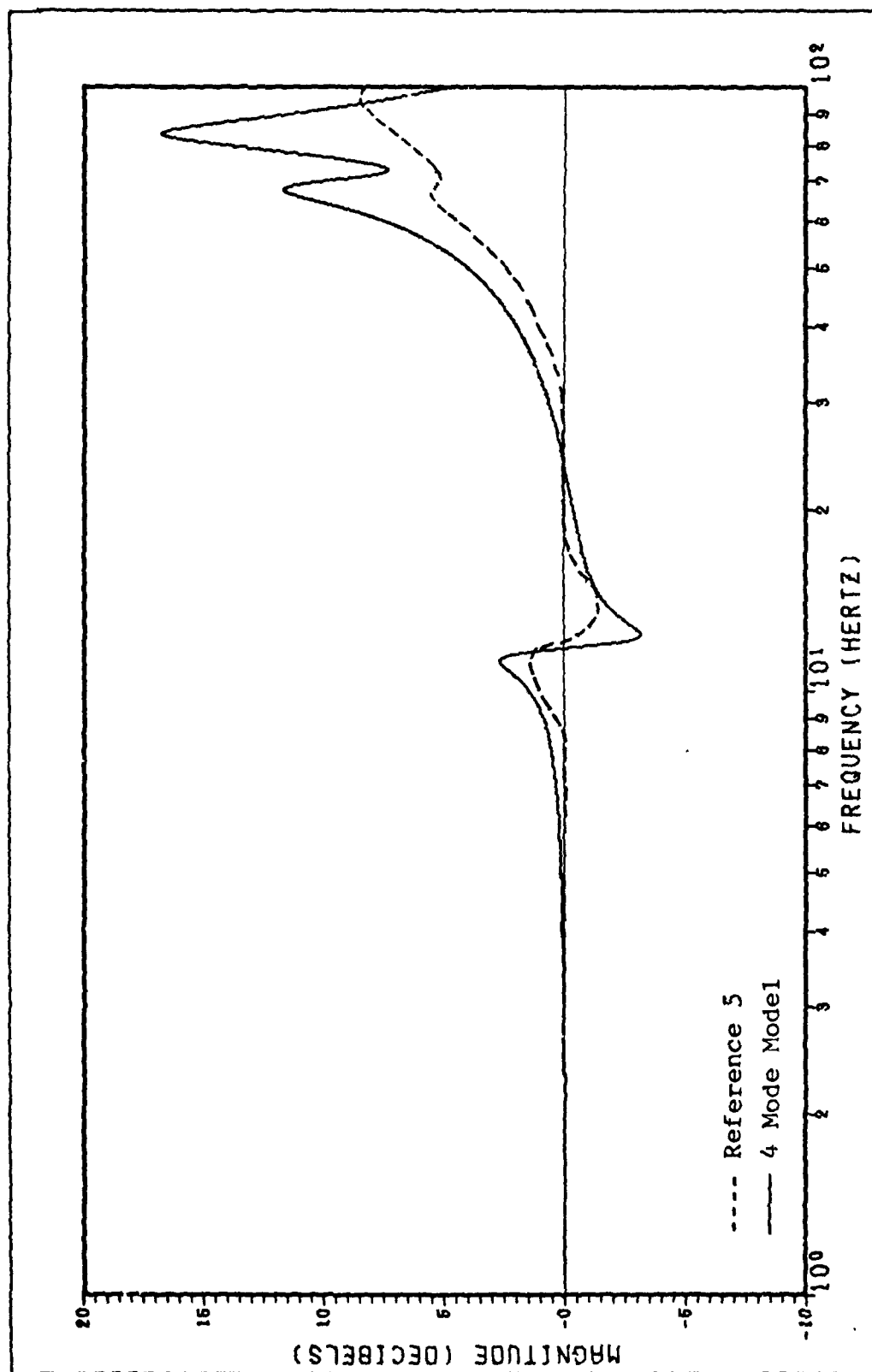


Figure 30a. Modeled Sensor Frequency Response.

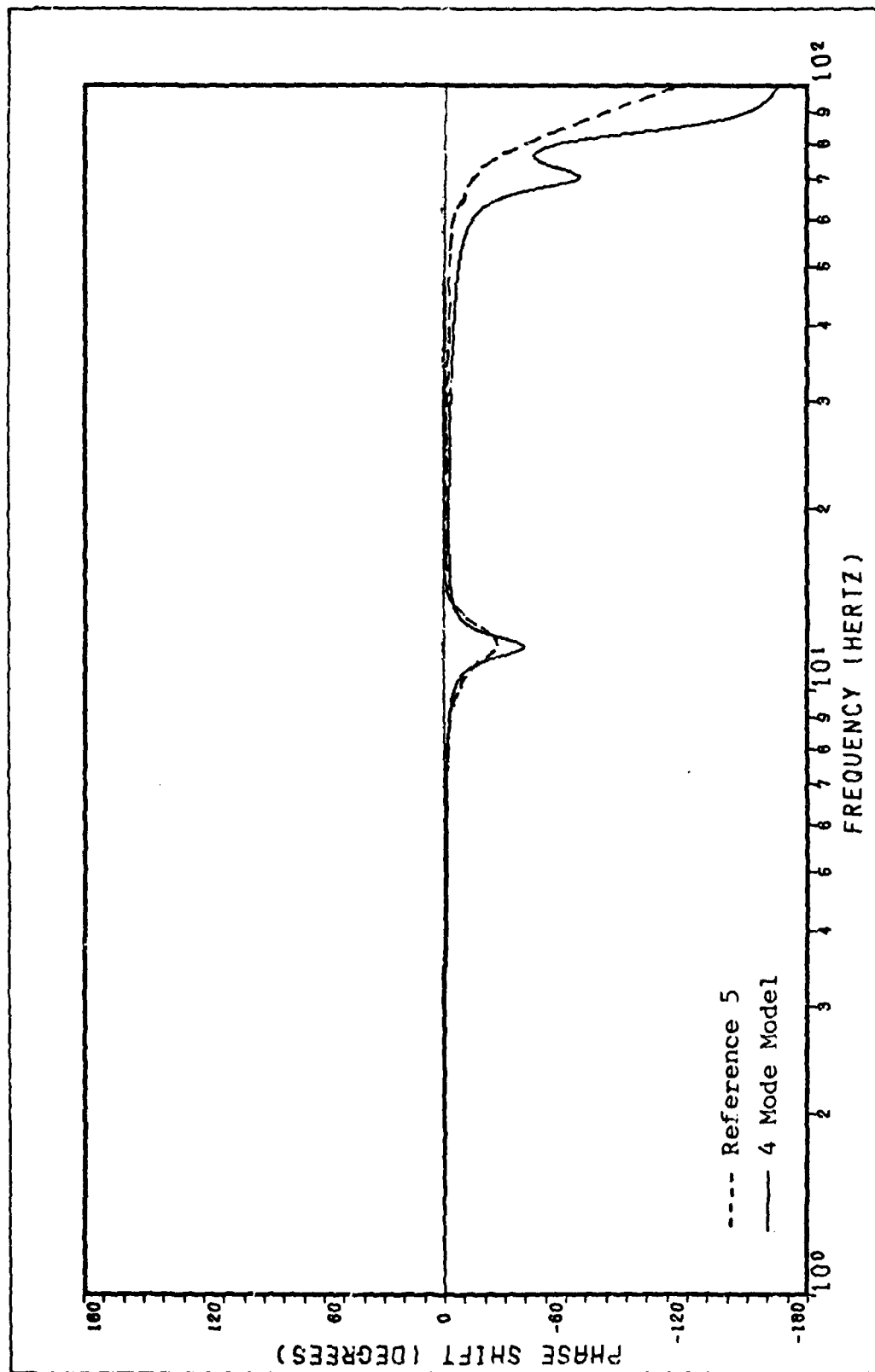


Figure 30b. Modeled Sensor Frequency Response.

Appendix C

Gun Servo Subsystem State Variable Representation

The gun servo subsystem dynamics must be put into state variable form for the computer simulation. A physical variable form composed of phase variable blocks was chosen to represent the system.

The state variable model is formed by first considering each transfer function individually and then connecting inputs and outputs according to the functional block diagram of Figure 31.

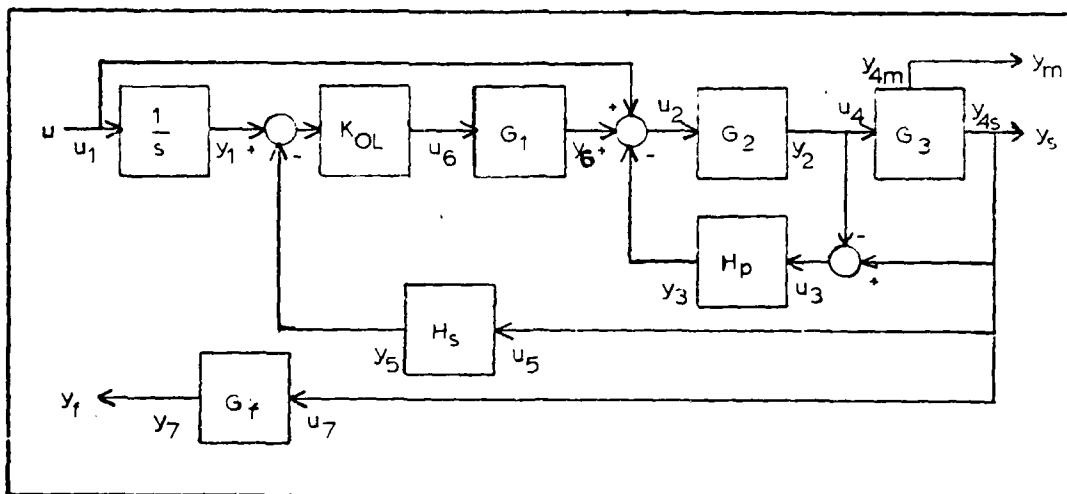


Figure 31. State Variable Block Diagram.

Phase Variable Form (Ref 18)

The phase variable form places the transfer function

$$\frac{U(s)}{Y(s)} = \frac{b_n s^n + \dots + b_2 s^2 + b_1 s + b_0}{s^n + \dots + a_2 s^2 + a_1 s + a_0}$$

into the form

$$\begin{aligned}\dot{x}_1 &= x_2 \\ \dot{x}_2 &= x_3 \\ &\vdots \\ \dot{x}_n &= -a_0 x_1 - a_1 x_2 - \dots - a_{n-1} x_n + u(t)\end{aligned}\quad (54)$$

$$\begin{aligned}y(t) &= (b_0 - a_0 b_n) x_1 + (b_1 - a_1 b_n) x_2 \\ &\quad + \dots + (b_{n-1} - a_{n-1} b_n) x_n + b_n u(t)\end{aligned}$$

Integrator

$$G_I(s) = \frac{Y_I(s)}{U_I(s)} = \frac{1}{s}$$

Using Eq (54)

$$\begin{aligned}\dot{x}_1 &= u_1 \\ y_1 &= x_1\end{aligned}\quad (55)$$

Servo valve Dynamics

$$G_2(s) = \frac{Y_2(s)}{U_2(s)} = \frac{A_v}{s^3 + 2\zeta \omega_v s^2 + \omega_v^2 s + 0}$$

Using Eq (54)

$$\begin{bmatrix} \dot{x}_2 \\ \dot{x}_3 \\ \dot{x}_4 \end{bmatrix} = \begin{bmatrix} 0 & 1 & 0 \\ 0 & 0 & 1 \\ 0 & -\omega_v^2 & -2\zeta \omega_v \end{bmatrix} \begin{bmatrix} x_2 \\ x_3 \\ x_4 \end{bmatrix} + \begin{bmatrix} 0 \\ 0 \\ 1 \end{bmatrix} u_2$$

$$y_2 = \begin{bmatrix} A_v & 0 & 0 \end{bmatrix} \begin{bmatrix} x_2 \\ x_3 \\ x_4 \end{bmatrix} \quad (56)$$

Differential Pressure Compensator

$$H_p(s) = \frac{Y_3(s)}{U_3(s)} = \frac{A_c}{(s + 1/\tau_1)(s + 1/\tau_2)}$$

Since the differential pressure compensator has no complex eigenvalues, it is easily implemented in a Jordan form (Ref 18).

Taking the partial fraction expansion of Eq (56),

$$H_p(s) = A_c \left[\frac{A}{1 + 1/\tau_1} + \frac{B}{1 + 1/\tau_2} \right]$$

where

$$A = \tau_2 / (\tau_2 - \tau_1)$$

$$B = \tau_1 / (\tau_1 - \tau_2)$$

The state variable representation is then

$$\begin{bmatrix} \dot{x}_5 \\ \dot{x}_6 \end{bmatrix} = \begin{bmatrix} 1/\tau_1 & 0 \\ 0 & 1/\tau_2 \end{bmatrix} \begin{bmatrix} x_5 \\ x_6 \end{bmatrix} + \begin{bmatrix} A_c \\ A_c \end{bmatrix} u_3$$

$$y_3 = \begin{bmatrix} A & B \end{bmatrix} \begin{bmatrix} x_5 \\ x_6 \end{bmatrix} \quad (57)$$

Note that the simulation program uses $T = 1/\tau$.

Gun Dynamics

The Gun Dynamics are treated as a set of decoupled modes each represented by a phase variable block.

$$G_3(s) = \frac{Y_4(s)}{U_4(s)} = \sum_{i=1}^5 \frac{A_i}{(s^2 + 2\zeta_i \omega_i s + \omega_i^2)}$$

One of these phase variable blocks is given by

$$\begin{bmatrix} \dot{x}_7 \\ \dot{x}_8 \end{bmatrix} = \begin{bmatrix} 0 & 1 \\ -\omega_1^2 & -2\zeta\omega_1 \end{bmatrix} \begin{bmatrix} x_7 \\ x_8 \end{bmatrix} + \begin{bmatrix} 0 \\ 1 \end{bmatrix} u_4 \quad (58a)$$

Similar blocks exist for states 9 through 16. The output equation is given by

$$y_4 = A_1 x_7 + A_2 x_9 + A_3 x_{11} + A_4 x_{13} + A_5 x_{15} \quad (58b)$$

where the output coefficients, A_i , will be different for sensor and muzzle output.

Feedback Compensator

$$H_s(s) = \frac{Y_5(s)}{U_5(s)} = \frac{C_{f1}s^2 + C_{f2}s^2 + C_{f3}s + C_{f4}}{s^2 + C_{f5}s^2 + C_{f6}s + C_{f7}}$$

Using Eq (54)

$$\begin{bmatrix} \dot{x}_{17} \\ \dot{x}_{18} \\ \dot{x}_{19} \end{bmatrix} = \begin{bmatrix} 0 & 1 & 0 \\ 0 & 0 & 1 \\ -C_{f7} & -C_{f6} & -C_{f5} \end{bmatrix} \begin{bmatrix} x_{17} \\ x_{18} \\ x_{19} \end{bmatrix} + \begin{bmatrix} 0 \\ 0 \\ 1 \end{bmatrix} u_5 \quad (59)$$

$$y_5 = [C_{f4} - C_{f7}C_{f1} \quad C_{f3} - C_{f6}C_{f1} \quad C_{f2} - C_{f5}C_{f1}] \begin{bmatrix} x_{17} \\ x_{18} \\ x_{19} \end{bmatrix} + C_{f1}u_5$$

AD-A081 893

AIR FORCE INST OF TECH WRIGHT-PATTERSON AFB OH SCHOO--ETC F/6 19/6
ANALYSIS OF A CONTROLLER FOR THE M61 MOVABLE GUN.(U)
DEC 78 D E JONES

UNCLASSIFIED

AFIT/6A/AA/78D-5

NL

2 of 2

3-8-88

END

DATE

FILED

4-80

DTIC

Feedforward Compensator

$$G_1(s) = \frac{Y_6}{U_6} = \frac{C_{11} s^2 + C_{12} s + C_{13}}{s^2 + C_{14} s + C_{15}}$$

$$\begin{bmatrix} \dot{x}_{20} \\ \dot{x}_{21} \end{bmatrix} = \begin{bmatrix} 0 & 1 \\ -C_{15} & -C_{14} \end{bmatrix} \begin{bmatrix} x_{20} \\ x_{21} \end{bmatrix} + \begin{bmatrix} 0 \\ 1 \end{bmatrix} u_6 \quad (60)$$

$$y_6 = [C_{12} - C_{15} C_{11} \quad C_{12} - C_{14} C_{11}] \begin{bmatrix} x_{20} \\ x_{21} \end{bmatrix} + C_{11} u_6$$

Sensor Filter

$$G_F(s) = \frac{Y_7}{U_7} = \frac{C_{21} s^2 + C_{22} s + C_{23}}{s^2 + C_{24} s + C_{25}}$$

$$\begin{bmatrix} \dot{x}_{22} \\ \dot{x}_{23} \end{bmatrix} = \begin{bmatrix} 0 & 1 \\ -C_{25} & -C_{24} \end{bmatrix} \begin{bmatrix} x_{22} \\ x_{23} \end{bmatrix} + \begin{bmatrix} 0 \\ 1 \end{bmatrix} u_7 \quad (61)$$

$$y_7 = [C_{23} - C_{25} C_{21} \quad C_{22} - C_{24} C_{21}] \begin{bmatrix} x_{22} \\ x_{23} \end{bmatrix} + C_{21} u_7$$

From Figure 31 it can be seen that

$$u_1 = u$$

$$u_2 = u + y_6 + y_3$$

$$u_3 = y_{4s} - y_2$$

$$u_4 = y_2$$

$$u_5 = y_{4s}$$

$$u_6 = K_{OL} (y_1 - y_5)$$

$$u_7 = y_{4s}$$

and

$$y_{\text{sensor}} = y_4$$

$$y_{\text{muzzle}} = y_{4m}$$

$$y_{\text{filter}} = y_7$$

where y_4 uses the sensor output coefficients in Eq (58b) and y_{4m} uses the muzzle output coefficients.

Using Eqs (55), (56), (57), (58), (59), (60), (61), and (62), the entire state variable representation is given by

$$\begin{aligned} \dot{x}_1 &= \dot{y}_c \\ \dot{x}_2 &= x_3 \\ \dot{x}_3 &= x_4 \\ \dot{x}_4 &= C_{11} K_{OL} x_1 - \omega_v^2 x_3 - 2\zeta_v \omega_v x_4 + \frac{1}{1-\tau_1/\tau_2} x_5 \\ &\quad + \frac{1}{1-\tau_2/\tau_1} x_6 + C_{11} K_{OL} C_{f1} (A_1 x_7 + A_2 x_9 + A_3 x_{11} \\ &\quad + A_4 x_{17} + A_5 x_{15}) \\ &\quad + C_{11} K_{OL} [(C_{f4} - C_{f5} C_{f1}) x_{17} + (C_{f3} - C_{f6} C_{f1}) x_{18} \\ &\quad + (C_{f2} - C_{f5} C_{f1}) x_{19}] \\ &\quad + (C_{13} - C_{15} C_{11}) x_{20} + (C_{12} - C_{14} C_{11}) x_{21} \\ \dot{x}_5 &= -1/\tau_1 x_5 + A_c [-A_v x_2 + A_1 x_7 + A_2 x_9 + A_3 x_{11} + A_4 x_{13} + A_5 x_{15}] \\ \dot{x}_6 &= -1/\tau_1 x_6 + A_c [-A_v x_2 + A_1 x_7 + A_2 x_9 + A_3 x_{11} + A_4 x_{13} + A_5 x_{15}] \end{aligned}$$

$$\begin{aligned}
\dot{x}_7 &= x_8 \\
\dot{x}_8 &= A_1 x_2 - \omega_1^2 x_7 - 2\beta \omega_1 x_8 \\
\dot{x}_9 &= x_{10} \\
\dot{x}_{10} &= A_1 x_2 - \omega_2^2 x_9 - 2\beta \omega_2 x_{10} \\
\dot{x}_{11} &= x_{12} \\
\dot{x}_{12} &= A_1 x_2 - \omega_3^2 x_{11} - 2\beta \omega_3 x_{12} \\
\dot{x}_{13} &= x_{14} \\
\dot{x}_{14} &= A_1 x_2 - \omega_4^2 x_{13} - 2\beta \omega_4 x_{14} \\
\dot{x}_{15} &= x_{16} \\
\dot{x}_{16} &= A_1 x_2 - \omega_5^2 x_{15} - 2\beta \omega_5 x_{16} \\
\dot{x}_{17} &= x_{18} \\
\dot{x}_{18} &= x_{19} \\
\dot{x}_{19} &= A_1 x_7 + A_2 x_9 + A_3 x_{11} + A_4 x_{13} + A_5 x_{15} \\
&\quad - C_{f7} x_{17} - C_{f6} x_{18} - C_{f5} x_{19} \\
\dot{x}_{20} &= x_{21} \\
\dot{x}_{21} &= K_{OL} x_1 - C_{f1} (A_1 x_7 + A_2 x_9 + A_3 x_{11} + A_4 x_{13} + A_5 x_{15}) \\
&\quad - K_{OL} [(C_{f4} - C_{f7} C_{f1}) x_{17} + (C_{f3} - C_{f6} C_{f1}) x_{18} + (C_{f2} - C_{f5} C_{f1}) x_{19}] \\
&\quad - C_{15} x_{20} - C_{14} x_{21} \\
\dot{x}_{22} &= x_{23} \\
\dot{x}_{23} &= A_1 x_7 + A_2 x_9 + A_3 x_{11} + A_4 x_{13} + A_5 x_{15} - C_{25} x_{22} - C_{24} x_{23}
\end{aligned}$$

The output equations are then given by

$$\begin{aligned}
y_{\text{sensor}} &= [A_1 x_7 + A_2 x_9 + A_3 x_{11} + A_4 x_{13} + A_5 x_{15}] \\
y_{\text{barrel}} &= [A_{b1} x_7 + A_{b2} x_9 + A_{b3} x_{11} + A_{b4} x_{13} + A_{b5} x_{15}] \\
y_{\text{filter}} &= (C_{23} - C_{25} C_{21}) x_{22} + (C_{22} - C_{24} C_{21}) x_{23} \\
&\quad + C_{21} (A_1 x_7 + A_2 x_9 + A_3 x_{11} + A_4 x_{13} + A_5 x_{15})
\end{aligned}$$

Appendix D

M61 Simulation Program

The M61 Simulation Program is designed to provide gun system response as a function of time for a variety of commanded inputs. The program is coded in CDC FORTRAN IV and requires 64K core memory for execution. The simulation requires approximately 15 seconds of CP time per second of simulation time.

The main program is responsible for data input, output and reduction, and acts as the simulation executive. All gun, control, and simulation parameters are read from the input file in free format. The main program then echos the inputs and processes them for use in the simulation. After initializing values, the simulation begins.

The program uses the integration package ODE (Ref 8) to integrate the GSS state equation between sampling instants. The actuator outputs are found at the sensor, barrel, and sensor filter locations and converted to gun angles by subroutine LNTQAN. At the sample instant, the control input is formed by subroutine CONTROL. If T_c is not zero, the input is delayed by the appropriate number of time intervals. Note that the computation time may not be exactly as specified due to the quantization of DT , the integration interval. DT is selected to provide 250 data points for the CALCOMP plotter based on the final time.

After the simulation is complete, the azimuth and elevation errors for both the sensor and barrel location are computed and printed along with the commands and positions.

Rise time, settling time, peak time and peak overshoot are determined for the azimuth. Mean and mean squared errors are calculated for elevation. Subroutine PLOTTER then plots the barrel and sensor angles if desired.

Subroutine GUN contains the state equation for the X and Y channels of the gun. Since the channels are identical, the same equations are used for each channel. Actuator position, rate, and acceleration limits are incorporated in the servovalve equations.

Subroutine LNTQAN transforms the actuator length to gun angles for obtaining GSS outputs. Subroutine ANTQIN transforms gun angles to actuator lengths for the digital controller. This subroutine returns both actual length and change in length from center.

Subroutine COMMAND generates position and rate commands for the gun system. The azimuth and elevation can be commanded independently with several different functions, including steps, ramps, parabolas, sines, cosines, and a random acceleration input. Subroutine NOISE generates the random input.

Subroutine PLOTTER plots gun azimuth and elevation positions and position commands against time using standard CALCMP routines.

Subroutine CONTROL uses the algorithm of section II in simulating the mission computer. K_2 is used as a switch for the rate feedforward.

```

PROGRAM M61A1 (INPUT,OUTPUT,PLOT,RESULT,TAPE5=RESULT)
DIMENSION T(253),AZM(253),ELM(253),A7C(253),ELC(253)
DIMENSION EL(253),A7(253)
DIMENSION WORK(1066),IWORK(5),X(46)
DIMENSION AS(5),ZH(5),W2(5),AB(5),C(5,2),CF(7)
COMMON /MISC/K1,K2,K3,KOL,DXC,DYC
COMMON /ACTUAT/A,B,D,XL0,YL0
COMMON/COEFF/AV,HV2,ZHV,AC,T1,T2,AS,W2,ZH,AB,C,CF
COMMON/MAX/TMAX,DTMAX,DDTMAX
REAL K1,K2,K3,KOL
EXTERNAL GUN
DATA NPPTS/251/
DATA A,3,D /10.25,10.25,24.1/
DATA X/46*0./
PI=2.*ASIN(1.)

```

C*****

INPUT AND ECHO DATA

C*****

C**** INPUT VALVE PARAMETERS

READ*,AV,HV2,ZHV

C**** INPUT DELTA PRESSURE PARAMETERS (T=1/TAU)

READ*,AC,T1,T2

C**** INPUT 5 SENSOR OUTPUT COEFFICIENTS, 5 MUZ7LE OUTPUT COEFFICIENTS

C**** 5 NORMAL GUN FREQUENCIES(HERTZ) AND GUN DAMPING RATIO

READ*,AS,AB,W2,ZETA

C**** INPUT GUN LIMITS DEGREES DEGREES/SEC DEGREES/SEC/SEC

READ*,TMAX,DTMAX,DDTMAX

C**** INPUT SYSTEM GAIN, DIGITAL RATE FEEDFORWARD GAIN (0 OR 1),

C**** DIGITAL SENSOR FILTER GAIN, AND GUN SERVO SUBSYSTEM GAIN (KOL)

READ*,K1,K2,K3,KOL

C**** INPUT FINAL TIME,SAMPLE TIME,COMPUTATION TIME,AND PRINT INCREMENT

READ*,T*,TS,TC,PRINC

C**** INPUT PLOT FLAG (0= NO PLOT)

READ*,IPLT

```

C**** INPUT 7 FEEDBACK PARAMETERS OF FORM
C HS(S)=(C1 S**3 + C2 S**2 + C3 S + C4)/( S**3 +C5 S**2 + C6 S +C7)
C**** INPUT 5 FEEDFORWARD COMPENSATOR COEFFICIENTS OF FORM
C G1(S)=(C1 S**2 + C2 S + C3)/( S**2 + C4 S + C5 )
C**** INPUT 5 SENSOR FILTER COEFFICIENTS OF FORM
C GF(S)=(C1 S**2 + C2 S + C3)/( S**2 + C4 S + C5 )
  READ*,C5,C
C**** INPUT AZIMUTH COMMAND TYPE, MAGINTUDE(MRAD), AND FREQUENCY(HERTZ)
C**** INPUT ELEVATION COMMAND TYPE, MAGINTUDE(MRAD), AND FREQUENCY(HERTZ)
C  COMMAND TYPES 1-STEP 2-RAMP 3-PARAB. 1-SIN 5-COS 5-RANDOM
  READ*,NAZTYPE,AZMAG,AZFREQ
  READ*,NELTYPE,ELMAG,ELFFREQ
  PRINT HEADER
C**** WRITE 3000
  PRINT*,"THIS PROGRAM SIMULATES THE MOVABLE M61A1 AERIAL CANNON AND
1 CONTROLLER"
  PRINT*," "
  PRINT*," "
  PRINT*,"GUN DAMPING RATIO IS: ",ZETA
  PRINT*," "
  PRINT*,"GUN RESONANT FREQUENCIES ARE: ",W2," HERTZ"
  PRINT*," "
  PRINT*,"SENSOR OUTPUT COEFFICIENTS ARE: ",AS
  PRINT*," "
  PRINT*,"MUZZLE OUTPUT COEFFICIENTS ARE: ",AB
  PRINT*," "
  PRINT*,"VALVE PARAMETERS ARE: ",AV,WV2,ZWV
  PRINT*," "
  PRINT*,"INNER LOOP COMPENSATOR PARAMETERS ARE: ",AC,T1,T2
  PRINT*," "
  PRINT*,"MAXIMUM ANGLE = ",TMAX,"DEGREES"
  PRINT*," "
  PRINT*,"MAXIMUM ANGULAR RATE = ",OTMAX,"DEGREES / SEC"
  PRINT*," "
  PRINT*,"MAXIMUM ANGULAR ACCELERATION = ",ODTMAX,"DEGREES/SEC/SEC"
  PRINT*," "

```



```

PRINT*, " "
PRINT*, "CONTROL VARIABLES ARE:"
PRINT*, " "
PRINT*, "K1=", K1
PRINT*, "K2=", K2
PRINT*, "K3=", K3
PRINT*, "KOL=", KOL
PRINT*, "SAMPLE TIME=", TS
PRINT*, "COMPUTATION TIME=", TC
PRINT*, " "
PRINT*, "FEEDBACK COMPENSATOR:"
PRINT 4000, CF
PRINT*, "FEEDFORWARD COMPENSATOR:"
PRINT 5000, (C(I,1), I=1,5)
PRINT*, "SENSOR FILTER:"
PRINT 5000, (C(I,2), I=1,5)
PRINT*, " "
PRINT*, " "
PRINT*, " "
C*****
C
C      SET UP FOR SIMULATION
C*****
C*** SCALE INPUT MAGNITUDE
    AZMAG=AZMAG/1000.
    ELMAG=ELMAG/1000.
C*** CONVERT GUN FREQUENCY AND DAMP RATIO TO PHASE VAR FORM
    DO 1 I=1,5
      W2(I)=2.*PI*W2(I)
      ZW(I)=2.*ZETA*W2(I)
      W2(I)=W2(I)**2
    1
C*** CONVERT ANGULAR MINIMUMS TO LENGTH MAXIMUMS
    TMAX=TMAX*.01745*D/AV
    OTMAX=OTMAX*.01745*D/AV
    OOTMAX=OOTMAX*.01745*D/AV

```

C**** CONVERT COMPENSATOR PARAMETERS FOR PHASE VARIABLE IMPLEMENTATION

```

DO 5 I=1,2
  C(2,I)=C(2,I)-C(4,I)*C(1,I)
  C(3,I)=C(3,I)-C(5,I)*C(1,I)
  CF(2)=CF(2)-CF(5)*CF(1)
  CF(3)=CF(3)-CF(6)*CF(1)
  CF(4)=CF(4)-CF(7)*CF(1)
  INITIALIZE TIME AND OUTPUTS
  AMAX=D*SIN(52./1000.)
  BMAX=AMAX/.707
  N=1
  T(1)=0.
  AZ(1)=0.
  EL(1)=0.
  AZM(1)=0.
  ELM(1)=0.
  ALPHA=0.
  BETA=0.
  XLI=0.
  YLI=0.
  OXC=0.
  OYC=0.
  DEFINE ACTUATOR LENGTHS
  XLD=SQRT(A**2+B**2)
  YLD=SQRT(A**2+B**2)
  COMPUTE SAMPLE INCREMENTS AND TIMES
  NCSAMP=(NPPTS-1)*TS/TF
  NCCOMP=(NPPTS-1)*TC/TF
  DT=TS/NCSAMP
  TC=DT*NCCOMP
  INCPR=PRINC/DT
  IF(INCPR.LE.0) INCPR=1
  ICONT=1

```

```

C**** DEFINE ODE PARAMETERS
      IFLAG=1
      RELERR=.000001
      ABSERR=.000001
      NEQN=46
C*****
C      PERFORM SIMULATION
C*****
C      10 CONTINUE
      DO 30 J=1,NCSAMP
      CALL COMMAND(T(N),AZC(N),ELC(N),NAZTYPE,NELTYPE,AZMAG,ELMAG,AZFREQ
      1,ELFREQ,DT,AZR,ELR)
C**** CHECK FOR CONTROL INPUT
      IF(J.NE.1) GO TO 15
      AZRC=AZR
      ELRC=ELR
      AZPC=AZC(N)
      ELPC=ELC(N)
      15 CONTINUE
C**** CHECK FOR FINAL INTERVAL
      IF (N.GE.NPPTS) GO TO 40
C**** CHECK FOR CONTROL OUTPUT
      IF ((J-1).NE.NCCOMP) GO TO 20
      CALL CONTROL(AZPC,AZRC,ELPC,ELRC,ALPHA,BETA,XLI,YLI,DT,ICONT)
C**** INTEGRATE STATE EQUATIONS
      20 TOUT=T(N)+DT
      T(N+1)=T(N)
      N=N+1
      CALL ODE (GUN,NEQN,X,T(N),TOUT,RELERR,ABSFRR,IFLAG,MDR<,IWORK)
      IF (IFLAG.GT.3) GO TO 999
      IF (IFLAG.EQ.3) PRINT*,"RELERR INCREASED"

```

```

C*** FIND AZ AND EL AT SENSOR POSITIONS
XX=AS(1)*X(7)+AS(2)*X(9)+AS(3)*X(11)+AS(4)*X(13)+AS(5)*X(15)
YY=AS(1)*X(30)+AS(2)*X(32)+AS(3)*X(34)+AS(4)*X(36)+AS(5)*X(38)
IF(XX.GT.AMAX) XX=AMAX
IF(XX.LT.-AMAX) XX=-AMAX
IF(YY.GT.AMAX) YY=AMAX
IF(YY.LT.-AMAX) YY=-AMAX
XL=XLO+XX
YL=YLO+YY
CALL LNT0AN (XL,YL,AZM(N),ELM(N))
C*** FIND AZ AND EL AT END OF BARREL
XX=AB(1)*X(7)+AB(2)*X(9)+AB(3)*X(11)+AB(4)*X(13)+AB(5)*X(15)
YY=AB(1)*X(30)+AB(2)*X(32)+AB(3)*X(34)+AB(4)*X(36)+AB(5)*X(38)
IF(XX.GT.BMAX) XX=BMAX
IF(XX.LT.-BMAX) XX=-BMAX
IF(YY.GT.BMAX) YY=BMAX
IF(YY.LT.-BMAX) YY=-BMAX
XL=XLO+XX
YL=YLO+YY
CALL LNT0AN (XL,YL,AZ(N),EL(N))
C*** FIND INPUT TO FC COMPUTER
IF(J.NE.NCSAMP) GO TO 30
XX=C(3,2)*X(22)+C(2,2)*X(23)+C(1,2)*(AS(1)*X(7)+AS(2)*X(9)+AS(3)
1*X(11)+AS(4)*X(13)+AS(5)*X(15))
YY=C(3,2)*X(45)+C(2,2)*X(46)+C(1,2)*(AS(1)*X(30)+AS(2)*X(32)+AS(3)
1*X(34)+AS(4)*X(36)+AS(5)*X(38))
XL=XLO+XX
YL=YLO+YY
CALL LNT0AN (XL,YL,ALPHA,BETA)
XLI=X(1)
YLI=X(24)
30 CONTINUE
GO TO 10
40 CONTINUE

```



```

C**** FIND BARREL ELEVATION ERRORS
      BELERRM=BELERRM+BELERR
      BELERRS=BELERRS+BELERR**2
C**** FIND AZIMUTH SENSOR FIGURES OF MERIT
      IF((ABS(AZERR).LE.A7ERR1).AND.(AZERR1.GT.AZERR2)) AZPK=AZERR1
      IF(AZERR1.GT.SC) GO TO 100
      IF(TSAZ.LT.999.) GO TO 200
      TSAZ=T(J-1)
      GO TO 200
100 TSAZ=999.
200 AZERR2=AZERR1
      AZERR1=ABS(AZERR)
C
      IF(TRAZ.LT.999.) GO TO 300
      IF(ABS(AZM(J)).GE.ABS(AZMAG)) TRAZ=T(J)
300 CONTINUE
C
      IF(ABS(AZM(J)).LT.PMAZ) GO TO 400
      PMAZ=AZM(J)
      TPAZ=T(J)
400 CONTINUE
C**** FIND AZIMUTH BARREL FIGURES OF MERIT
      IF((ABS(BAZERR).LE.BAZERR1).AND.(BAZERR1.GT.BAZERR2)) BAZPK=BAZERR1
      IF(BAZERR1.GT.SC) GO TO 500
      IF(TSBAZ.LT.999.) GO TO 600
      TSBAZ=T(J-1)
      GO TO 600
500 TSBAZ=999.
500 BAZERR2=BAZERR1
      BAZERR1=ABS(BAZERR)
C
      IF(TRBAZ.LT.999.) GO TO 700
      IF(ABS(AZ(J)).GE.ABS(AZMAG)) TRBAZ=T(J)
700 CONTINUE

```

```

C
IF(ABS(AZ(J)).LT.PMBAZ) GO TO 800
PMBAZ=AZ(J)
TPBAZ=T(J)
800 CONTINUE

C
IF(I.NE.INCPR) GO TO 49
WRITE 2000,T(J),AZC(J),ELC(J),AZM(J),ELM(J),AZERR,E-ERR,AZ(J),
1EL(J),BAZERR,BELERR
I=1
GO TO 50
49 I=I+1
50 CONTINUE
BELERRM=BELERRM/NPPTS
BELERRS= SORT(BELERRS/NPPTS)
IF(AZPK.GT.SC) TSAZ=999.
IF(BAZPK.GT.SC) TSBAZ=999.
PRINT*," "
PRINT*," "
PRINT*," "
PRINT*,"MEAN BARREL ELEVATION ERROR =",BELERRM
PRINT*," "
PRINT*,"SORT MEAN SQUARE BARREL ELEVATION ERROR =",BELERRS
PRINT*," "
PRINT*," "
PRINT*,"SENSOR AZIMUTH FIGURES OF MERIT"
WRITE 6000,TSAZ,TRAZ,TPAZ,PMAZ
PRINT*," "
PRINT*," "
PRINT*," "
PRINT*,"BARREL AZIMUTH FIGURES OF MERIT"
WRITE 6000,TSBAZ,TRBAZ,TPBAZ,PMBAZ
PLOT MEASURED ANGLES AND COMMANDED ANGLES
IF(IPLT.EQ.0) GO TO 998
CALL PLOTTER(T,A7,EL,AZC,ELC,TF,1,1-M)
CALL PLOTTER(T,A7M,ELM,AZC,ELC,TF,0,1-HS)
C****

```

```

C*****
998 STOP
999 PRINT*, "ODE ERROR", IFLAG, "AT", TOUT
      STOP "ODE ERROR"
C*****
1000 FORMAT (//6X, "TIME", 9X, "COMMAND (MRAD)", 10X, "SENSOR (MRAD)", 11X,
1"ERROR (MRAD)", 11X, "MUZZLE (MRAD)", 12X, "ERROR (MRAD)" /
25X, "(SEC)      AZIMUTH      ELEVATION      AZIMUTH      ELEVATION", 4X,
3"AZIMUTH      ELEVATION      AZIMUTH      ELEVATION      AZIMUTH      ELEVATION", 4X,
4"ELEVATION" /)
2000 FORMAT (11(4X, F8.4))
3000 FORMAT (1H1)
4000 FORMAT (10X, G10.4, "S**3 +", G10.4, "S**2 +", G10.4, "S +", 510.4 /
110X, 55 (" - ") / 20X, "S**3 +", G10.4, "S**2 +", G10.4, "S +", 510.4 /)
5000 FORMAT (10X, G10.4, "S**2 +", G10.4, "S +", 510.4 / 10X, 39 (" - ") /
120X, "S**2 +", G10.4, "S +", G10.4 /)
5000 FORMAT (1X, *TS=*, F10.4, 4X, *TR=*, F10.4, 5X, *TP=*, F10.4, 5X, *MP=*, 510.4
1)
C
      END

```



```

C**** SUBROUTINE GUN (T,X,DX)
C**** THIS SUBROUTINE CONTAINS THE X AND Y STATE EQUATIONS FOR THE
M61-A1 GUN SERVO SUBSYSTEM WITH DELTA P AND RATE FEEDFORWARD
DIMENSION X(46),DX(46),W2(5),ZW(5),AB(5),DC(2)
DIMENSION C1(5),C2(5),CF(7),Y(2)
COMMON/COEF/AV,WV2,ZWV,AC,T1,T2,A1,A2,A3,A4,A5,W2,A3,C1,C2,CF
COMMON /MISC/K1,K2,K3,KOL,DC
COMMON/MAX/TMAX,DTMAX,DDTMAX
REAL K1,K2,K3,KOL
H1=1/(1-T2/T1)
H2=1/(1-T1/T2)
DO 20 I=1,2
J=23*(I-1)
C**** INTEGRATOR
DX(J+1)=DC(I)
C**** SERVO-VALVE
IF(X(J+2).GT.TMAX) X(J+2)=TMAX
IF(X(J+2).LT.-TMAX) X(J+2)=-TMAX
DX(J+2)=X(J+3)
IF(DX(J+2).GT.DTMAX) DX(J+2)=DTMAX
IF(DX(J+2).LT.-DTMAX) DX(J+2)=-DTMAX
DX(J+3)=X(J+4)
IF(DX(J+3).GT.DDTMAX) DX(J+3)=DDTMAX
IF(DX(J+3).LT.-DDTMAX) DX(J+3)=-DDTMAX
Y(I)=(A1*X(J+7)+A2*X(J+9)+A3*X(J+11)+A4*X(J+13)+A5*X(J+15))
DX(J+4)=DC(I)+KOL*C1(1)+X(J+1)-WV2*X(J+3)-ZWV*X(J+4)+H1*X(J+5)
1+H2*X(J+5)-KOL*C1(1)+CF(1)+Y(I)+CF(4)+X(J+17)+CF(3)+X(J+18)
2+CF(2)+X(J+19))+C1(3)+X(J+20)+C1(2)+X(J+21)

```

```

C**** DELTA P COMPENSATOR
DX(J+5)=AC*(-AV*X(J+2)+Y(I))-T1*X(J+5)
DX(J+6)=AC*(-AV*X(J+2)+Y(I))-T2*X(J+5)
C**** GUN DYNAMICS
DO 10 M=1,5
L=J+2*(M-1)
DX(L+7)=X(L+8)
DX(L+8)=AV*X(J+2)-W2(M)*X(L+7)-ZW(M)*X(L+8)
10 CONTINUE
C**** FEEDBACK COMPENSATOR
Y(I)=(A1*X(J+7)+A2*X(J+9)+A3*X(J+11)+A4*X(J+13)+A5*X(J+15))
DX(J+17)=X(J+18)
DX(J+18)=X(J+19)
DX(J+19)=-CF(7)*X(J+17)-CF(6)*X(J+18)-CF(5)*X(J+19)+Y(I)
C**** FEEDFORWARD COMPENSATOR
DX(J+20)=X(J+21)
DX(J+21)=-C1(5)*X(J+20)-C1(4)*X(J+21)+KOL*(X(J+1)-C*(4)*X(J+17)
1-CF(3)*X(J+18)-CF(2)*X(J+19)-CF(1)*Y(I))
C**** SENSOR FILTER
DX(J+22)=X(J+23)
DX(J+23)=-C2(5)*X(J+22)-C2(4)*X(J+23)+Y(I)
20 CONTINUE
RETURN
END

```

```

SUBROUTINE LNTOLN (LX,LY,AZG,ELG)
C*****THIS SUBROUTINE TRANSFORMS ACTUATOR LENGTHS TO
C*****GUN AZIMUTH AND ELEVATION
COMMON /ACTUAT/A,B,D,XL0,YL0
REAL LX,LY
X1=((LX**2)-(LY**2))/(4*B*D)
Y1=((SQRT(2*(LX**2)*(LY**2)+2*(LX**2)*((2*B)**2)
1+2*(LY**2)*((2*B)**2)-(LX**4)-(LY**4))-((2*B)**4)))/(4*3))-A)/D
IF (Y1.GT.1.) Y1=1.
AZG=ASIN(Y1)
ELG=(-1)*ASIN(X1)
RETURN
END
SUBROUTINE ANTOLN (LX,LY,AZG,ELG,ELX,ELY)
C*****THIS SUBROUTINE TRANSFORMS GUN AZIMUTH AND ELEVATION
C*****TO ACTUATOR LENGTHS
COMMON /ACTUAT/A,B,D,XL0,YL0
REAL LX,LY
LX=SQRT((D*A7G+A)**2+(D*ELG-B)**2)
LY=SQRT((D*A7G+A)**2+(D*ELG+B)**2)
ELX=LX-XL0
ELY=LY-YL0
RETURN
END

```

```

SUBROUTINE COMMAND(T,AZ,EL,NATYPE,NETYPE,AMAG,EMAG,1=REQ,EFREQ,DT,
1AZR,ELR)
DIMENSION X(2),Y(2)
GO TO (10,20,30,40,50,60)NATYPE
10 AZ=AMAG
   AZR=0.
   GO TO 100
20 AZ=AMAG*T
   AZR=AMAG
   GO TO 100
30 AZ=AMAG*T**2
   AZR=2.*AMAG*T
   GO TO 100
40 AZ=AMAG*SIN(2*3.1416*AFREQ*T)
   AZR=2.*3.1416*AFREQ*AMAG*COS(2.*3.1416*AFREQ*T)
   GO TO 100
50 AZ=AMAG*COS(2*3.1416*AFREQ*T)
   AZR=-2.*3.1416*AFREQ*AMAG*SIN(2.*3.1416*AFREQ*T)
   GO TO 100
60 CALL NOISE(AZ,AZR,ADUM,AMAG,AFREQ,DT)
100 CONTINUE
   GO TO (110,120,130,140,150,160) NETYPE
110 EL=EMAG
   ELR=0.
   RETURN

```

```

120 EL=EMAG*T
    ELR=EMAG
    RETURN
130 EL=EMAG*T**2
    ELR=2.*EMAG*T
    RETURN
140 EL=EMAG*SIN(2*3.1416*EFREQ*T)
    ELR=2.*3.1416*EFREQ*EMAG*COS(2.*3.1416*EFREQ*T)
    RETURN
150 EL=EMAG*COS(2*3.1416*EFREQ*T)
    ELR=-2.*3.1416*EFREQ*EMAG*SIN(2.*3.1416*EFREQ*T)
    RETURN
160 CALL NOISE(EL,ELR,EDUM,EMAG,EFREQ,DT)
    RETURN
END
SUBROUTINE NOISE(X,DX,DDX,MAG,T,DT)
C*** THIS SUBROUTINE GENERATES POSITION BASED ON EXPONENTIALLY CORRELATED
C*** ACCELERATION
    REAL MAG
    GAUSS=0.
    DO 10 I=1,12
10 GAUSS=GAUSS+RANF(DUM)-.5
    X=X+DX*DT+.5*DDX*DT*DT
    DX=DX+DDX*DT
    DDX=DDX*EXP(-DT/T)+GAUSS*MAG
    RETURN
END

```

```

SUBROUTINE PLCTTER(T,AZ,EL,AZC,ELC,TF,IFLAG,IPOS)
THIS SUBROUTINE PLOTS TWO GRAPHS, EACH HAVING TWO P.PTS.
DIMENSION T(253),AZ(253),EL(253),AZC(253),ELC(253)
DEFINE ORIGIN AT MARGIN AND DRAW BOX AROUND PLOT AREAS

CALL PLOT(0.0,-3.0,-3)
CALL PLOT(0.0,1.5,-3)
CALL PLOT(0.0,8.5,2)
IF (IPOS.EQ.1H) GO TO 1
CALL SYMBOL(2.0,8.1,.175,15HSENSOR RESPONSE,0.0,15)
GO TO 2
1 CALL SYMBOL(2.0,8.1,.175,15HMUZZLE RESPONSE,0.0,15)
2 CALL PLOT(0.0,8.5,3)
CALL PLOT(6.0,8.5,2)
CALL PLOT(6.0,0.0,2)
CALL SYMBOL(4.0,.1,.105,15H* ANGLE COMMAND,0.0,15)
CALL PLOT(5.0,0.0,3)
CALL PLOT(0.0,0.0,2)

DEFINE SCALE FACTORS
T(252)=0.
T(253)=TF/5.
AZ(252)=-50.
AZC(252)=-50.
EL(252)=-50.
ELC(252)=-50.
ALEN=4.
AZ(253)=100./ALEN
AZC(253)=100./ALEN
EL(253)=100./ALEN
ELC(253)=100./ALEN

```

```

C
C      DRAW TIME AXIS
C      CALL PLOT(.6,4.25,-3)
C      CALL AXIS (0.,.20,10TIME (SEC),-10,3,0.,T(252),T(253))
C
C      SCALE FOR AZ AND EL PLOTS
C      FACT=7./8.
C      T(253)=T(253)*FACT
C      CALL FACTOR (FACT)
C
C      DRAW AZIMUTH AXIS AND PLOT AZ INFORMATION
C      CALL PLOT (0.,.343,-3)
C      CALL AXIS (0.,0.,9HAZ (MRAD),9,ALEN,90.,AZ(252),AZ(253))
C      CALL LINE (T,AZ,251,1,0,0)
C      CALL LINE (T,AZC,251,1,50,11)
C
C      DRAW ELEVATION AXIS AND PLOT EL INFORMATION
C      CALL PLOT (0.,-4.857,-3)
C      CALL AXIS (0.,0.,9HEL (MRAD),9,ALEN,30.,EL(252),EL(253))
C      CALL LINE (T,EL,251,1,0,0)
C      CALL LINE (T,ELC,251,1,50,11)
C      CALL FACTOR (1.)
C
C      IF THIS IS LAST PLOT, END PLOT
C      IF(IFLAS.NE.0) GO TO 10
C      CALL PLOT (0.,0.,3)
C      CALL PLOTE
C      GO TO 20
C      IF NOT LAST PLOT,SET UP FOR NEXT PLOT
C
C      10 CALL PLOT (8.,0.,-3)
C      20 RETURN
C      END

```

```

C**** SUBROUTINE CONTROL(AZPC,AZRC,ELPC,ELRC,AZM,ELM,XI,YI,DI,N)
THIS SUBROUTINE PERFORMS THE DIGITAL PORTION OF THE CONTROL LAW
COMMON/MISC/K1,K2,K3,KOL,DXC,DYC
COMMON /ACTUAT/A,B,D,XL0,YL0
REAL K1,K2,K3,KOL
C**** IF FIRST CALL INITIALIZE
IF (N.NE.1) GO TO 10
PHI=1-K3
XIO=0.
YIO=0.
X=0.
Y=0.
TMAX=18.93
N=2
10 CONTINUE
C**** TRANSFORM COMMANDS AND MEASUREMENTS
CALL ANFOLN (XPOS,YPOS,AZPC,ELPC,XPC,YPC)
CALL ANFOLN(DUM1,DUM2,AZM,ELM,XM,YM)
XRC=((D*A7PC+A)*AZRC+(D*ELPC-B)*ELRC)*J/XPOS
YRC=((D*A7PC+A)*AZRC+(D*ELPC-B)*ELRC)*D/YPOS
C**** FILTER MEASUREMENTS
X=K3*(X-XI)+XI+PHI*(X-XIO)
Y=K3*(Y-YI)+YI+PHI*(Y-YIO)
XIO=XI
YIO=YI
C**** CONTROL LAW
DXC=K1*(XPC-X)+K2*XRC
DYC=K1*(YPC-Y)+K2*YRC
C**** LIMITER
IF (DYC.LT.-TMAX) DYC=-TMAX
IF (DYC.GT.TMAX) DYC=TMAX
IF (DXC.LT.-TMAX) DXC=-TMAX
IF (DXC.GT.TMAX) DXC=TMAX
RETURN
END

```


Appendix E

Z and S Plane Relationships

Pole locations in the Z plane can be related to S plane poles and associated response using Figure 32. Lines of constant σ in the plane correspond to circles centered at the origin in the Z plane and lines of constant damped frequency are radical lines. While stability in the S plane is indicated by left half plane poles, Z domain stability is indicated by poles with a magnitude less than 1.

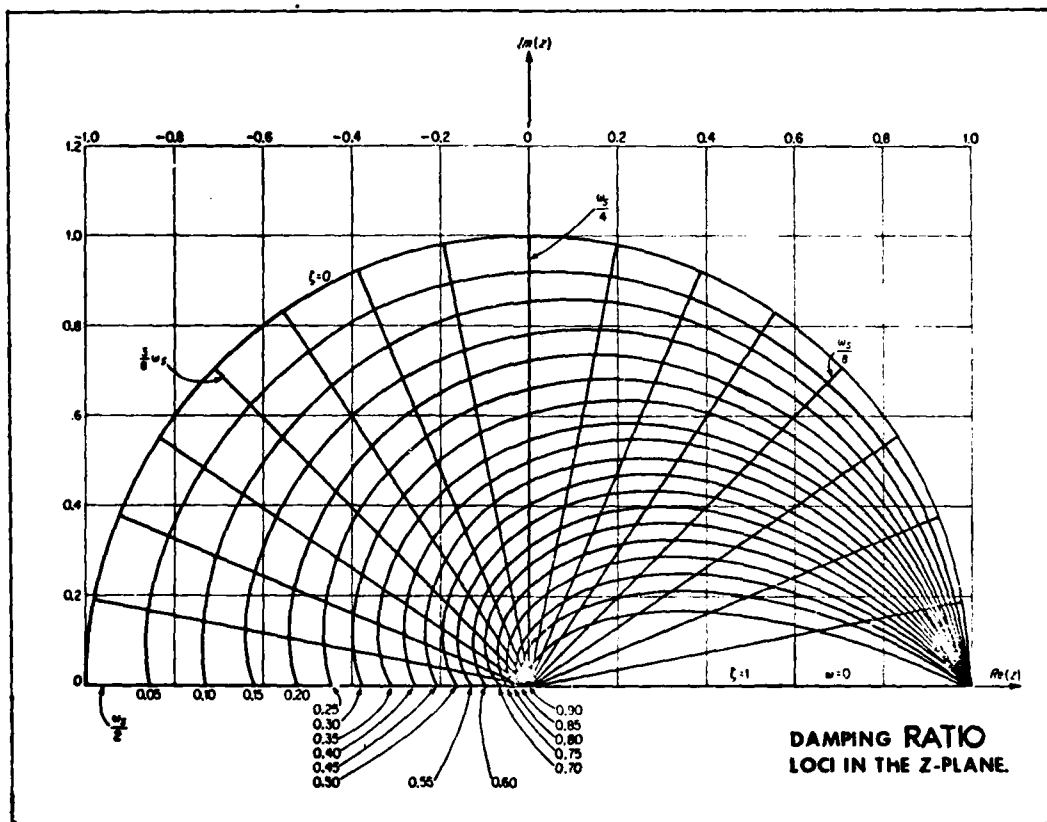


Figure 32. Z Domain Unit Circle.

VITA

Donald E. Jones was born on May 17, 1955, in Longmont, Colorado. He attended school in Berthoud, Colorado until graduation from Berthoud High in 1973. After spending four years at Colorado State University, he graduated with distinction in August 1977, receiving the Bachelor of Science Degree in Engineering Science. At this time, he received his commission as a Second Lieutenant in the United States Air Force. His first assignment, entering active duty in September 1977, was to the School of Engineering, Air Force Institute of Technology. Lt Jones is a member of I.E.E.E., A.I.A.A., Tau Beta Pi, and Phi Kappa Phi.

Permanent address: 621 4th Street
Berthoud, Colorado 80513

UNCLASSIFIED

SECURITY CLASSIFICATION OF THIS PAGE (When Data Entered)

REPORT DOCUMENTATION PAGE		READ INSTRUCTIONS BEFORE COMPLETING FORM
1. REPORT NUMBER AFIT/GA/AA/78D-5	2. GOVT ACCESSION NO.	3. RECIPIENT'S CATALOG NUMBER
4. TITLE (and Subtitle) ANALYSIS OF A CONTROLLER FOR THE M61 MOVABLE GUN		5. TYPE OF REPORT & PERIOD COVERED MS Thesis
		6. PERFORMING ORG. REPORT NUMBER
7. AUTHOR(s) Donald E. Jones Second Lieutenant, USAF		8. CONTRACT OR GRANT NUMBER(s)
9. PERFORMING ORGANIZATION NAME AND ADDRESS Air Force Institute of Technology (AFIT-EN) Wright-Patterson AFB, Ohio 45433		10. PROGRAM ELEMENT, PROJECT, TASK AREA & WORK UNIT NUMBERS
11. CONTROLLING OFFICE NAME AND ADDRESS		12. REPORT DATE December 1978
		13. NUMBER OF PAGES 122
14. MONITORING AGENCY NAME & ADDRESS (if different from Controlling Office)		15. SECURITY CLASS. (of this report) Unclassified
		15a. DECLASSIFICATION/DOWNGRADING SCHEDULE
16. DISTRIBUTION STATEMENT (of this Report) Approved for public release; distribution unlimited		
17. DISTRIBUTION STATEMENT (of the abstract entered in Block 20. If different from Report)		
18. SUPPLEMENTARY NOTES Approved for public release; LAW AFR 140-17 JOSEPH P. HIEPS, Major, USAF Director of Information		
19. KEY WORDS (Continue on reverse side if necessary and identify by block number) Movable Gun Digital Control Structural Vibration		
20. ABSTRACT (Continue on reverse side if necessary and identify by block number) The effects of changing control parameters of the movable M61 gun system proposed for the F-15 aircraft are examined using time response and root locus methods. In the course of the analysis, a Fortran IV simulation program, state space model, and gun servo subsystem Z transform are developed. The gun servo subsystem design has little effect on system response. The system settled in under 0.2 sec and had less than 10% overshoot for any open		

UNCLASSIFIED

SECURITY CLASSIFICATION OF THIS PAGE(When Data Entered)

Continuation
Block 20. ABSTRACT

loop gain from 0 to 200 sec^{-1} and with or without differential pressure compensation.

The overall system is stable for a system gain of 0 to 39 and exhibits nearly deadbeat responses for a gain of 20. Digital rate feedforward is required to keep ramp following error below 1 mrad for a $5^\circ/\text{sec}$ ramp. Digital filtering improves response and analog low-pass sensor filters with a cutoff of 30 Hz eliminate aliasing while moderately reducing system performance. Computation delays of less than 0.005 sec were found to have negligible effect on the system response.

The muzzle response is examined and a compensator, which neglects barrel cluster rotation, is designed to reduce the 50% overshoot and over 2 sec settling time for a step input. This, however, degraded tracking of more realistic (lower frequency content) inputs indicating that a better compensator should be designed or that muzzle response at target acquisition should be allowed to settle before firing.

Overall, the movable M61 was found to be an extremely fast gun system, insensitive to most control parameters.

UNCLASSIFIED

SECURITY CLASSIFICATION OF THIS PAGE(When Data Entered)